CONSORZIO RFX
Ricerca Formazione Innovazione

Activity Report 2019

1. INTRODUCTION 3

2. ITER PROJECT 5

2.1. ACTIVITY FOR THE DEVELOPMENT OF NEUTRAL BEAM INJECTORS FOR ITER 5

2.1.1. PRIMA and host activities 6

2.1.2. SPIDER 12

2.1.3. MITICA 25

2.1.4. ITER Neutral Beam Injector Physics 35

2.1.5. Vacuum high voltage holding modeling and experiments 40

2.1.6. RF Research and Development 45

2.1.7. Caesium R&D 46

2.2. ITER DIAGNOSTICS 47

2.2.1. Diagnostic systems Engineering Services 47

3. EUROFUSION PROGRAMME 48

3.1. RFX-MOD: EXPERIMENTAL, MODELING ACTIVITIES AND UPGRADES 48

3.1.1. Introduction 48

3.1.2. Implementation of the machine toroidal assembly modifications 48

3.1.3. Preparation of the RFX-mod2 scientific programme 55

3.1.4. Design/upgrade of new diagnostic systems for RFX-mod2 57

3.1.5. Mod Theory and modelling related to RFP helical states 61

3.1.6. Edge physics 67

3.1.7. Effect of RFP reconnections in global power balance 69

3.1.8. Studies of m=1 wall-locking in RFX-mod and RFX-mod2 69

3.1.9. MHD equilibrium and control 72

3.1.10. Studies on RFP machine as Neutron Source 73

3.2. ITER PHYSICS WORK PACKAGES 75

3.2.1. Introduction 75

3.2.2. MST1 75

3.2.3. JET1 79
3.2.4. DTT 86
3.2.5. WPSA 91
3.2.6. WPS1 94
3.2.7. WPISA 96
3.2.8. Collaborations: Interfacing VMEC and Cariddi to study dymnamic plasma equilibria (F4E OPE0951) 97
3.3. ITER NBI PHYSICS ACTIVITIES AND ACCOMPANYING PROGRAM 97
3.3.1. NIO1 Experiment 97
3.3.2. NBI Complex system and controllability 100
3.3.3. RAID 100
3.4. PPPT PROJECTS 101
3.4.1. WPBoP - Balance of Plant - DEMO Plant Electrical System (PES) 101
3.4.2. WPBoP - Balance of Plant - Thermal-Hydraulic Design of DEMO PHTS+BOP and Aux System. 103
3.4.3. WPHCD – Heating and Current Drive systems 104
3.4.4. WPFTV - Tritium, Fuelling and Vacuum Pumping Systems 105
3.4.5. WPMAG – Magnet System: Quench Protection Circuit Studies 106
3.5. SOCIO ECONOMIC STUDIES (SES) AND DEMO 107
3.5.1. Fusion power plant economic assessment 107
3.5.2. The role of fusion in long term energy scenarios 107
3.6. EDUCATION AND TRAINING 109
3.7. SCIENTIFIC CONFERENCES AND MEETINGS 109
3.8. COMMUNICATION AND OUTREACH 110
4. BROADER APPROACH 112
4.1. CONTRIBUTION TO THE JT-60SA PS COMBINATION TESTS PRELIMINARY TO THE INTEGRATED COMMISSIONING 112
4.2. POWER SUPPLIES FOR IN-VESSEL SECTOR COILS FOR RWM CONTROL 113
5. INDUSTRIAL AND NON-FUSION RELATED COLLABORATIONS 114
5.1. DESIGN OF VACUUM INTERRUPTERS WITH THE VOLTAGE HOLDING PREDICTION MODEL (VHPM) 114
5.2. BIOMEDICAL PLASMA APPLICATIONS 115
5.3. PLASMA STUDY FOR GALILEO PASSIVE HYDROGEN MASER 116

1. Introduction

This Report describes the activities and the results obtained in the year 2019, developed along the guidelines of the 2019 Activity Programme approved by the Consorzio RFX partners meeting held on 5 December 2018.

In 2019 on SPIDER the first extraction and acceleration of a negative beam has been obtained from volume production of negative ions. A limited number of 80 beamlets, over a total of 1280, have been left unmasked to allow operating in a wider pressure range. The experimental activities have been performed along the year with only limited shut downs phases for improvements and integration works.

In parallel in MITICA the Beam Source Vessel and the Bushing have been installed allowing to complete the High Voltage tests up to 1.2 MV (1.0 MV for the bushing in agreement with the requirements) for all the SF6 and air insulated components of MITICA. The beam line vessel at the end of the year has passed the last factory tests and is now ready for the delivery. The Beam Source procurement is proceeding in time, in November the Beam Line Components procurement contract has been signed, whereas the cryogenic pump procurement is ongoing with some delay presently not yet in the critical line.

The PRIMA and MITICA plant systems have been completed and most of them have been already transferred for use or under the final site acceptance tests.

Side activities on specific facilities, NIO1, CATS, HVPTF have been performed to support to development and the understanding of specific aspects of the ITER and DEMO negative neutral beam injectors.

With regards to RFX-mod2 the activities of both contracts have suffered the financial crisis of the main industrial partner E. Zanon Spa responsible for the main activities on the torus assembly. In consequence to this event the manufacturing activities have not been initiated, the procurements of components have been delayed as well as the final tests planned on specific mock ups to support the evolution of some technical choices. The last part of the year has been dedicated to identify the solution to restructure the contracts with the new company that has taken the place of E. Zanon SpA.

In parallel the analysis and the studies for the refurbishment and revamping of diagnostics and plant systems, that are no more in operation since the end of 2015, have been performed or initiated to identify the costs and the required resources to reestablish the previous operability.

A draft of the scientific plan of exploitation of RFX-mod2 has been developed and used as a basis for the work to develop a comprehensive plan ready for the restart of the exploitation phase.

The activities on the different Tokamaks being part of the European programme in support to the development of ITER plasma scenario (JET, AUG and TCV), the participation to the design of DTT, the participation to the conceptual design of DEMO and finally the participation to the commissioning and the preparation the first phase of operation in JT-60SA have continued with an increasing effort. It has to be mentioned the increasing effort in the DTT design activities in parallel with the process to establish the design team.

Other significant activities and achievements are described in the document we highlight here: the studies to the identification of the role of Fusion Nuclear Power Plant in the mix of energy sources in the evolving energy scenario of this century, the paper on the density limit across different toroidal configurations, the development of atmospheric plasma sources in view of the biomedical use, the organization of the 8th MEVARC (8th International Workshop on Mechanisms of Vacuum Arcs) and the numerous public information activities.

In 2019, 134 papers with co-authors of Consorzio RFX have been published in International Journals, 67 of them submitted by a Consorzio RFX first author; there have been 134 participations of Consorzio RFX researchers to National and International Workshops and Conferences, 110 of them submitting a contribution as a first author, of the latter ones 11 were invited talks and 20 oral presentations.

2. ITER Project

2.1. *Activity for the development of Neutral Beam Injectors for ITER*

The SPIDER experiment was regularly operated during 2019 with interleaved short shut down periods, in order to apply changes and integrations as required by the experimental outcomes and commonly agreed among all the involved partners and organizations. In particular all the experimental activity has been performed operating the Beam Source by masking part of the plasma grid apertures by a metallic mask, 93% of the apertures masked, in order to maintain the residual pressure in the vessel lower than 40 mPa, which is the pressure limit below which in-vacuum RF discharge probability is strongly reduced. The first negative ion beam was extracted from the SPIDER ion source and accelerated at the end of May 2019. Further details in the next sections.

Installation, commissioning and SAT (Site Acceptance Tests) of MITICA power supplies and other auxiliary plant systems were well advanced. In particular, after installation and SAT of MITICA Beam Source Vessel, the High Voltage Bushing, the TL3 bend and the last piece of the HV Transmission Line were installed, so decreeing the substantial completion of the Japanese component installations. In 2019, also electrical insulation tests of HV components were carried out. These tests were repeated each time a new part of the system, under different DA (Domestic Agency) responsibility, was connected to the previous ones. This test sequence was necessary to ensure that responsibilities were clearly associated to the different DAs during the tests.

In Q4 2019 the contract for procurement of the Beam Line Components, the last procurement for components of MITICA experiment, was finally awarded after completion of Stage 1 review by three competitors. So presently all the contracts for procurement of MITICA components are launched and in progress.

The main activities performed in 2019 can be so summarized:

- Technical support to the F4E procurement contracts of MITICA plant and components;
- Support to installation and tests of components procured by JADA and INDA;
- Integration activities for installation and tests of SPIDER and MITICA components and management of the interfaces with PRIMA buildings and plants;
- Development of MITICA diagnostics, control and protection systems;

- Host activities to support on-site works and safety coordination during installation of equipment of F4E and other DAs;
- Management and execution of commissioning and integrated tests;
- Execution of SPIDER experiments with technical support and scientific exploitation managed and performed by NBTF Team and with the contribution from other parties;
- Development of physics modelling in support of SPIDER experiments;
- Specific R&D activities in support of design and experiments including: experimental campaigns using the HV Test Facility to validate the electrostatic models and study the voltage holding in vacuum; experimental campaigns in the RF laboratory to study and characterize RF circuit properties of plasma sources in support of SPIDER operation; experimental campaigns using the CAesium ovens Test Stand (CATS) to check and optimize the SPIDER Cs Ovens design and operations.

A comprehensive update about the progress of NBTF and the results obtained with SPIDER operation in 2019 can be found in [1] [2].

2.1.1. *PRIMA and host activities*

2.1.1.1. Building and auxiliaries

As regards the NBTF building in 2019 only minor procurements and completions were done. In particular:

- installation of concrete door of MITICA bio-shield;
- design and procurement of fire extinguish systems of 1 MV insulating transformer;
- installation of a water discharge system for the cooling plant in the industrial sewer system.

The integration and interface management work continued in 2019 to ensure the coherent integration of the experimental devices by monitoring the construction activities and the full

[1] V. Toigo, et al., “Progress in the ITER neutral beam test facility”, Nuclear Fusion, Volume 59, Number 8

[2] G. Serianni et al., “SPIDER in the roadmap of the ITER neutral beams”, Fusion Engineering and Design, Volume 146 (2019) 2539-2546

3D CAD model of the facility, including both the infrastructures and the experimental plant systems and injectors.

Finally, in 2019 the procurements of the rotating platform for BS and BSV Rear Lid removal were well advanced. Installation and tests on-site will be completed within Q1 2020.

2.1.1.2. Cooling Plant

Commissioning and site acceptance tests of the SPIDER Plant Unit were already completed during 2018 and allowed the use of the Plant Units for SPIDER operations during 2019. The technical solution identified and agreed to recover the pumps and equipment affected by the flood occurred at the end of November 2017 in Building 2 at level -4.0 m was finally implemented in May-June 2019. This allowed the removal of the temporary equipment that were installed and used to allow SPIDER operations till June 2019. Secondary and tertiary circuits for SPIDER and MITICA were finally available for the overall commissioning and Site Acceptance Tests performed during the second half of 2019. To be noted that during 2019 the SPIDER cooling plant was always used in local or manual mode, waiting for the final integrated commissioning with CODAS, expected in 2020 after the closure of procurement contract.

In parallel, hydraulic installation works for MITICA Plant Unit were almost completed in 2019 and continuous activities have been carried out by NBTF Team to support, verify and witness the supplier's activities, commissioning and Overall Site Acceptance Tests on-site. Installation of electrical parts and sensors were also completed in 2019; follow-up for activities on electrical subsystem and control system was guaranteed. I&C development is presently under review for final adjustments after Overall Acceptance Tests.

Some non-conformities found during the Overall Acceptance Tests entail a number of issues to solve, requiring further effort by NBTF Team both for hydraulic aspects (new pressurizing systems for PC01, PC08 and PC09) and sensors/control system adjustments. Technical documents, procedures and schedule for commissioning and acceptance tests of MITICA and Shared Plant Units were reviewed and discussed among the Supplier, NBTF Team and F4E, aiming to prepare the final Acceptance Data Package (ADP) for closure of the contract within Q1 2020. Transfer for Use of MITICA Plant Unit is foreseen within Q2 2020.

A team of engineers and technicians was trained for plant operations, tuning and maintenance. Continuous presence and follow-up during SPIDER operations was also guaranteed, with particular effort for managing issues about water resistivity degradation and the use of off-line Chemical Control System.

Overall views of Cooling Plant equipment inside Building 2 are shown in Fig. 2.1. Pictures of hydraulic pipes installed on the back wall of SPIDER Neutron Shield and inside the MITICA Neutron Shield are shown in Fig. 2.2.

2.1.1.3. Vacuum, gas injection and gas storage for SPIDER and MITICA

SPIDER GVS plant [3] was routinely used and maintained for SPIDER operations in 2019, including the installation of new cryopump displecers. Studies and analyses to optimize the gas pressure distribution inside the SPIDER Vacuum Vessel were performed, contributing to the design optimization for masking of SPIDER grids apertures, in order to reduce gas pressure on the back of the source and associated electrical discharge probability.

[3] S. Dal Bello et al., "SPIDER gas injection and vacuum system: From design to commissioning", Fusion Engineering and Design, Volume 146 (2019) 1485-1489

a)  b) 

Fig. 2.1 (a) Pumps of secondary and tertiary circuits in Building 2 at level -4.0 m; (b) Overall view of the equipment of SPIDER, MITICA and Shared Plant Units inside Building 2

a)  b) 

Fig. 2.2 Overall view of (a) SPIDER distribution circuits on the back wall of SPIDER Neutron Shield and (b) Primary Circuits pipes inside MITICA Neutron Shield

A pressure gauge was installed in the source and two new mass spectrometers for real-time and off-line RGA analyses are under procurement. Preparation and follow-up of maintenance contracts with several companies were carried out in 2019.

As regards the MITICA GVS, the design review well progressed in 2019 and installation of gas cabinets, vacuum system, manifolds and cabling are going to be completed within end of 2019. Site Acceptance Tests are scheduled by Q1 2020. Pictures of SPIDER and MITICA pumping units connected to the vessels are shown in Fig. 2.3.

Engineers and technicians of NBTF Team were deeply involved on the technical follow-up during 2019: participation to periodic technical meetings, controls and solving of problems due to integration issues, review of documents submitted in F4E-IDM, preparation of maintenance contracts (with several companies), continuous presence and follow-up during the SPIDER operational period.

a)  b) 

Fig. 2.3 Views of GVS pumping units installed on SPIDER Vacuum Vessel (a) and beside the MITICA Beam Source Vessel (b)

2.1.1.4. Host activities

During 2019 significant amount of resources were invested on activities for construction supervision and coordination, mainly concerning the installation and integration of MITICA experimental plants, and the conduction of SPIDER experiment. Particular effort was required to manage interfaces between buildings and experimental plant units. Also the management of the interfaces between plant units themselves required large effort: specifically to this end, the interface management structure, run by NBTF Team, worked in a coordinate way with the aim of reducing as much as possible clashes during installation of plants being able to define in real-time the modifications required in any of the plants. Significant activities relevant to integration management are represented by the installation of some MITICA components and plant systems, such as the HV Transmission Line (JADA), the HV Bushing (JADA), the HVD1-TL2 HV Bushing (F4E), the Cryoplant (F4E) and the Cooling Plant (F4E).

The NBTF metrology team continued the site and components survey activities, where and when necessary. Just as an example, metrology activities were fundamental during the installation phase of the MITICA Beam Source Vessel (BSV) and during the installation of the MITICA HV Bushing (HVB).

The support to F4E and the other Domestic Agencies for the management of the Construction-Erection All Risks insurance contract for the NBTF (CEAR), directly managed by Consorzio RFX, continued. A flooding event in building #2, happened in 2017 November the 13th, was claimed to the insurance. Long negotiations were necessary due to difficulties in finding agreement with the Cooling Plant supplier. At the end of 2018 an agreement was found (between F4E, IO, Consorzio RFX and Delta-T company) and the recovery activity performed in 2019 (ended in May) through a contract with a company, expert on this type of activities (Belfor), directly issued and managed by Consorzio RFX.

The NBTF-site management, with reference to “Titolo IV of D.Lgs. 81/08” (Health and Safety on-site), whose structure had been set up through the Implementation Agreement, continued

in 2019: the Responsible of Works and the Safety Coordinator continuously monitored and periodically reported the state of the site. Significant resources were spent to assist F4E, in particular by the Safety Coordinator who is in charge for issuing all the Plans for Safety and Coordination (called PSC documents), being the latter an essential part for both the procurement call for tenders and contracts management. To this end, Consorzio RFX personnel (such as the Work Package Managers) closely collaborated with the Safety Coordinator and his collaborator.

With the support of the Coordinator of the Directors of Works (namely CDL) the time schedule for MITICA on-site activities was prepared and discussed among Consorzio RFX, IO and all involved Domestic Agencies during the year. Furthermore, as a coordination method, more than 30 weekly Site Progress Coordination Meetings (SPCMs) have been held, and the minutes distributed and uploaded in F4E IDM. The MITICA time schedule has been managed by preparing, discussing and verifying weekly the activity plan with a visibility of one week, 3 weeks and 3 months.

On weekly basis, a Safety Coordination Meeting amog the CSE, the RSPP of Consorzio RFX and the Site Manager was held to discuss and manage the interferential risks between the yard activities (managed by the CSE) and the activities performed by Consorzio RFX, as for example the SPIDER operation and the maintenance contracts, but not only. The minute of these meeting were distributed to the CDL, F4E Supervisor and Director of Works. Several site inspections were performed by nearly all of the Companies and Domestic Agencies that were operating.

General follow up activities were performed for all the companies working on-site and all the companies working under “Balance of Plant” procurements. Further activities were devoted to the follow-up of companies involved into the three signed Framework Contracts (CODAS-Interlock-Safety, Diagnostics, Assembly).

Big effort has been given by the NBTF team for the SPIDER AGPS system transfer for use by managing the process to obtain the authorization of the use for the whole SPIDER experiment.

As for the Licence to operate the two experiments:

- SPIDER is already authorized from the Radioprotection point of view to use (nulla osta as per DLgs 230/95); in 2019 the CPI (Fire Prevention Certificate) was obtained from the Local Authority (Fire Brigades);
- for MITICA, following the submission of the radioprotection technical reports, in October 2019 we received the Nulla Osta with prescriptions (as per DLgs 230/95).

In 2019 the Transfer for Use to Consorzio RFX of some plants (such as SPIDER Gas and Vacuum, SF6 Gas Handling and Storage, SPIDER AGPS, MITICA HVD1) was obtained; for other systems, such as MITICA BSV and AGPS-CS, Consorzio RFX signed the Tranfer of Right to Use in order to perform, for example, the commissioning activities.

The management of safety and the organization of personnel works on roster for the commissioning (SPIDER and MITICA) and experimental activities (SPIDER) prosecuted during the whole year.

Futhermore the NBTF Team guaranteed a continuous support in the management of the insulating SF6 Gas in order to fill and empty HV components for the HV acceptance test, also managing a contract of assistance with an external company expert on this kind of activities. In particular, Consorzio RFX accepted the responsibility of the HV tests of QST systems, from the safety point of view, through the appointment of the Responsible for the Test and the emergency coordinator and squads.

Finally, NBTF Team managed and performed activities on SPIDER plant system in order to guarantee the correct maintenance and intervention to solve troubleshooting and minor/major faults.

2.1.2. ***SPIDER***

2.1.2.1. SPIDER Beam Source

The delivery of SPIDER Beam Source (BS) occurred in October 2017 [4]. Then the BS was tested on-site and installed inside the Vacuum Vessel in February 2018 [5]. From April 2018 onwards, the BS was used for SPIDER integrated commissioning and experiments. Tests carried out at the end of 2018 highlighted that the pressure inside the vessel was a key factor to trigger electrical discharges around the rear side of the source; this prevented both the increase of performances and the simultaneous utilization of the four RF power supply circuits. Aiming to limit the gas pressure increase during SPIDER pulses, a mask was designed and installed downstream of the Plasma Grid, leaving only 80 apertures open among 1280. This change led to an increased ratio between gas pressure inside the source and outside the source. Limiting the latter under the critical threshold for discharges allowed to enlarge sensibly the operational space and the simultaneous use of RF generators.

The following main works and changes were carried out on the SPIDER BS during 2019:

---

[4] A. Masiello et al., “The fabrication and assembly of the beam source for the SPIDER experiment”, Fusion Engineering and Design, Volume 146 (2019) 839-844

[5] M. Pavei et al., “Spider beam source ready for operation”, Fusion Engineering and Design, Volume 146 (2019) 736-740

- Several inspections to the BS, identify possible damage and marks of arc discharges;
- Installation of a PG mask (80 apertures left open) to reduce gas conductance, so allowing beam extraction and acceleration w/o discharges;
- Final electrostatic shield installation, with adaptations of some parts to avoid interferences and to allow a smooth assembly;
- New thermocouples and signal boxes installed after damage during operation;
- Preliminary tests of PG thermal expansion in air up to 140°C;
- Connection of cooling plant to the Grounded Grid inlet/outlet, excluding the leaky GG4 segment;
- Procurement and installation of a thicker PG mask and pyrex; after this change up to about 6-8 minutes pulse length will be allowed during operations in 2020.

Pictures of SPIDER BS while applying some changes during 2019 shutdowns are shown in Fig. 2.4 and Fig. 2.5.

The tests and relevant activities carried out on the BS during 2019 required a huge amount of resources (engineers and technicians) competent on vacuum and hydraulic technologies,

Fig. 2.4 Installation of the final electrostatic shield around the BS

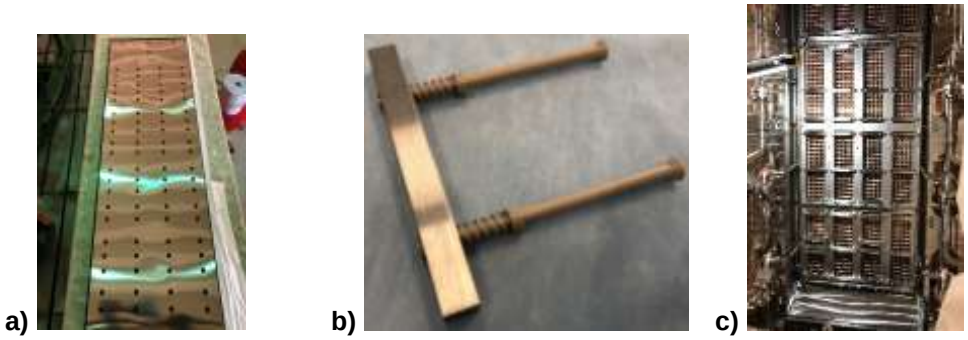

Fig. 2.5 a) The mask molybdenum plate 0.25mm thick; b) Pushers pressing the mask against Plasma Grid, acting from Grounded Grid side; c) View of the BS with pushers and mask installed (from GG side)

electrical insulation in air and in vacuum, radio frequency circuits, diagnostics, metrology and magnetic measurements. During the period of SPIDER operations a big effort was kept to investigate the issue of electrical discharges during pulses, both inside the BS and towards the vacuum vessel. Accurate measurements, monitoring and studies were performed investigating the effects of different RF parameters/configurations and of the hydrogen pressure inside the vacuum vessel. During short shutdowns, a lot of inspections and minor modifications were carried out, involving a high number of people.

In parallel to the activity and exploitation of the mask, temporarily solving the issue of the pressure, waiting for the necessary upgrade of the pumping system to be designed and put in place, a thorough assessment of the RF circuit was undertaken, ranging from the power supplies in the High Voltage Deck to the in-vacuum zone. With regard to the beam source itself, a revision of the RF driver configuration was assessed, which led to a set of modifications, in part already pre-tested in ELISE experiment at IPP, that was discussed among all stakeholders, approved, and will be put in place during the long shutdown in 2020, after completion of the procurements being set up.

One of the Grounded Grid segments (GG4) was non-conform in terms of vacuum sealing of the hydraulic circuit, so the procurement of a new replacing segment was agreed among IO, F4E and Consorzio RFX. Two different orders were placed in 2018 by Consorzio RFX: order n. 1 for manufacturing and tests of the Cu segment and order n. 2 for manufacturing and tests of two hydraulic manifolds to be connected to Cu segment. Both procurements were completed successfully during 2019. Completion of activities, welding the hydraulic manifolds to the Cu segment and executing the final vacuum leak tests, are foreseen on-site within Q1 2020, in time for GG4 replacing during SPIDER shutdown.

2.1.2.2. SPIDER Power Supplies and modeling

The SPIDER Power Supplies include the Ion Source Power Supply (ISEPS), hosted in a Faraday cage - called HVD (High Voltage Deck) - air insulated with respect to ground for -100 kV and the Acceleration Grid Power Supply (AGPS). A Transmission Line connects the HVD to the BS through the HV Bushing installed on the Vacuum Vessel (VV). A 3D view of the SPIDER layout is shown in Fig. 2.6.

AGPS has been procured by INDA, while all the other SPIDER PSs and auxiliary plants necessary to operate SPIDER have been procured by F4E. As of 2019, the SPIDER Power Supplies have been completely commissioned and used extensively during experimental sessions.

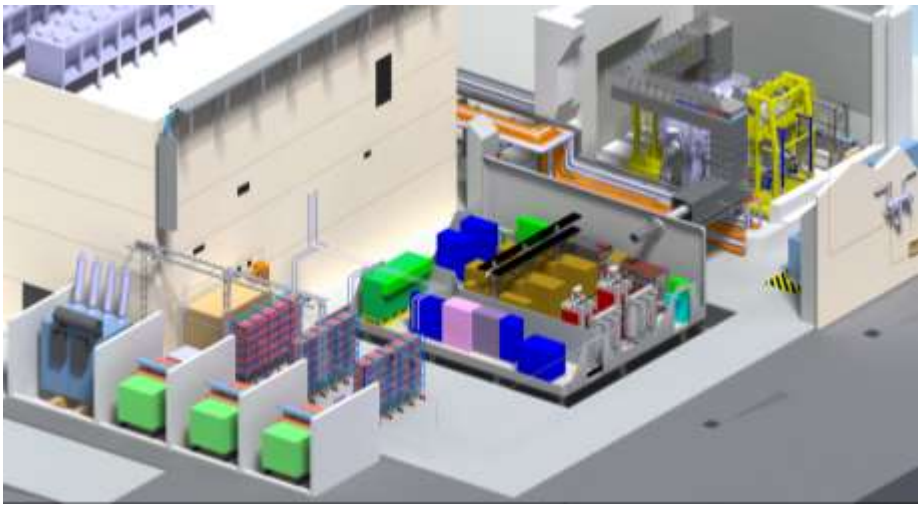

Fig. 2.6 3D view of SPIDER power supply system

Ion Source and Extraction Power Supply (ISEPS) system

ISEPS is in operation since 2017. In 2019 ISEPS has been extensively used in SPIDER experimental campaigns. Understanding, troubleshooting and optimization activities continued to reach a reliable operation. In particular, a large effort has been devoted to increase the maximum RF power delivered to the source with simultaneous operation of all 4 generators, enhancing the operational stability. Reliable recipes to operate up to 4x100kW have been developed.

On the plant, a rearrangement of ISEPS small power supplies has been performed to increase Bias and Bias Plate power supply voltage capability, while the ISEG output filter, after initial damage due to an unexpected additional RF current (see Fig. 2.7), has been modified and improved to withstand the additional dissipated energy coming from RF coupling phenomena.

Initial studies to get rid of the coupling and for other enhancements to the power supplies have started. In parallel, the activity on the modeling of the SPIDER power supplies progressed in particular for the improvement and validation of the RF circuit models, which took advantage from the availability of more experimental data. The performed activities included a review of the tetrode screen grid voltage limits and of the Screen-Grid-Control fault on SPIDER and analyses of SPIDER breakdown protections. The task of finding the best matching parallel capacitor maximising the

Fig. 2.7 Burning of filter resistors at ISEG output occurred, due to RF-induced currents

power exploitation of the RF generators has been first experimentally investigated mounting different capacitance values (5nF, 6.5nF, 10nF and 15nF) and then the findings have been used to assess and validate the models developed for the four configurations. Other relevant modelling activities concerned:

- development of a model to assess the efficiency of the radiofrequency power transfer to the SPIDER plasma;
- study of the operational envelope of the SPIDER RF oscillators;
- analyses on potential modifications of the SPIDER matching network to avoid frequency flips 6.

Further work has been devoted for estimating the maximum power achievable with the oscillators, with frequency control to improve matching after ignition.

Acceleration Grid Power Supply (AGPS) system

In 2018, the AGPS installation was finally completed and all pending non-conformities were solved. In 2019 the system has been integrated in the control system (Fig. 2.8) and then extensively used for SPIDER operations to extract and accelerate the beams. At the moment the system is certified to operate at reduced voltage, up to 30 kV. Discussions for definition of requirements have been performed in 2019 to launch the activity for modifying the circuit to extend the certification beyond 30 kV and up to 100 kV.

Fig. 2.8 Control room for SPIDER AGPS integrated commissioning performed in 2019

2.1.2.3. SPIDER & MITICA diagnostics

The first set of SPIDER diagnostics, delivered in 2018 under the first F4E procurement contract OFC-531-01, have been extensively exploited during the 2019 experimental campaigns, characterizing the source plasma and the accelerated beam.

Source emission spectroscopy comprises fast acquisition with photodiodes (10 kHz) of the absolutely calibrated Hα hydrogen line emission from each driver, particularly useful to

[6] F. Gasparini, et al., “An Eigenvalue Approach to Study SPIDER RF Oscillator Operating Space”, 2019 IEEE Pulsed Power and Plasma Science Conference (PPPS 2019), 23-28 June 2019, Orlando, FL, USA

assist operation[7], and 44 lines of sight, some through the drivers, others parallel to the grids, also absolutely calibrated; the signals are detected through either low or high dispersion imaging spectrometers, to measure the atomic Balmer series or the molecular Fulcher band and to monitor the presence of impurities, like Cu, O, OH, especially present soon after pumpdown. These measurements, available since beginning of SPIDER operation, have been analysed first using line ratios, then a Collisionaly Radiative model developed for this purpose by ISTP-Bari, to evaluate electron density and temperature, vibrational and rotational temperature and plasma composition. Plasma parameters uniformity across the large source and their variation with operation parameters like RF power or magnetic filter intensity were extensively studied.[8]

Other electrical source diagnostics installed in 2018 are source thermocouples and electrostatic probes, both suffering strong EM noise for several months, which prevented their effective use. Actually most MIC thermocouples melted in one shot because of high current induced by the RF circuit; they have then been replaced with kapton insulated thermocouples routed through a more carefully selected path, which still survive. For both diagnostics an unceasing analysis of the noise sources and test of potential remedial actions have eventually led to meaningful measurements. Thermocouples are now used for calorimetry, while electrostatic probes operate either in ion saturation current or scanning the full characteristic, providing electron density and temperature estimates near the grids.

More specific source diagnostics are laser absorption and cavity ring down spectroscopy (CRDS), to measure cesium and negative hydrogen density respectively. The former was installed in 2018 on the cesium test bed, where it has been operated throughout 2019, and will be moved to SPIDER in 2020.[9,10] CRDS has been procured and installed in 2019 within the second F4E procurement contract OFC-531-02; it will be commissioned early in 2020, before the first operation with cesium.

The main novelty in 2019 has been the exploitation of beam diagnostics: beam emission spectroscopy (BES) and visible imaging installed in 2018, the latter improved this year, towards the full tomographic system, and STRIKE partially installed, with one of the panels inside the vessel intercepting half of the beam. Tomography and STRIKE will be completed in 2020. They have provided meaningful measurements since the very first beam operation, proving good sensitivity even for a partial weak initial beam (see Fig. 2.9).

---

[7] R.Pasqualotto et al., Fusion Engineering and Design, 146 (2019) 709-713

[8] B.Zaniol et al., submitted to Review of Scientific Instruments

[9] M.Barbisan et al., accepted in Journal of Instrumentation

[10] M.Barbisan et al., Fusion Engineering and Design, 146 (2019) 2707-2711

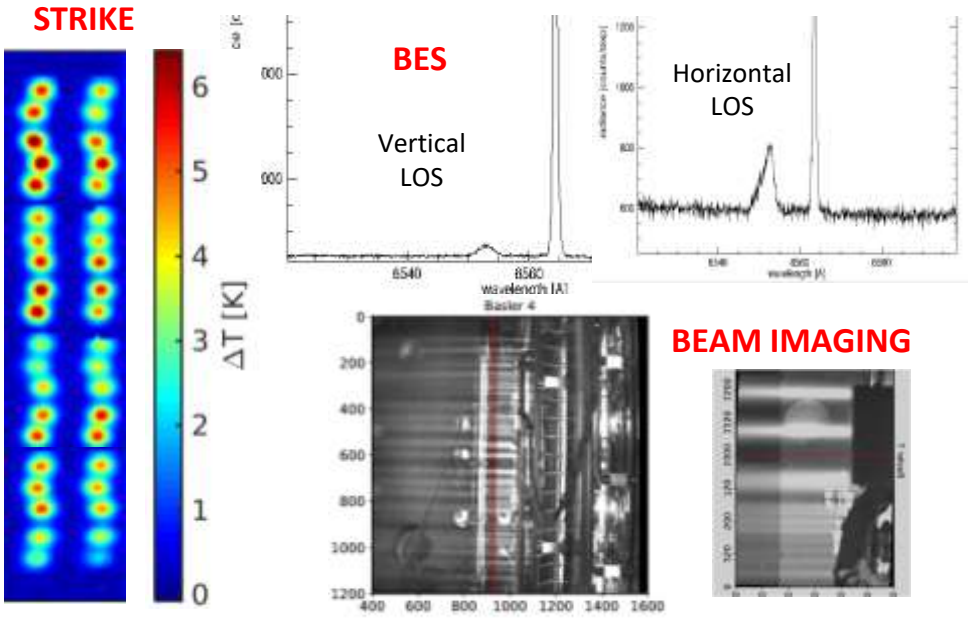

Fig. 2.9 Examples of beam measurements – STRIKE: half beam footprint on CFC-1D tiles measured with infrared thermography; BES: small high energy peak; Beam Imaging: trajectories of individual beamlets from two cameras.

The experience with the initial beam operation in SPIDER will be useful to decide which diagnostics to implement in the early phase of ITER injectors, whose calorimetry will likely be insensitive at the beginning.

Taking advantage of the mask between grids, which selects only 80 beamlets out of 1280, STRIKE can measure the footprint of each beamlet of the half intercepted beam, allowing estimates of beamlets divergence, deflection and shape.[11] The second panel will be installed by mid 2020. BES can estimate the divergence and the different aiming of beamlets covered by the same line of sight (LOS). Beam imaging is an online tool to assist operation; it also provides divergence and will be a training benchmark of tomographic inversions using the views from five installed cameras. The neutron imaging diagnostic has been installed and commissioned and is now being optimised in terms of signal to noise.[12,13]

The OFC-531-02 contract also includes three MITICA diagnostics:

- electrostatic sensor prototypes for the beam line components, produced in house this year

[11] A.Pimazzoni et al., submitted to Review of Scientific Instruments
[12] G.Croci et al., Fusion Engineering and Design, 146 (2019) 660-665
[13] A.Muraro et al., Nuclear Inst. and Methods in Physics Research, A 916 (2019) 47–50

Fig. 2.10 SPIDER operation managed from the control room

- fiber optic sensors to perform thermo-mechanical measurements on the beam line components, specified and ordered this year, to be delivered by mid 2020
- custom radiation-hard magnetic sensors, as prototypes for the ITER HNB, manufactured in 2019.

2.1.2.4. SPIDER CODAS, Central Interlock and Safety Systems

The development activity on the SPIDER CODAS, Central Interlock and Central Safety Systems was carried out in 2019 under the task orders #02 and #03 of the F4E framework contract on the NBTF control systems (F4E-OFC-280). In parallel to the development activity, much effort was devoted to the optimization of SPIDER CODAS and central interlock during SPIDER operation, by fixing progressively unavoidable software bugs and developing new tools for quasi real-time data streaming visualization, with the goal of a better interactive participation in the operation of scientists and operators [14].

A set of completion activities were executed, aiming to:

- install and make operational the SPIDER control room (see Fig. 2.10);
- develop, install and test the SPIDER central safety system15;
- optimize the management of the SPIDER power supply system;
- develop the control system of the SPIDER Caesium ovens;
- support data acquisition of the diagnostics in operation and under development.

The implementation of the SPIDER Central System required many efforts, especially in the test phase, due to the complexity of life cycle prescribed by the functional safety technical

[14] G.Manduchi et al, Fusion Engineering and Design, to appear

[15] A.Luchetta et al., Fusion Engineering and Design, 146 (2019) 246-249

standards IEC 61508 for electrical/electronic/programmable electronic systems and IEC 61511 for industrial processes. The safety instrumented system architecture was significantly expanded to manage a much wider input/output signal set (from about 270 to 450 signals) and cover additional risks; the Safety Instrumented Functions were redefined; the safety risk analysis was updated and the allocation of Safety Integrity Levels of the Safety Instrumented Functions was revised. The optimization of the management of the power supply systems was targeted to introduce high flexibility in switching on/off the single power supply units. The hardware of the control system of the Caesium ovens was procured, installed and tested, whereas the control programs are being developed. The site tests of the whole system including control software is scheduled for early 2020. The development of the data acquisition for the diagnostics was focused to the manufacturing design of the interface of the neutrons and cavity ring-down spectroscopy diagnostics and to support the development of the SPIDER tomography diagnostic.

2.1.2.5. SPIDER integration and commissioning

The SPIDER integrated commissioning continued in 2019 with the completion of the integration of the SPIDER AGPS with CODAS and Central Interlock System.

Activity was also carried out to integrate the electrostatic probe diagnostic system.

2.1.2.6. SPIDER experiments: main results and issues

SPIDER experiments resumed in April 2019, after a shutdown period to apply changes to the Beam Source and auxiliary systems that could allow reliable and effective SPIDER operation in 2019. Three experimental campaigns were performed and the preparation for a fourth one will be completed by December 2019:

- investigation of single RF circuits;
- first characterisation of source and beam with no caesium;
- investigation of simultaneously operating RF circuits;
- characterisation of the source by electrostatic sensors (under preparation).

SPIDER is a key asset in the development of the negative-ion beam source for ITER. For the first time the vacuum-insulated concept is fully applied to an ion source for fusion: the multi-aperture multi-electrode electrostatic accelerator and the RF-driven plasma source (at high voltage) are completely contained in the same vacuum as the beam drift region (see Fig. 2.11).

Electrical insulation from the vessel is achieved by maintaining a sufficiently low gas pressure. Unlike the other existing prototype sources for fusion applications, SPIDER allows

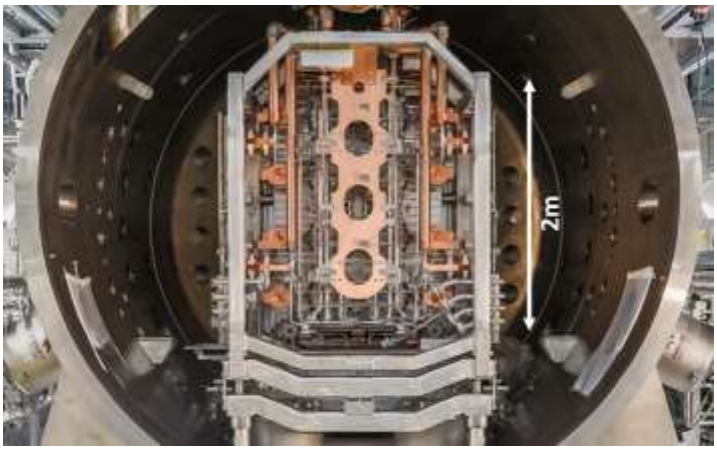

Fig. 2.11 Rear view of SPIDER beam source inside the vacuum vessel

to develop procedures and technical solutions that are specific of this vacuum-insulated concept. In this sense, during the first year of operation, the experimental activities addressed a pressing issue related to electrical insulation in the presence of RF fields, a condition that is more difficult than in steady state. More than one year after the first plasma was ignited and after a large effort dedicated to the commissioning of diagnostics and to the optimisation of the RF generators, SPIDER routinely operates the negative-ion beam produced in the plasma volume. Presently, the experimental work focusses on concluding the commissioning and on improving the reliability of all SPIDER plants, in view of caesium operation. The vacuum-insulated source concept indeed does not allow accessing any part of the beam source for maintenance or mechanical improvements, without breaking the same vacuum in which the caesium layer is being built-up and conditioned for negative ion production.

During SPIDER operations in 2018 an issue regarding the occurrence of RF-induced discharges on the rear side of the beam source emerged, which impeded simultaneous operation of all RF drivers as well as the operation above a total RF power of ~100 kW. It was recognised that above a vessel pressure of 40 mPa the probability of discharges quickly increases; such a pressure corresponds to only 0.1 Pa inside the ion source [16]. In parallel to the definition of a long-term major modification of SPIDER pumping system, it was decided to carry on with the experimental programme, upon reducing the gas conductance between the source and the vessel by installation of a mask on the downstream side of the plasma grid provided with 80 apertures (out of 1280).

SPIDER operations resumed at mid-April 2019. As of 2019 most of SPIDER diagnostic systems were operating: the list of source diagnostics includes source emission

[16] G. Serianni et al., “SPIDER in the roadmap of the ITER neutral beams”, Fusion Engineering and Design, Volume 146 (2019) 2539-2546

spectroscopy, surface and calorimetry thermocouples, H_α detectors, visible cameras and electrical measurements at the various power supplies. The operating diagnostic systems allowed the measurement of the plasma and beam parameters in different experimental conditions, which can be explored even within single pulses, thanks to the very flexible SPIDER control system.

A first characterisation of the RF circuits was carried out in parallel to the implementation of a feedforward control of the internal capacitors of the RF generators and to the development of a model reproducing the behaviour of the RF system. The experiments focussed on the parallel capacitance of the matching network, after the temporary installation of different capacitors on the 4 circuits (5nF, 6.5nF, 10nF, 15nF). The experiments confirmed the presence of hysteresis resulting in a "forbidden" region of frequencies (unfortunately the optimal frequency for transfer of RF to the coils lies in this region) and provided a benchmark for the numerical simulations of the RF circuits. Thus it was possible to thoroughly assess the features of the generators, although in single-generator operation only, so as to attain an RF power per generator up to 125-145 kW (depending on the generator). Based on this campaign and on the numerical codes, it was subsequently possible to simultaneously and reliably operate the 4 RF generators up to 100 kW per generator, after restoring the original 10nF parallel capacitance of all matching networks. Increasing the RF power above that value will be the subject of further investigations. Reference pulses were identified for different experimental conditions, in terms of RF power, magnetic filter field intensity and source pressure.

As for the characterisation of the ion source [17], signals from H_{alpha} detectors and emission spectra indicate that, both in the drivers and close to the plasma grid, plasma emission increases with RF power; moreover the plasma completely fills the drivers and the expansion chamber.

The ratio between H_{gamma} and Fulcher band seems to increase with the RF power (see Fig. 2.12), suggesting a corresponding increase of the dissociation degree of hydrogen.

The rotational temperature of the hydrogen molecules increases with RF power and gas pressure. No major influence of electron and beam extraction on the plasma surrounding the plasma grid is suggested by spectroscopy (but it shall be remembered that no caesium has been used in SPIDER to enhance the negative ion amount yet). The magnetic filter field was found to affect the plasma even far away from the plasma grid (see section 2.1.4.1); the light

[17] B. Zaniol et al., First measurements of Optical Emission Spectroscopy on SPIDER Negative Ion Source, presented at ICIS2019, submitted to Rev. Sci. Instrum.

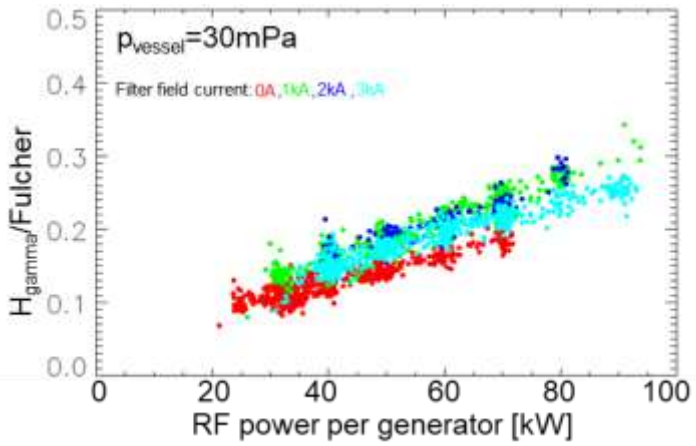

Fig. 2.12 Ratio of H_{gamma} and Fulcher brightness versus RF power for different values of the magnetic filter field current.

emitted by the plasma reaches a maximum for a certain value of the filter field current, depending on pressure and RF power, and decreases for larger values (at low RF power the plasma can be even switched off for large filter field). This evidence was ascribed to the specific topology of the magnetic filter field, which features magnetic field lines intersecting the walls of the RF drivers, thus distorting the electron trajectories, as confirmed by the increase of the heat deposited onto these surfaces as the filter field increases. The magnetic configuration will be improved in the future.

The first negative ion beam was extracted from the SPIDER ion source and accelerated at the end of May 2019 [18]. The signature of the negative hydrogen beam can be clearly seen by the light emitted when the beam interacts with the background gas (see Fig. 2.13). A first characterisation was performed of the beam features and of the amount of co-extracted electrons. The bias voltages applied to the plasma grid and to the bias plate were found to reduce the amount of co-extracted electrons; combinations of the two voltages were tested and the condition in which one is more positive than the other seems more effective. The magnetic filter field was found to selectively reduce the amount of co-extracted electrons with respect to the negative ions.

The SPIDER beam features can be studied by means of several diagnostic systems: apart from the electrical measurements provided by the power supplies, dedicated diagnostics include visible cameras, beam emission spectroscopy and the STRIKE diagnostic calorimeter. An emittance scanner is also under preparation.

[18] G. Serianni et al., “First operation in SPIDER and the path to complete MITICA”, presented at ICIS 2019, submitted to Rev. Sci. Instrum.

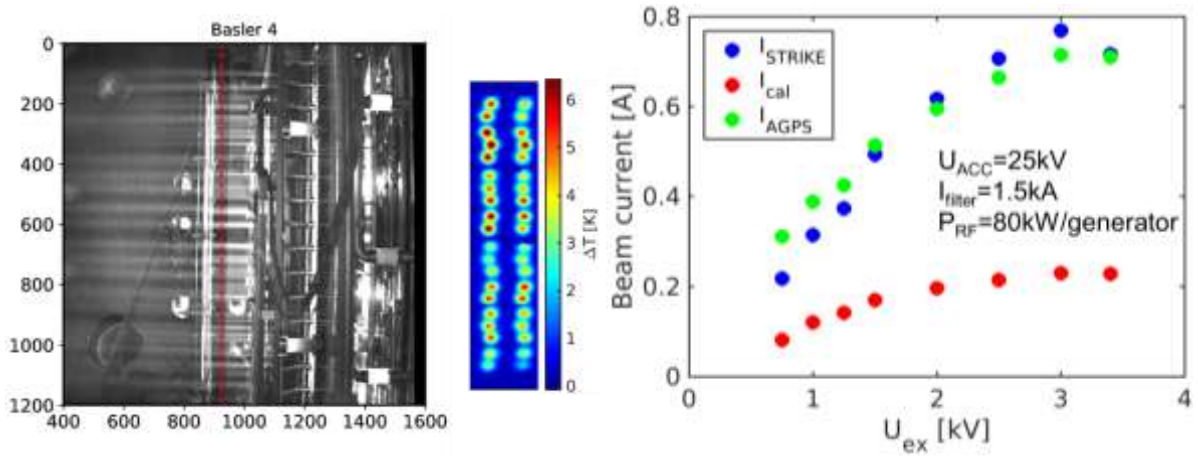

Fig. 2.13 Image of the beam provided by the visible camera (left); footprint of the beamlets onto the STRIKE tiles (right).

The electrical measurement of the beam current at the accelerator power supply and the electrical current collected by STRIKE were found to be comparable and to increase with the extraction voltage. The negative ion flux measured calorimetrically at STRIKE exhibits a similar trend, but the equivalent current is a factor of 2.5 lower than the electrical current; this is common evidence: the electrical current usually exceeds the calorimetrical estimate since the latter is not affected by secondary electrons.

The installation of the plasma grid mask in SPIDER leaves only isolated beamlets, for a total number of 80 beamlets out of 1280. This configuration of the accelerator gives a unique, albeit temporary, opportunity for the detailed investigation of the beamlet properties. The beam divergence can be measured in SPIDER by several diagnostic systems. Many visible cameras are installed on the vacuum vessel in different positions and with different field of view; the Doppler-shifted light emitted by the beam particles is measured by beam emission spectroscopy along several lines-of-sight; the STRIKE calorimeter records the thermal footprints of the single beamlets on the CFC tiles [19] (see Fig. 2.13). Similar values of the beamlet divergence, down to 20-30 mrad, were estimated by the various beam diagnostics and the same dependency on the extraction voltage was found.

A system of electrostatic sensors is being installed inside the SPIDER vessel to characterise the source features. The system will involve: planar Langmuir probes in the single-probe configuration (to deduce the plasma parameters); Mach probes (to study the plasma flows and drifts); retarding field energy analysers (to study the probability distribution function of the various particles). Commissioning of the system is planned in December 2019.

[19] A. Pimazzoni et al., “Assessment of the SPIDER beam features by diagnostic calorimetry and thermography”, presented at ICIS 2019, submitted to Rev. Sci. Instrum.

2.1.3. *MITICA*

2.1.3.1. MITICA Vacuum Vessel

The MITICA Vacuum Vessel (VV) is composed by three main parts: the VV support structure, the Beam Source Vessel (BSV) (containing the Beam Source and connected to the PS Transmission Line) and the Beam Line Vessel (BLV) (containing the Beam Line Components). The main characteristics are shown in Fig. 2.14. The procurement contract is on-going since January 2015 and the Supplier is De Pretto Industrie (I). The MITICA VV support structure and the Rear Lid Handling System were already manufactured, installed and tested on-site in 2017. The BSV, manufactured and tested at the factory during 2018, was finally installed and tested inside the MITICA Neutron Shield during 2019, as shown in Fig. 2.15.

As regards the BLV the final machining of all the parts, accurate finishing of critical surfaces for vacuum tightness and thorough cleaning were carried out in 2019. After positive dimensional tests carried out at the factory in Oct/Nov 2019, the BLV is ready for vacuum leak tests at the factory, foreseen by the end of 2019 and January 2020. Pictures of BLV at the supplier's factory are shown in Fig. 2.16. BLV delivery on-site is presently expected by mid January 2020; installation and tests on-site will follow according to the overall MITICA schedule.

All these activities and relevant milestones, both for BSV and BLV, were carefully controlled and verified in order to get an armonized and integrated schedule for MITICA Injector and auxiliaries, considering the parallel on-going activities at PRIMA site for integration and tests of auxiliaries and power supplies.

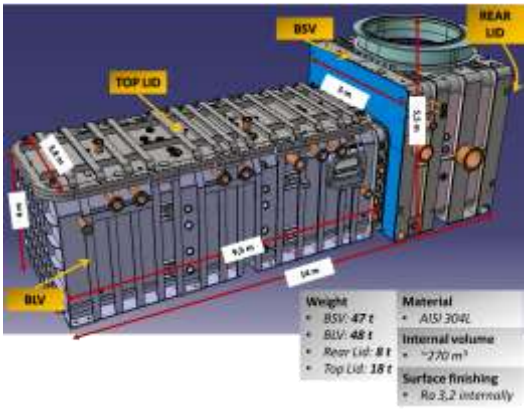

Fig. 2.14 CAD view and main characteristics of MITICA VV

Fig. 2.15 BSV installation inside the MITICA Neutron Shield

The NBTF Team guaranteed the technical follow-up during 2019. Frequent meetings and inspections at Supplier's premises were carried out for continuous verifications and support during machining, cleaning and tests. In particular specific support was given by NBTF metrology and vacuum teams during installation and tests of BSV on-site. Review of documents and drawings for BSV and BLV were also performed, and support was given for re-organization and updating of the supply quality documents.

Fig. 2.16 BLV machining and preparation for vacuum leak tests at the factory (pictures taken in De Pretto Industrie)

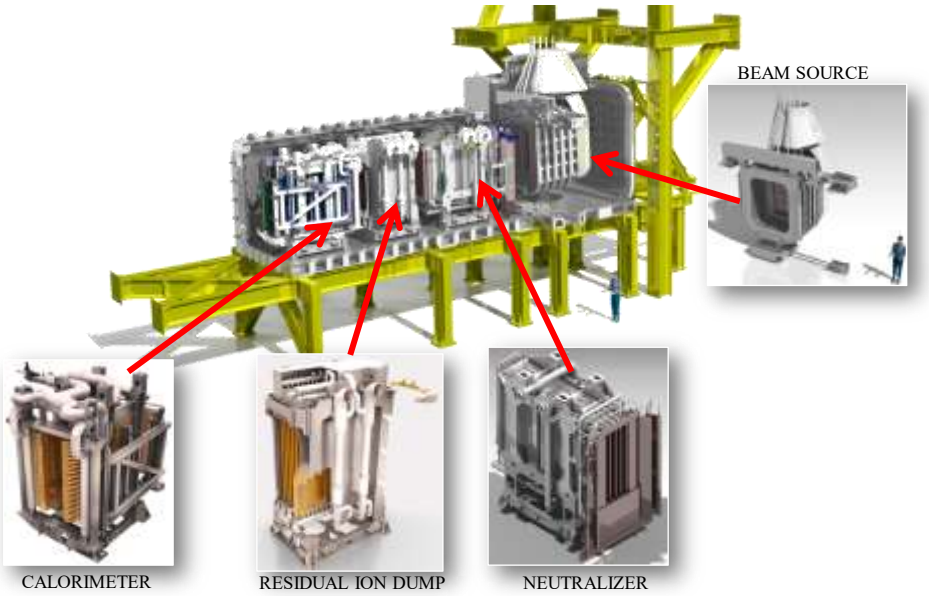

Fig. 2.17 CAD section view of the MITICA Injector with Beam Source and Beam Line Components

2.1.3.2. MITICA Beam Source

The main in-vessel components of MITICA Injector are shown in Fig. 2.17. All these components are actually full size prototypes of the ones to be manufactured and installed on the ITER Heating Neutral Beam Injectors. Procurements for manufacturing and tests of all these components are on-going.

The MITICA Beam Source is the key component for Negative Ion Beam generation and acceleration. The negative ion beam will be generated and extracted by a RF plasma source operating at an applied electric potential of about −1 MV. Five additional acceleration grids (AG1, AG2, AG3, AG4, GG) at intermediate electric potential increasing by 200 kV steps, are located downstream the RF source, thus constituting a 5-stage electrostatic accelerator (see Fig. 2.18 and Fig. 2.19).

The procurement strategy for MITICA Beam Source (BS) manufacturing consists in a framework contract divided in three specific stages: stage 1 is the baseline design review, stage 2 is the MITICA Beam Source procurement and stage 3 is ITER HNB Beam Source procurement. Stage 2, assigned to Alsyom-Seiv, started in October 2018.

In 2019 the supplier set up the organization of the procurement, signed the contracts with all major sub-suppliers, prepared documentation to pass Manufacturing Readiness Review for a good part of the source subsystems and started to produce some prototypes.

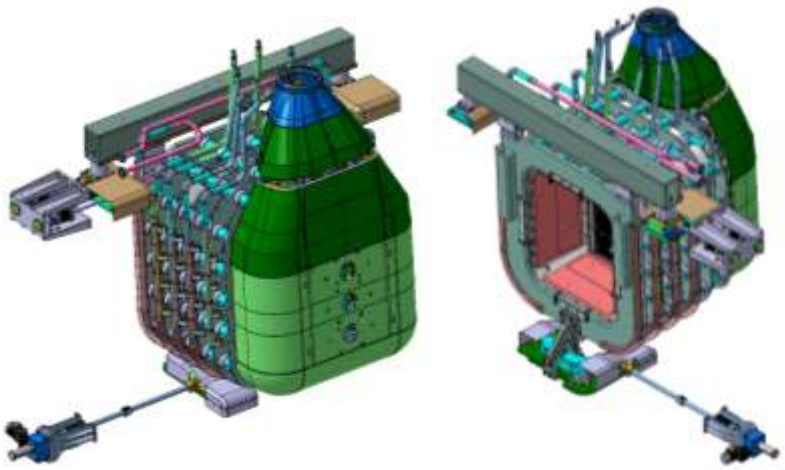

Fig. 2.18 CAD views of the MITICA Beam Source

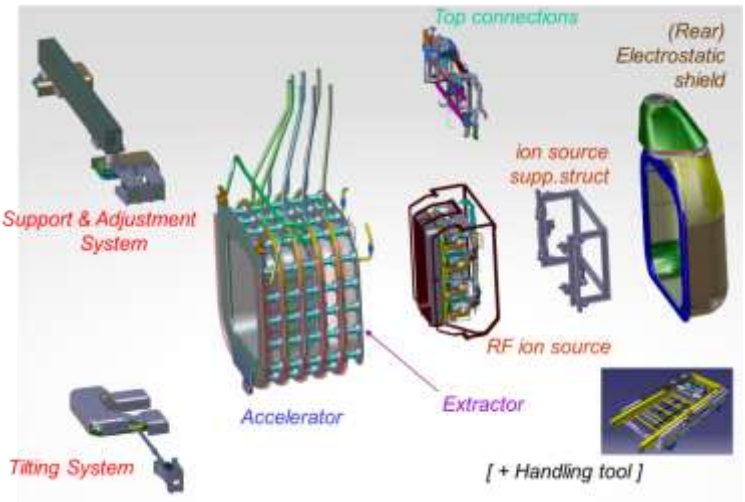

Fig. 2.19 CAD exploded view of the MITICA Beam Source

NBTF Team provided feedback and technical support for discussions and review of technical/quality documents submitted by the supplier, and attended several meetings, both for formal progress and for technical follow up of manufacturing advancement or prototype tests. Fig. 2.20 shows some pictures of the prototype of AG4 acceleration stage during manufacturing, assembly and mounting on the BS Assembly Tool. Factory tests were completed in December 2019.

2.1.3.3. MITICA Beam Line Components

Three Beam Line Components are foreseen downstream the Beam Source, as shown in the previous Fig. 2.17. The negative ion beam generated by the Beam Source at 1 MeV, after passing through a gas cell Neutraliser and an Electrostatic Residual Ion Dump (RID), shall produce a ~17 MW D^0 or H^0 neutral beam focused onto a target Calorimeter for a duration up to 3600 s.

Fig. 2.20 Pictures of the prototype of AG4 acceleration stage manufactured and tested at the factory

A two stages contract was launched in 2018: Stage 1 for baseline review, Stage 2 for MITICA BLCs procurement. Three different competitors were awarded for Stage 1 activities that were completed in 2018.

Issue of Call for tender, tender evaluation and awarding of Stage 2 were carried out during 2019. Technical support was guaranteed by NBTF Team devoting a substantial amount of resources for review/update of several documents and drawings, preparation of Call for Tender documents and finally for tender evaluation.

The BLCs contract was awarded to the Spanish company AVS–Tecnalia in December 2019 and the procurement activities will start in January 2020.

2.1.3.4. Cryogenic Pumps

Two large Cryogenic Pumps will be installed inside the MITICA Beam Line Vessel to guarantee proper vacuum conditions inside the vessel during MITICA operation (see Fig. 2.21). The Cryopumps are based on adsorption pumping by charcoal coated cryopanels (CPs), 8 m long, 2.8 m high and 0.45 m deep, operated between 4.5 K and 400 K. These cryopanels are surrounded by a Thermal Radiation Shield (TRS) operated between 80 K and 400 K. The CPs will be at the lower temperatures during normal operations, while 100 K or 400 K will be achieved during periodic pump regenerations necessary to remove from the

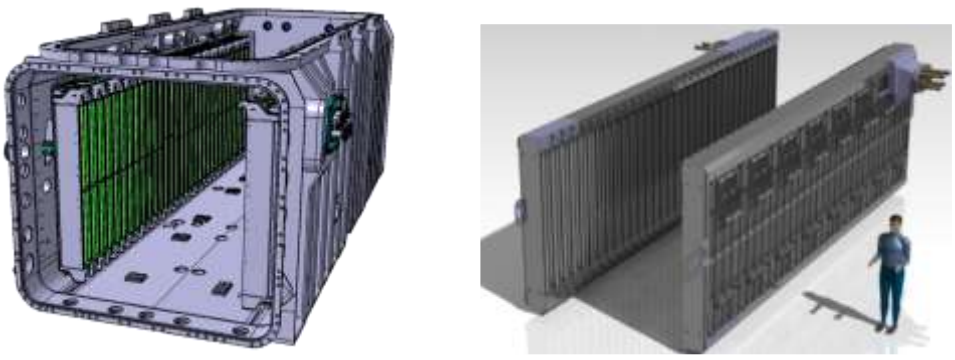

Fig. 2.21 CAD Views of MITICA Cryogenic Pumps

Fig. 2.22 Pictures of extruded aluminium profiles and charcoal coating process for MITICA Cryopumps

CPs the adsorbed gas (H_2 or D_2). The pumping speed estimated for the two pumps operating in parallel are 5000 m^3/s for H_2 and 3800 m^3/s for D_2.

The complex procurement of Cryopumps is subdivided into three lots, corresponding to specific kowledge and expertise of different suppliers: Lot 1 for support frame and assembly, Lot 2 for expansion profiles and Lot 3 for charcoal coating of pumping surfaces.

The contract for procurement was awarded in 2018 and the procurement activities are on-going. During 2019 technical follow-up was carried out by NBTF Team to support F4E during the procurement phases. In particular material purchase and specific manufacturing processes and prototypes for qualification were thoroughly discussed.

Some technical issues regarding the qualification of hydroforming process for Cryopanels, charcoal coating and surface finishing are presently creating problems and delays on procurement, requiring careful follow-up. Some pictures showing prototypes for process qualification are shown in Fig. 2.22. Further activities were performed in 2019 to complete the design of the Cryopump Assembly Tool that will be necessary for the installation of Cryopumps inside the MITICA VV. The development of a detailed assembly sequence, of the Assembly Tool design (see Fig. 2.23) and of Technical Specification for procurement were carried out. These activities have been managed by NBTF Team and carried out with the support by CCFE as third part under the Work Programme WP2019.

2.1.3.5. Cryogenic Plant

The MITICA Cryogenic Plant is designed to produce supercritical Helium (ScHe) at 4.6K and gaseous Helium (GHe) at 81K and to feed these cryogenic fluids respectively to the cryosorption panel (CP) and to the thermal radiation shield (TRS) assemblies of the cryopumps. The expected heat loads to be removed in pulse-on scenario are 800 W on CP and 17.4 kW on TRS assembly. The same plant shall also manage the regeneration of Cryopumps at different temperatures.

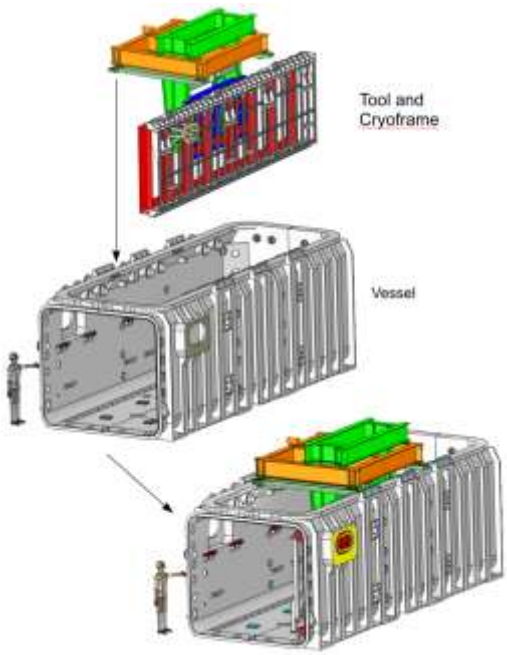

Fig. 2.23 CAD view of the MITICA Cryogenic Pumps Assembly Tool

The procurement contract for MITICA Cryogenic Plant was launched in September 2016 and the supplier is ALAT (Air Liquide Advanced Technologies). All the equipment, components, warm lines and cryo lines, sensors, electrical boards and cabling have been delivered and installed in 2019. After completion of assembly, commissioning started in Q3 2019 and is going to be completed within the year.

The NBTF Team guaranteed the technical follow-up during 2019. Frequent meetings were necessary for continuous verifications and support during on-site installation activities. Reviews of several documents submitted by the Supplier were also performed.

Some additional activities of NBTF Team were devoted to the follow-up, monitoring and maintenance/repair of the auxiliary cooling system for He compressor, solving some critical issues occurred during the commissioning phase of the plant.

Development of control system and integration with CODAS are on-going. Site Acceptance Tests and training of NBTF personnel are foreseen within Q1 2020. Picturea of the Cryogenic Plant installation are shown in Fig. 2.24.

2.1.3.6. MITICA Conversion system (AGPS-CS, ISEPS, GRPS)

The MITICA Conversion system includes all the power supplies necessary for the operation of the MITICA experiment, excluding the components for the generation of the High Voltage, i.e. the AGPS Conversion System (AGPS-CS), the Ion Source and Extraction Power Supplies (ISEPS) and the Ground Related Power Supplies (GRPS). Substantial progress in

Fig. 2.24 Pictures of MITICA Cryogenic Plant components and piping inside Building 2

the installation and commissioning of these power supplies has been made. NBTF Team supported all the involved companies during the design, factory tests and activities at Site.

In the following, the progress achieved in 2019 for each subsystem is described.

The MITICA AGPS Conversion System

The AGPS is a special conversion system feeding around 60 MW at -1MV dc to the acceleration grids, and able to interrupt the power delivery in some tens of microseconds in case of grid breakdown, which is a condition expected to occur rather frequently during a pulse.

The ITER AGPS reference scheme consists of an ac/dc stage feeding five three-phase inverters, each connected to a step-up transformer feeding a diode rectifier and a DC filter. The rectifiers are connected in series at the output side to obtain the nominal acceleration voltage of -1 MV dc, with availability of the intermediate potentials.

The AGPS-CS includes two step-down transformers, the ac/dc converter, the dc/ac inverters and the control system. In 2018 the installation and commissioning of the system have been completed[20]. In 2019 the activity progressed on the review of the documentation to achieve the Authorization for Use, which has been obtained in December. In parallel, activities for the integration of the system with CODAS have been launched, and integration tests started in late 2019. The design and procurement of the Voltage Ringing Filters (VRFs), necessary to mitigate the overvoltage at the input of the AGPS-DCG, has been also launched, and the installation has been completed in 2019 (see Fig. 2.25).

[20] L. Zanotto et al., “Acceleration grid power supply conversion system of the MITICA neutral beam injector: On site integration activities and tests”, Fusion Engineering and Design, Volume 146, Part B, September 2019, Pages 2238-2241

Finally, discussions with QST have started in late 2019 to prepare the AGPS-CS for integration with AGPS-DCG and Transmission Line, to be performed in early 2020.

Fig. 2.25 AGPS-CS ringing filters installed in 2019

The MITICA ISEPS

The ISEPS design adaptation to MITICA were completed in 2017. In 2018, the follow-up of the contract progressed up to the positioning of the equipment inside HVD1. In 2019, the bulk of the installation activities took place and finally the installation phase has been completed. Initial commissioning started in late 2019 and will continue and finish in 2020.

The MITICA GRPS

The MITICA GRPS is actually composed by the Residual Ion Dump (RID) power supply only. This power supply has to provide an average voltage up to 25 kV, plus an ac low-frequency voltage component with maximum amplitude of 5 kV, to spread the power deposited over the RID plates. The nominal output current is 60 A, and the maximum pulse duration is 1 hr. The selected topology is the Pulse-Step-Modulator (PSM), including a multi-winding dry transformer and 42 water-cooled switching power modules, connected in series at the output.

In 2018, on-site installation of the system was completed (see Fig. 2.26). In 2019, the follow-up of the contract with OCEM progressed with completion of the commissioning activities and the review of the documentation. In late 2019 the training on-site has been performed and the system is now going to be transferred to Consorzio RFX for use.

Fig. 2.26 Picture of the GRPS installed inside Building 3

2.1.3.7. MITICA HV Components and insulating tests

The installation activities of JADA HV components started in December 2015 and continued till the first half of 2018. In June 2018, after completion of installation activities and preliminary checks and verifications, the HV components have been tested with the following insulating tests:

- 1.2 MV dc for 1 hour
- 1.06 MV dc for 5 hours, followed by five fast ramps up to 1.26 MV

Tests were successfully passed in November 2018. A second set of HV tests have been performed in order to test the TLs. Also in this case the test was successfully passed.

In 2019 the installation of all DCG components, the 1MV insulating transformer and Transmission Line (TL) have been completed. It also included the HV Bushing interfacing BSV and TL and the last piece of TL. In July 2019 the 1MV insulating transformer has been successfully tested in a combined test with the HVD1. In September 2019, the first attempt to test the last part of TL and HVB failed at 900 kV due to a fault in the Testing Power Supply (TPS). After TPS troubleshooting and repair, the test was repeated and passed in November[21]. In Fig. 2.27 some pictures are shown, taken during installation of HV Bushing, TL3 bend (last piece of TL) and Short Circuit Device inside the Beam Source Vessel. Concerning the HVD1, the system was transferred for use to RFX in 2019, and the Site Tests were successfully performed in July[22]. The HVD1 was subject to the following insulating test voltage patterns:

- -1.2 MV for 1h on Insulating Transformer (via HVD1)
- -1.06 MV for 5h on HVD1 + Insulating Transformer
- 5 final pulses from -1.06 MV up to -1.265 MV

HVD1 is now accepted. HV equipment is ready for the final integration with the AGPS conversion system.

2.1.3.8. MITICA I&C

The activity on MITICA Instrumentation and Control (I&C) was carried out within the F4E 2019 Work Program until the autumn. Subsequently, the activity was passed under the task order F4E-OFC-280-04 that was signed in July 2019 (entered into force in autumn) to develop MITICA CODAS and procure the I&C equipment needed for the integrated commissioning of the MITICA power supply systems. Significant activity was required to prepare the requirement documents for launching the task order F4E-OFC-280-04, including MITICA plant control CODAS (interface with AGPS, ISEPS and GRPS) and the plant operation and time communication networks. To this end, two meetings were carried out in spring with IO and F4E to define the ITER requirements for the MITICA I&C.

The activities performed in 2019 were targeted to:

---

[21] M. Kashiwagi et al., “Achievement of DC 1 MV Insulation in High-Voltage Power Supply for ITER Neutral Beam Test Facility”, 14th International Symposium on Fusion Nuclear Technology, Budapest (Hungary), 22-27 September 2019.

[22] M. Boldrin et al., “The High Voltage Deck 1 and Bushing for the ITER Neutral Beam Injector: Integrated design and installation in MITICA experiment”, Fusion Engineering and Design, Volume 146, Part B, September 2019, Pages 1895-1898

a)  b) 

c)  d) 

Fig. 2.27 a) Installation of HV Bushing over the BSV; b) Installation of TL3 bend; c) and d) Installation of Short Circuiting Device (SCD) inside the BSV

- develop the interface with MITICA/Shared Cooling and Gas and Vacuum Systems;
- develop the interface with the MITICA Cryogenic System;
- prepare miniCODAS and miniInterlock, the CODAS and interlock test instrumentation, for the site acceptance tests of MITICA ISEPS, Cooling, and Cryogenic System;
- procure the provisional MITICA HNB plant interlock system to carry out the power supply integration in the next year.

2.1.4. *ITER Neutral Beam Injector Physics*

2.1.4.1. Beam physics simulations and benchmarking in support to the design and operation of SPIDER and MITICA - Magnetic configuration of BS

Effect of PG and EG geometry and magnetic configuration on beamlet divergence: comparison of NITS experiments at QST and BUG experiments at IPP

In Jan-Feb 2019, an investigation was started in order to understand the reason for the large difference of beamlet divergence experimentally found between experiments on NITS (Negative Ion Test Stand) at QST and experiments having similar parameters on BUG (BATMAN UpGrade) experiment at IPP. The different magnetic field configuration and/or some small differences in the Plasma Grid and Extraction Grid geometry were considered among the possible causes of this mismatch. To this purpose, detailed numerical models of NITS device and BUG device were set-up using both SLACCAD and OPERA. The comparison of the beamlet divergence of both devices carried out by numerical simulations showed that the difference could not be attributed to differences in the geometry or in the magnetic field configuration.

Participation to Joint experiments on the Megavolt Test Facility (MTF) at QST and benchmark of beam optics and heat loads codes

During May and June, Consorzio RFX personnel participated to collaborative experiments carried out at the QST lab in Naka on the MTF (Megavolt Test Facility) facility with voltage applied up to 500 kV (3 stages), long-pulse (100 s) and high current (190 A/m^2). The beam optics simulation models previously prepared by Consorzio RFX (beam optics with SLACCAD, OPERA, vacuum pressure profile with AVOCADO and COMSOL, power loads on grids with EAMCC) have been benchmarked against the MTF experimental results (currents and thermal power deposited on grids and IR image on CFC target) also using the models developed during the previous NITS joint experiments.

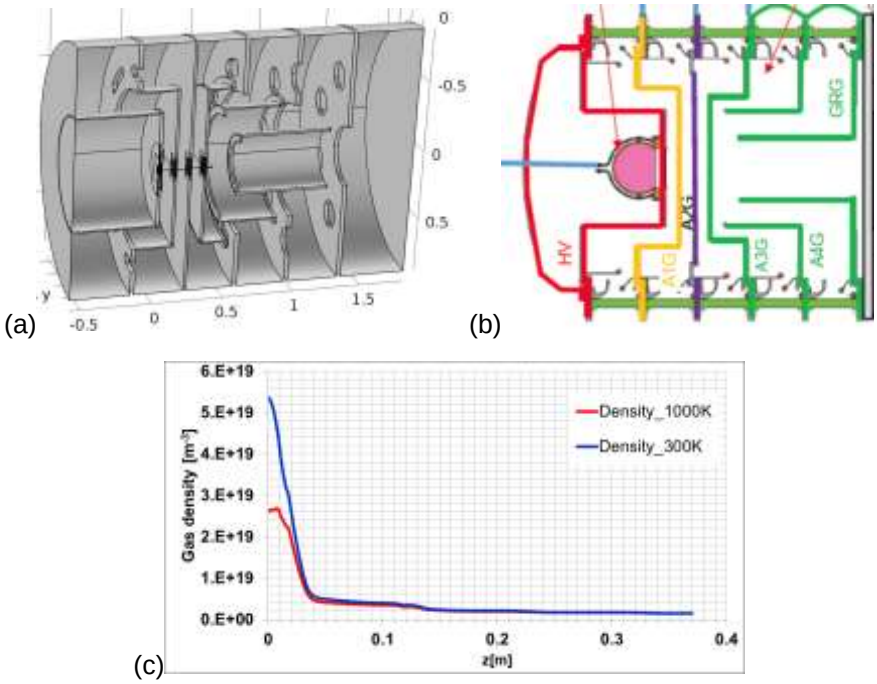

Fig. 2.28 a) and b): accelerator geometry used for accurate gas density calculation, c) Gas density profile as obtained from the COMSOL model for a source pressure of 0.24 Pa.

A good agreement was found concerning the beam optics and the evaluation of additional beamlet deflection due to asymmetry of the extracted current density at the meniscus. Considerable improvements were obtained in the accuracy of the numerical model describing the gas flow and the gas pressure profile in the accelerator (Fig. 2.28)

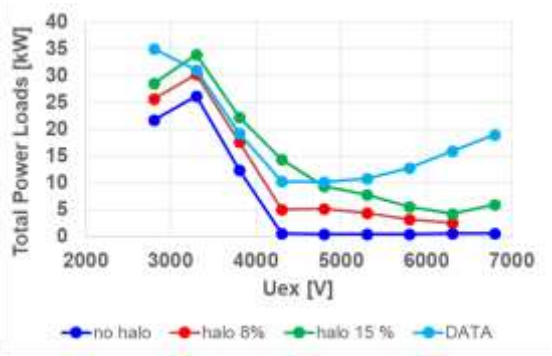

Fig. 2.30 Total heat load measured by water calorimetry in MTF as a function of the extraction voltage Uex, compared with corresponding heat load calculated using EAMCC3D.

However, the comparison of thermal power deposited on grids, measured by water calorimetry during the MTF experiments, indicated that the power load due to stripped electrons (and maybe also due to negative ions) during experiments is considerably larger than the heat load calculated using EAMCC3D numerical models, under corresponding beam optics conditions (see Fig. 2.30).

This is true even assuming a large beam halo current fraction (see Fig. 2.29). Additional interpretations have been developed to explain this power mismatch, however a fully consistent explanation has not yet been found.

<u>Experimental and numerical investigation on the asymmetry of the current density through meniscus</u>

Based on the analysis of thermal images of the beamlets on CFC target during the Joint experimental campaigns on NITS (QST lab. Naka) in 2016-2017, an empirical scaling law was found describing the asymmetric distribution of negative ion current density extracted at the meniscus. This empirical scaling law can describe the current density distribution at the meniscus as a stepwise function of the transverse magnetic field at meniscus, according to

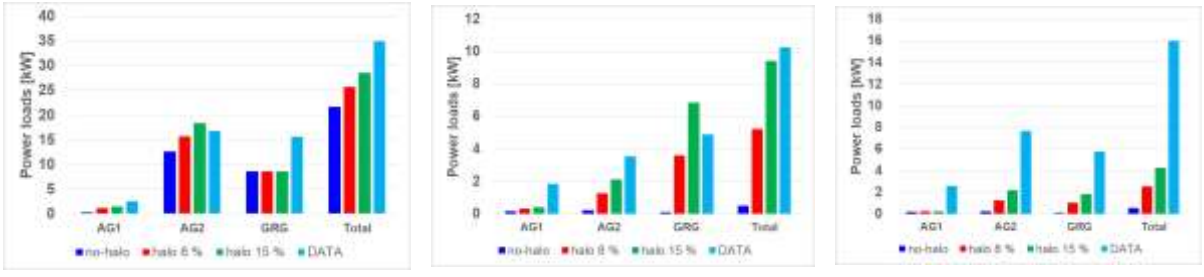

(a) (b) (c)

Fig. 2.29 Experimentally measured and calculated heat loads on accelerator grids for 3 different operating conditions: (a) U_{ex} = 2.8 kV; (b) U_{ex} = 4.8 kV; (c) U_{ex} = 6.3 kV. The effect of different halo fraction assumptions (respectively 0%, 8% and 15%) in the simulations is also shown.

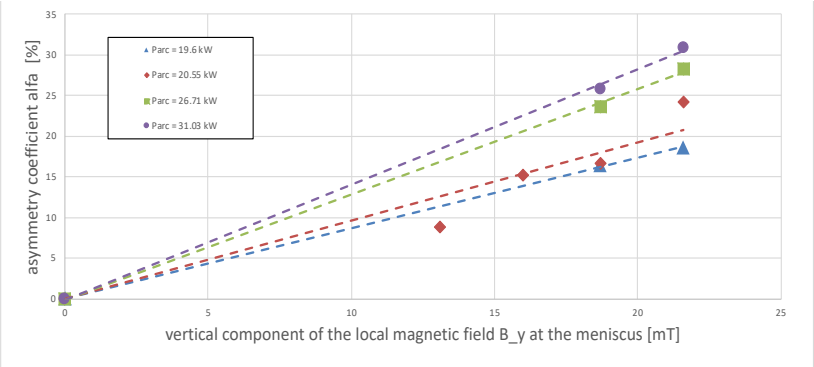

Fig. 2.31 Asymmetry coefficient α_{unb} of the current density at meniscus obtained from a analysis of the Joint experiments (2016-2017) on the NITS accelerator; the asymmetry coefficient α_{unb} is well fitted by a linear function of the vertical magnetic field component B_y at the meniscus.

the equations:

- $\begin{cases} j_{left} = (1 + \alpha_{unb}) j_{tot} \\ j_{right} = (1 - \alpha_{unb}) j_{tot} \end{cases}$

where the asymmetry coefficient α_{unb} appears to be linearly dependent on the transverse magnetic field By at the meniscus (for a given value of the Kamaboko arc power), as shown in Fig. 2.31.

Two Particle-In-Cell (PIC) models of the Kamaboko plasma source of NITS, developed respectively by LAPLACE/CNRS and by NanoTec Bar, were set up to support a physical explanation of non-uniform ion current extraction at meniscus and of its relationship to the local magnetic field. The numerical results obtained using a Particle In Cell (PIC) model confirmed the existence of:

- An intra-aperture asymmetry of the extracted current density, which linearly depends on the local “electron suppression magnetic field” applied on each aperture of the PG;
- An inter-aperture asymmetry of the extracted current density, which exhibits a non-uniform distribution and depends on the “magnetic filter field” globally applied on the kamaboko plasma source.

The effect of the local “electron suppression magnetic field” is shown in Fig. 2.32, where also the linearity of the asymmetry coefficient α_{unb} is shown.

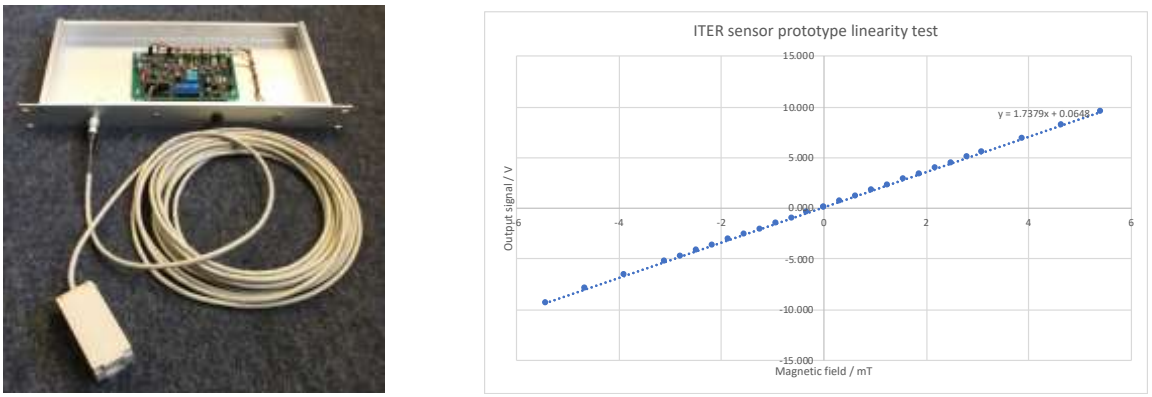

Fig. 2.33 ***Prototype flux-gate magnetic field sensor and results of the linearity tests at Stefan Mayer GmbH***

Realization of two engineered flux-gate magnetic field sensor prototypes

Following the finalization of an amendment of the F4E Framework Contract for MITICA Diagnostics, a supply order has been issued to Stefan Mayer Instruments GmbH & Co. KG for the construction of two "engineered" flux-gate magnetic sensors suitable for MITICA/HNB. A kick-off meeting has been held concerning the supply contract of tow flux-gate magnetic sensor prototypes. According to the original plan, the construction of the sensors was to be completed in Sept. and the factory acceptance test was supposed to take place in Oct. 2019. However, due to the supply of Vespel material taking longer than expected, Stefan Mayer Instruments completed the construction and carried out factory acceptance tests in Nov. 2019, using provisional parts made of PEEK instead of Vespel material (see Fig. 2.33). On 29th Nov. the supplier confirmed that the construction of the final sensors was completed and that the tests could be performed during Dec. 2019.

Development of a new layout of the PG busbar in the SPIDER experiment, so as to avoid the formation of a null point of the filter field inside the RF drivers

Experimental results obtained in SPIDER have shown that a magnetic filter field above a certain level could compromise the operation of RF drivers. This effect appeared to be caused by a specific feature of the magnetic field configuration, which was designed to have

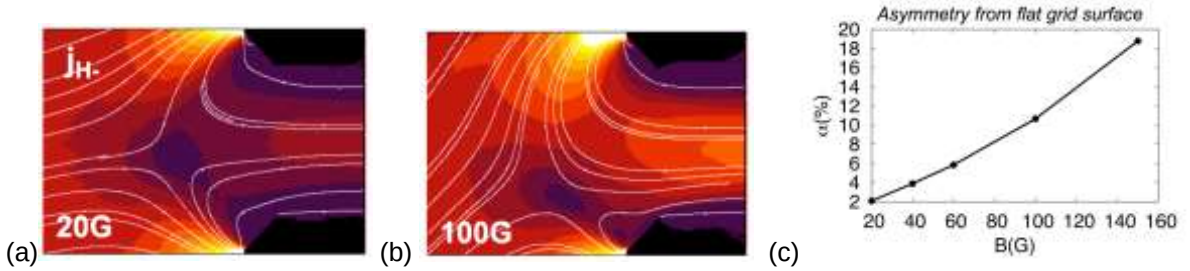

Fig. 2.32 (a) and (b) - pictures of the negative ion drift velocity inside the source in front of a grid aperture, with different strength of the transverse magnetic field; (c) - asymmetry coefficient α_{unb} as a function of the transverse magnetic field B_y at the meniscus

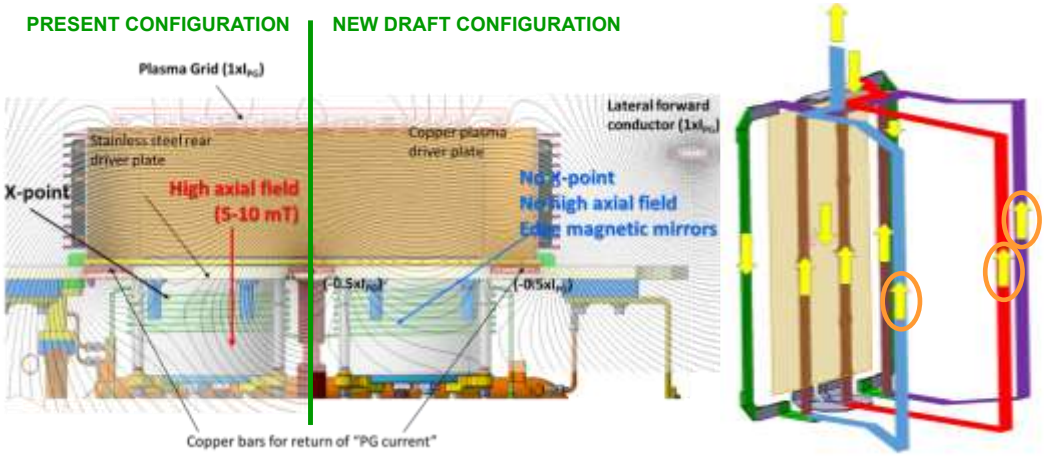

Fig. 2.34 ***Modification of the magnetic Filter Field configuration and corresponding new layout of the PG busbars planned to be implemented during the next shutdown***

minimum strength with a null point inside the RF driver. In order to address this problem, a new magnetic filter field configuration, based on a slightly different PG busbars layout, has been developed and optimized. The new configuration avoids the formation of a null-point inside the RF source (see Fig. 2.34) and will be implemented during the next long SPIDER shutdown.

2.1.5. *Vacuum high voltage holding modeling and experiments*

2.1.5.1. HVPTF experiments

During the first months of 2019, spherical stainless steel spheres (24 mm in diameter, gap length 30 mm) were tested on the HVPTF in double power supply configuration (V_{anode}=-$V_{cathode}$). Using the standard conditioning procedure in high vacuum, a maximum total voltage of 370 kVdc was achieved between electrodes. At the end of the conditioning procedure in high vacuum, the so called “pressure effect” was investigated by injecting a small flux of Argon into the vacuum chamber. In this case, a maximum total voltage of 470 kVdc was achieved when the Argon gas pressure was about 0.1 Pa.

Tests of the sphere (40 mm in diam.) - plane configuration, gap length 30 mm were also carried out, achieving a voltage up to 440 kV and 592 kV respectively in high-vacuum and low-pressure in Argon.

During April-May, specific Common Mode Voltage (CMV) experiments were undertaken (see Fig. 2.35).

Fig. 2.35 ***HVPTF vacuum chamber during the CMV electrode assembly***

The results did not allow to discriminate if the HV conditioning involves a modification of the cathode rather than of the anode surface, but indicated that the mutual exchange of charged particles between each single electrode and the vacuum chamber could be related to the micro-discharge onset.

Fig. 2.37 Picture of thick alumina cup during the HV test

An improved procedure for removing the dust deposited inside the vacuum chamber was also implemented, but no significant improvement of voltage holding was observed during subsequent HV tests in high vacuum.

In June, new electro-polished AISI 304 electrodes, a spherical (40 mm diameter) cathode, and a planar anode, with 30 mm gap length were installed in HVPTF. High voltage tests, similar to those already carried out during the previous months, were performed in HVPTF using accurately electropolished (plane – sphere) electrodes. No evidence of voltage holding improvements was found with respect to the reference case.

An experimental campaign was also carried out using a spherical cathode covered with a solid alumina cap (40 mm outer diameter, 10 mm thickness) and a stainless-steel plane anode. The electrodes are separated by a 33 mm vacuum gap, as shown in Fig. 2.37.

During the first phase of conditioning, some improvement of the hold-off voltage was observed with respect to the reference case (stainless steel cathode having the same cathode geometry and gap length). However, an unrecoverable degradation of the breakdown voltage occurred after breakdown #93 at 452 kV. The inspection of the electrode evidenced several mechanical fractures in the alumina ceramic cap, caused by the energy deposited during the electric breakdown.At the

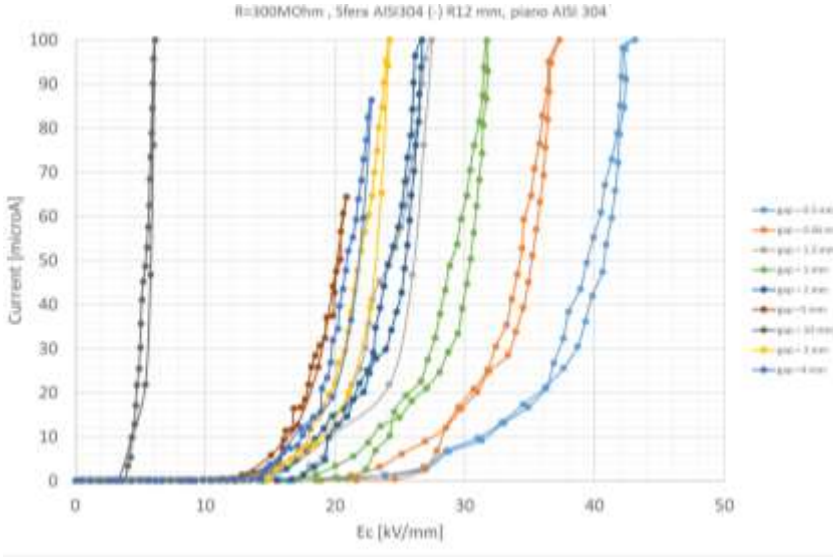

Fig. 2.36 Measured current vs. maximum Electric field at cathode for small gaps, stainless Steel electrodes

(a)  (b) 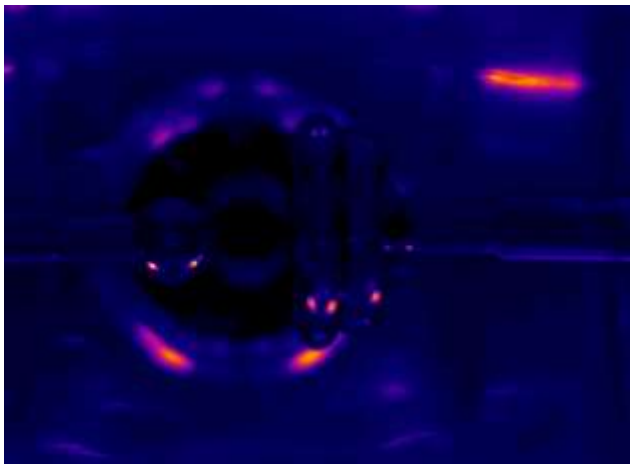

Fig. 2.38 a) Picture of the HV 800 NEG modules inside the HVPTF vacuum Vessel , b) Infra Red image during the activation of the NEG modules at ≈500°C

HVSGTF (High Voltage Short Gap Test Facility), systematic measurements of dark current were carried out with vacuum gap length of: 0.5, 0.66, 1.0, 1.25, 1.5, 3 ,4 and 10 mm and with an applied voltage up to 80 – 100 kV. As expected, the measured current was in the range between 1 and several tens of microA.The first Fowler-Nordheim (FN) fits with the experimental results were carried out, (Fig. 2.36). An interesting dependence, not described by the original FN model, between dark currents and the vacuum gap lengths was observed.

In October, a plane (anode) - sphere (cathode, 40 mm diam.) configuration with 33 mm gap length was installed in the HVPTF to help the measure of effectiveness of the NEG pumps. Four toroidal screens were also added near the inner wall of the vacuum vessel. A maximum voltage of 477 kVdc was achieved. During the high voltage test the signals of 3 types of scintillators (LaBr3(Ce), Cerium doped Lutetium -LYSO and Yttrium Aluminum Perovskite-YAP) were recorded in the same location. In November, a pair of Non-Evaporable Getter (NEG) modules (SAES Getter HV800) were installed in the HVPTF (Fig. 2.38).

The modules were specified to have a N_2 nominal pumping speed comparable to the pumping speed of the turbomolecular pump which is routinely used at the HVPTF. Both modules were positioned on the bottom of the vacuum vessel, under the structures supporting each electrode and were activated according to the operational procedure defined by the pumps supplier, using the main turbomolecolar pumping system. However, when the turbomolecular pumps were disconnected by closing a CF200 vacuum valve, it was not possible to keep the pressure below 1e-06 mbar by using the sole NEG pumps at room temperature. After starting the activation procedure again, the NEG pumps were operated at about 200°C.

In this case, after few tens of minutes, the RGA signals started to indicate that the small fraction of Argon contained in the atmospheric air (<1%) could not be pumped. After about

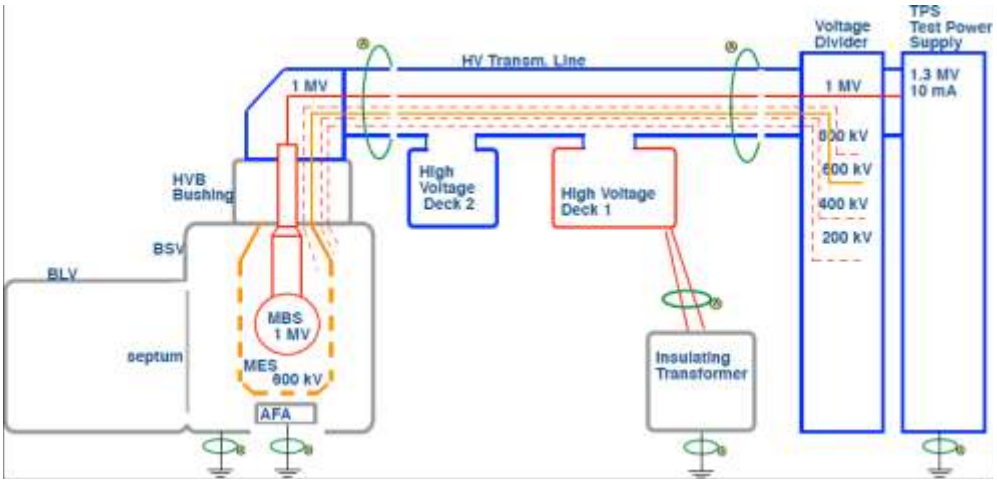

Fig. 2.39 Scheme of the electric circuit to be used for the HV tests in the MITICA vessel

24 hours of operations (without turbo pumps), the vacuum vessel drifted to 1e-04 mbar and the total pumping speed of NEG modules appeared to be reduced by one order of magnitude, the dominant molecule being CO_2. On the basis of these results, it was concluded that NEG pump cannot be used as a substitute of turbomolecular pumps in case of small air leakages, unless an auxiliary system dedicated to pumping noble gases is also used.

2.1.5.2. Vacuum High Voltage modelling and preparation of MITICA HV holding tests

During the first part of the year, the preparation of a specific HV test campaign to be implemented in the MITICA Vacuum Vessel using a mock-up of the Beam Source progressed according to the rationale and objectives defined during the previous work carried out in 2018.The tests have been designed with the aim of reducing the insulation problem to its most essential configuration (just 2 electrodes, possibly with an intermediate shield), so as to obtain reliable data on voltage holding at 1 MV and, if necessary, to focus on the most effective solutions. The tests were to be performed both in vacuum and in low-pressure gas, using the JADA 1.3 MV Test Power Supply TPS, after delivery and installation of MITICA Beam Source Vessel and Beam Line Vessel and before the delivery of the MITICA Beam Source. The electric scheme for the test is shown in Fig. 2.39. According to the development work carried out in 2018, the test configurations and procedures have been defined in detail and a schedule has been prepared, together with a list of test equipment. In preparation for an overall review meeting and discussion with ITER IO and experts, detailed design solutions for the realization of the main electrodes (Mock-up of the Beam Source, Additional Flat Anode and Intermediate Electrostatic Shield) have been prepared (see Fig. 2.40), including the optimization of the kinematics of the movable electrodes, the definition of the assembly procedures, the structural, static and dynamic analyses.

The list of auxiliary equipment (control and data acquisition, vacuum and gas injection, measurement equipment) necessary for the experimental campaign has also been defined.

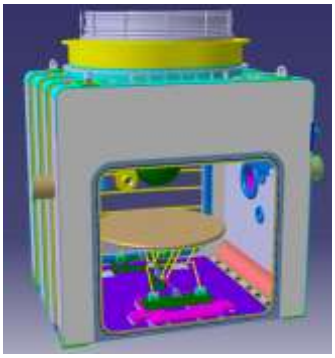

Fig. 2.40 Pantograph system and planar electrode inside the beam source vessel

The Vessel port usage was also preliminarily allocated for the tests. The actual outgassing rates of the MITICA BSV without and with the HVB were measured on site in order to define the requirements of the vacuum pumping and gas injection systems and measurement equipment necessary for the experiments. The vacuum pumping and gas injection scheme for the test is shown in Fig. 2.41.

While waiting for an overall review meeting, the status of the design of the HV tests has been shared with IO (L. Svensson) and QST experts (N. Umeda and K. Watanabe). To this purpose, informal discussions have been organized during the first months of the year concerning the HV test setup, the measurement equipment and the necessary devices for the protection of the HV bushing from overvoltage wave propagation in case of electric breakdown between the HV electrodes and the Beam Source Vessel during tests.

In Sept. – Oct. 2019 additional discussions were held with QST experts (A. Kojima and M. Kashiwagi). During these discussions it was suggested to consider the possibility of testing a much more realistic mock-up of the Beam Source, including grid supports and three or four intermediate shields, instead of a simplified sphere-cylinder mock-up with only one

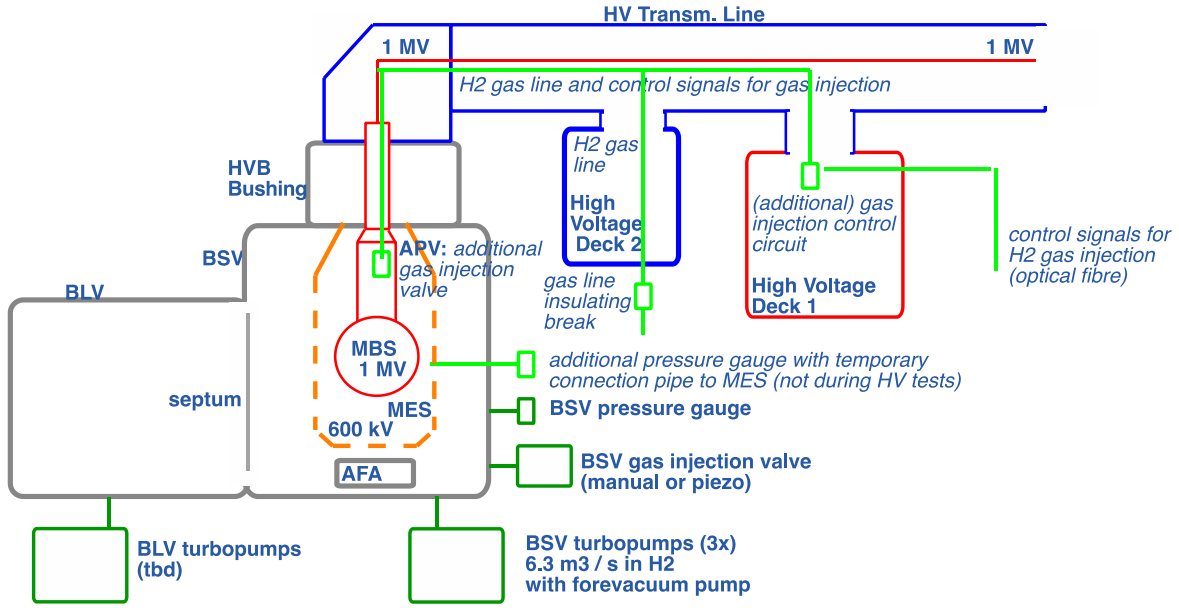

Fig. 2.41 Schematic of the MITICA pumping and gas injection system considered for HV tests in vacuum and low-pressure gas.

intermediate shield, as considered so far in the test plans.

On one hand, using such electrodes, the HV tests results would be directly applicable to assess the HV insulation system of the MITICA BS, avoiding the uncertainty due to the predictive models in presence of large area and long gaps. On the other hand, the new approach implies a change in the philosophy of the test and the design and realization of a much more complex “nested” electrode structure.

Presently the primary motivations and advantages/disadvantages of the two approaches are being analysed in detail with conflicting results. A plan for the implementation of this new approach is under development, in order to evaluate all the major implications of this choice, in terms of feasibility, time schedule, installation procedure and test procedure of such a complex electrode structure.

2.1.6. *RF Research and Development*

To enhance the knowledge in the field of Radio Frequency (RF) driven inductively coupled plasma sources and to investigate possible issues related to the voltage hold off at low pressure of the RF circuit and drivers of SPIDER and MITICA, a RF laboratory was set up at Consorzio RFX. The first developed testbed is the “High Voltage Radio Frequency Test Facility” (HVRFTF) devoted to the experimental validation of the driver insulation design criteria. In 2019, the activity has progressed as detailed hereinafter. In January, tests were carried out in support of finalising the design of SPIDER Plasma Grid masking activity. Components were installed in-vessel for the test of the “pushers”. The parts were then preassembled and checked and by the end of March, the electrodes were mounted and got ready for the test of the “pushers”. First tests were performed in Hydrogen on the 10 mm PEEK cylinder and continued through the year[23].In parallel, analyses have progressed on power transfer efficiency in the driver of SPIDER. Results have been obtained with the multi current filament model (with the variation of frequency and magnetic field, with and without stochastic heating). Validation of the Power Transfer Efficiency models has been investigated. A dedicated poster contribution has been presented at PPPS2019[24]. An alternative way is being explored to obtain the electron density within the driver and a dedicated meeting has been held with the IO to discuss the work and share the results. An

[23] A. Maistrello et al. “Voltage Hold Off Test of the Insulating Supports for the Plasma Grid Mask of SPIDER”, 14th International Symposium on Fusion Nuclear Technology, Budapest (Hungary), 22-27 September 2019.

[24] M. Recchia et al., “Studies on power transfer efficiency in the drivers of the SPIDER inductively coupled RF ion source”, 2019 IEEE Pulsed Power and Plasma Science Conference (PPPS 2019), 23-28 June 2019, Orlando, FL, USA

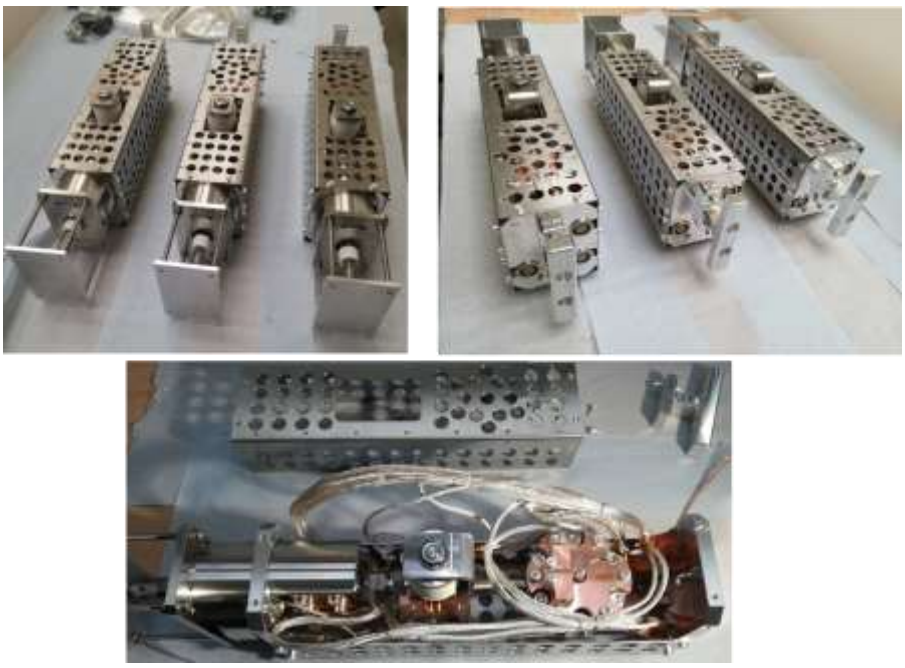

Fig. 2.42 Pictures of the 3 SPIDER Cs Ovens manufactured, delivered and tested in 2019

estimate of the electron density from the electrical parameters of the RF circuit has been proposed, taking into account ohmic heating only for the time being. Electrostatic measurements of plasma parameters have been performed in July and a COMSOL model is under development. Finally, to enhance the HVRFTF, some activity has started in 2019: the procurment of a new RF amplifier, a patch panel, an impedance meter and a current probe.

2.1.7. *Caesium R&D*

Caesium R&D activities on CATS facility started in 2018. In 2019 the procurement for the three SPIDER Cs ovens was completed, then the functional tests on the first two ovens were successfully carried out in CATS. See pictures of the three Cs ovens in Fig. 2.42.

Several tests were performed to calibrate and characterize the oven behavior and the performances of the related diagnostics, in order to estimate the flux of Cs at the various conditions imposed to the system, namely changing the set temperature and in short/long term operation.

Preliminary results indicate that:

- Cs emission is controllable and repeatable (between oven #01, #02 and prototype);
- an estimation of evaporation rate is possible;
- Cs oven filling procedures in glove box is confirmed;

- valve functionality had some early issues, but there are good lessons learned to prevent sticking;
- diagnostics (SID, LAS) provide valuable information, but require non-neligible efforts to maximize their effectiveness and reliability.

Some tests have also been carried out to assess different procedures to face experiment (un)foreseen shutdowns, in order not to incur in chemical reactions between Cs and water/oxygen/nitrogen that could prevent an acceptable restart of the oven operation.

Moreover, procurements for the materials and other preparatory activities were launched, with relation to the electrical and control systems necessary for the completion and integration of the SPIDER Caesium system, in order to be ready for the first Cs campaign in early 2020.

2.2. *ITER DIagnostics*

2.2.1. *Diagnostic systems Engineering Services*

During 2019 one of the two running Task Orders of the 'Diagnostic systems Engineering Services' Framework Contract (namely Task Order #05) has been completed, whereas the second (TO#06) has been postponed to early 2020 in order to allow the support of RFX team to the Preliminary Design Review of the Scientific Software for ITER Magnetic Diagnostic.

Concerning TO#05 (Engineering and coordination for the Outer Vessel Steady-state Sensors, PBS 55.A5/A6), the Task was completed with the last deliverables relative to:

- a technical assessment of the steady state magnetic sensors calibration procedure, proposed by ITER, and a market survey of the potential calibration suppliers25
- a cross calibration procedure between Outer Vessel Steady-state Sensors and inductive magnetic sensors, proposed as resolution of a chit raised at the steady-state sensors Final Design Review26.

Concerning TO#06 (Update of the design description and requirement documentation of the ITER magnetic diagnostic), a contribution was given to the ITER Diagnostic Team in the review and update of the "Design Description Document" of the ITER magnetic diagnostic

[25] M.Brombin, "Technical specifications for the steady state sensor calibration", <RFX_ITERDES_TN_006>, 03/07/2019

[26] N. Marconato, "1st progress report on the steady-state sensors FDR chit resolution", <RFX_ITERDES_TN_007>, 09/07/2019

system, with particular focus on performance assessment based on bespoke electronics component design[27].

3. EUROfusion Programme

3.1. *RFX-mod: experimental, modeling activities and upgrades*

3.1.1. *Introduction*

During 2019 the activities for the modification of RFX-mod experiment have been progressing in the framework of the industrial innovation project MIAIVO (granted by Regione Veneto POR-FESR 2014-2020), but they suffered significant delays both for technical and administrative issues.

The technical issues concerned the design of the vacuum-tight electrically-insulated crossed joints of the new vacuum vessel, which turned out to be not fully reliable at the expected operating conditions tested on a suitable mockup, and the need for the insulation of the entire copper stabilizing shell, which required a thorough study of the insulation coatings applicable on the specific in-vessel component.

The administrative issues concerned an important finacial crisis of the major industrial partner of the MIAIVO project (Ettore Zanon spa), which caused the interruption of the manufacturing activities in the last months, waiting for the involvement of a new company able to take over in the execution of the activities managed by Ettore Zanon spa.

Possible solutions to both technical and administrative problems have been identified and should be implemented at the beginning of 2020.

3.1.2. *Implementation of the machine toroidal assembly modifications*

3.1.2.1. Vacuum Tight Support Structure (VTSS)

As far as VTSS is concerned, the main activities had been focused on the validation of the vacuum-tight electrical-insulated crossed joints at the horizontal/vertical gaps of the new vessel, developed in the first phase of the MIAIVO project and based on a “CF-style flange” concept combining a particular geometrical shape and a selection of compatible materials (PEEK gaskets, Viton O-ring and epoxy adhesives).

The results of numerical simulations and experimental tests, executed on the reduced-scale “VTSS-mockup” (Fig. 3.1), demonstrated that the proposed soultion is not reliable due to

[27] N.Marconato, L.Pigatto, “Update of DDD and performance assessment based on bespoke electronics component design as submitted for PDR 1”, https://user.iter.org/?uid=UX4R6Q, 02/09/2019

Fig. 3.1 "VTSS-mock-up" during tests of the vacuum-tight electrical-insulated crossed joints[28]

eccessive stresses, among different materials facing at the vacuum boundary, which could occur owing to differential thermal expansion at the expected operating conditions up to 100°C[28].

An alternative solution has been studied, which implies the use of high-performance polymers combined with acrylic based syntactic foam materials, which provide proper vacuum tightness (required leak rates < 1E−9 mbar·l/s) and electrical insulation (required dielectric strength > 1 kV/mm), with suitable viscoelastic characteristic that guarantees the compensation of thermal deformations expected during operation. This solution has been successfully tested on a reduced-scale mockup (Fig. 3.2) and it is expected to be repeted on the VTSS mockup at the restart of the design activities with the new company replacing Ettore Zanon spa in the framework of the MIAIVO project.

3.1.2.2. Passive Stabilizing Shell (PSS)

The main activity related to the new PSS component has been focused on *R&D on ceramic coating of the RFX-mod2 copper shell*[29]. The 3mm thick stabilizing shell, that will be located in vacuum within the VTSS, will be characterized by overlapped gaps as shown in Fig. 3.3. Based on RFX-mod experience, during plasma operations the loop voltage can rapidly step up to 1.5 kV during fast plasma current terminations. Therefore, intense electric fields can generate between the shell flaps, only a few millimetres apart, along the overlapping region

[28] A. Rizzolo, et al., "Giunto Poloidale della VTSS di RFX-mod2: Analisi e soluzioni alternative", presentation at RFXmod2 internal meeting, 29/04/19

[29] L.Cordaro, presentation at the 8th International Workshop on Mechanisms of Vacuum Arcs (MeVArc 2019)

(Fig. 3.3). In RFX-mod2 the shell, which is in vacuum, is exposed to low temperature plasma so that the formation probability of harmful electric arcs is high[30].

In order to avoid arc formation, different kind of insulation ceramic coating on the copper (Alumina, Zirconia, Alumina-titania), able to withstand the applied electric fields in the presence of plasma, have been investigated and experimentally tested on a mock-up exposed to a weakly ionized plasma, a vacuum chamber in which a helium plasma was generated by means of a hot tungsten filament and a DC power supply (Fig. 3.4).

Zirconia and Alumina-Titania have been discarded after a preliminary megaohmeter resitivity measurement, as the measured resistence was lower than Alumina. In the tests with plasma, a bias voltage was applied between a copper plate and a cylindrical electrode (Ø 4

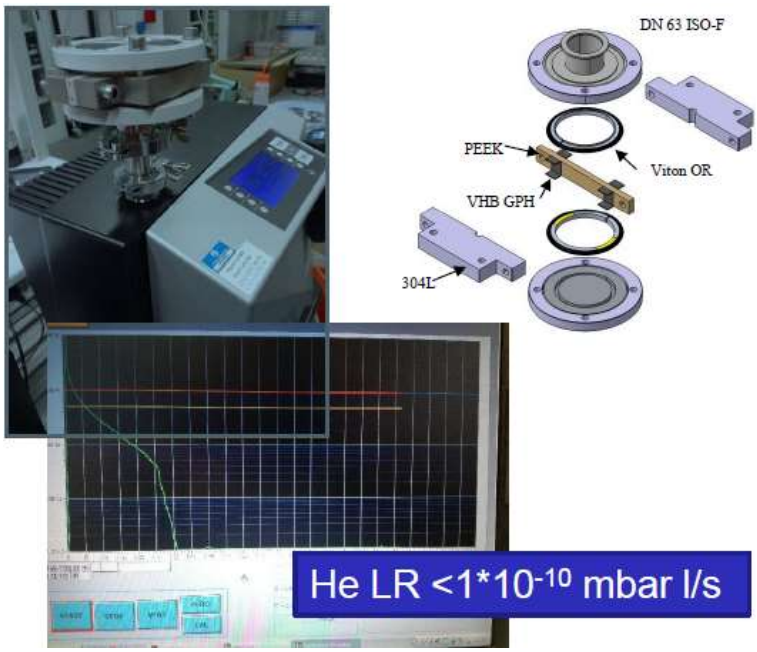

Fig. 3.2 Layout and result of the bench test of the new concept of the vacuum-tight electrical-insulated crossed joint based on acrylic based syntactic foam materials[28]

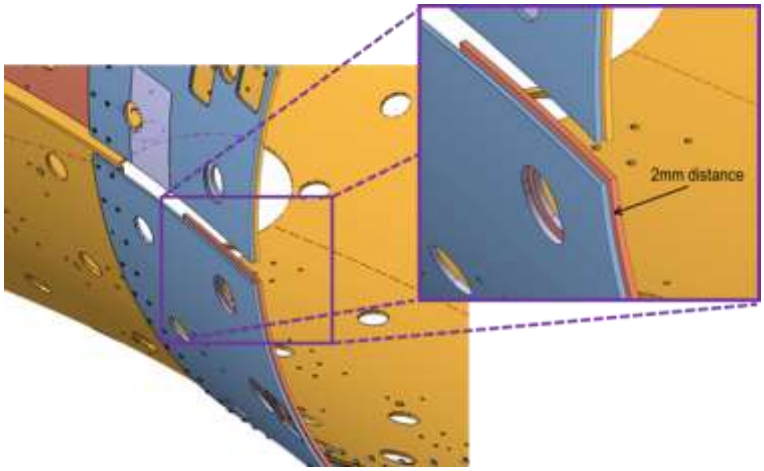

Fig. 3.3 Design of RFXmod2 stabilizing copper shell. A detail of overlapping region is shown (blue and orange flaps must be electrically insulated)

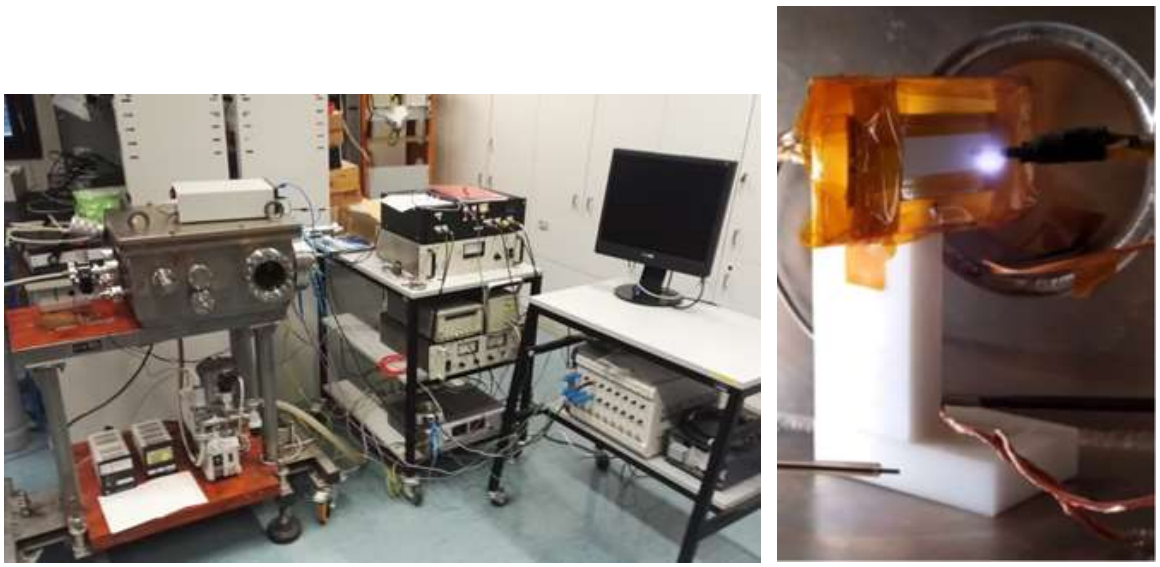

Fig. 3.4 (Left): experimental set-up for electrical insulation tests in vacuum and plasma. (Right): example of test with failure of insulation – arc between electrode and ceramic-coated copper sample

mm). The plate side facing the electrode was covered with alumina. The two electrodes were floating and biased by a small capacitor bank (0.3÷2 μF). Voltage pulses up to 2.6 kV were applied, with a background gas pressure in a range between 10^{-3} and 10 mbar. Furthermore, the electrodes were kept both in contact and spaced up to 5 mm. In these first tests, the formation of electric arcs between the rear sample surface and the pin was observed, showing that electric arcs can be formed even at relatively long distances between exposed metal surfaces. Further tests with completely isolated samples showed, instead, that alumina coating was able to guarantee insulation and it is therefore suitable for RFXmod2. For this reason, a modification of initial RFX-mod2 design has been proposed: i.e covering with insulation layer the entire copper shell. Further tests have been planned on a copper mockup with more realistic geometry with an alumina deposit, in order to simulate the overlap at the gap position. Several deposition techniques have been analyzed, including magnetron sputtering, detonation gun and plasma spray. The latter has been considered the most suitable for covering the entire RFX copper shell.

Locking bush insulation: Similar experiments have been conducted to evaluate the electrical insulation of an alumina layer on locking bushes, the steel supports on which the graphite tiles of the first wall will be fixed (Fig. 3.5). Air tests with a megohmmeter on the flat surface showed an excellent degree of isolation[31], however vacuum tests led to the formation of

[31] M. Spolaore, et al., <RFXmod2-TN-017> (11/07/19), <RFXmod2-TN-022> (13/11/19), Consorzio RFX internal Technical Notes

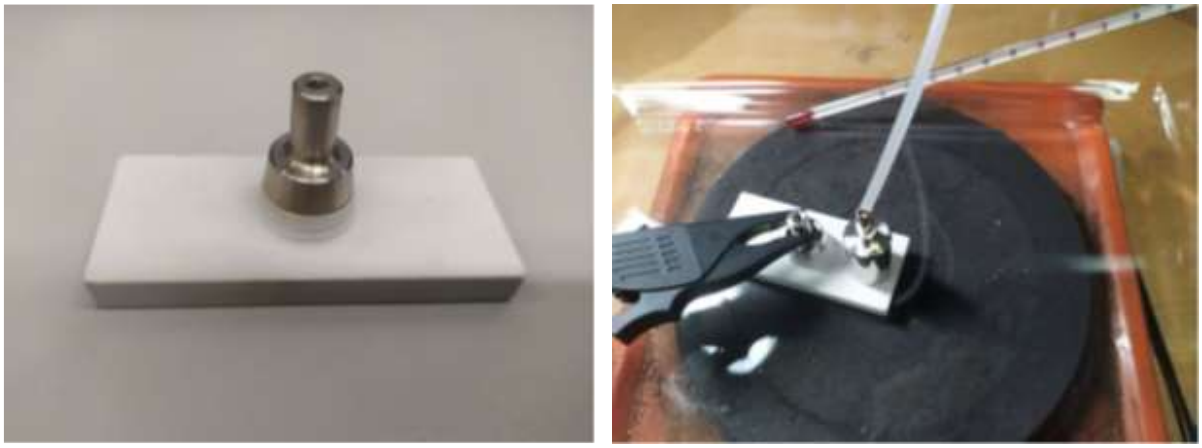

Fig. 3.5 (Left): prototype of "locking bush" made of Stainless Steel, with alumina coating. (Right): insulation test in atmosphere

holes on the base cone at a voltage of about 1.9 kV. These holes were formed at points where the insulation layer was smaller, showing a non-uniformity of the ceramic deposit.

Taking into account that it is not possible to guarantee a uniform alumina coating over the entire surface of the RFXmod2 shell, and considering that the electric fields expected in the worst scenario are comparable with those leading to the formation of breaks in the tested samples, the realization of a second gap in the copper shell has been proposed. Such a double gap design would have the advantage of halving the maximum electric field at each of the two overlapping regions, thus avoiding the establishment of the dielectric layer breaking conditions. Furthermore, the probability of having simultaneous electric arcs in both gaps, which could irreparably damage the stabilizing copper structure, would be considerably reduced.

Design of new PSS support structure: the design of the new support structure for the PSS has been developed up to an advanced stage and a procurement contract has been launched for the manufacture of the first prototypes of the supporting rings made of PAI-Torlon (Fig. 3.6).

The design activities of the PSS are expected to be completed with the restart of the activities with the new company replacing Ettore Zanon spa in the framework of the MIAIVO project.

3.1.2.3. First Wall

A significant modification of RFX-mod2 consists of replacing the first wall tiles, proposed as a key factor to improve the gas density with reduction of hydrogen retention. Polycrystalline graphite has been identified as tile material given its high thermal conductivity (up to about 165 $Wm^{-1}K^{-1}$), uniformity and small grain size (about 20μm), and high mechanical strength (100 MPa compressive strength, 30 MPa tensile strength).

Fig. 3.6 First prototypes of sectors of the PSS supporting rings made of PAI-Torlon

With respect to RFX-mod, the mechanical resistant section of tiles has been increased coherently with the magnetic front-end modification that foresees the tiles supported by the existing MHD passive stabilising shell, so decreasing the maximum stress at 3.5 MPa calculated from finite element analysis that simulates the operating condition. This low stress level together with a measurement of the experimental loads during next RFX-mod2 operations could qualify the use of extruded graphite for a possible further first wall change in the future. Indeed, extruded graphite is considered attractive given its high directional thermal diffusivity (about 50% better then polycrystalline graphite) to enhance the heat transmission and so improving the gas density control, and the low stress induced may allow use of this mechanically less performing graphite.

Each tile will be fastened through a bayonet mount realised through a male key with 2 radial pins connected to a female receptor modelled with matching slots; the female receptor is named locking bush and it is made of 304L. Four Belleville springs will keep the system parts locked together as shown in Fig. 3.7.

The design of RFX-mod2 first wall was presented at the ISFNT conference[32]. A call for tender for the procurement of the raw graphite material has been completed and the procurement for the machining of the complete set of 2016 first wall tiles is expected to be launched by mid 2020.

[32] M. Dalla Palma, et al. “Design of the RFX-mod2 first wall”, presented at the 14th International Symposium on Fusion Nuclear Technology (2019), submitted to Fusion Engineering and Design 2019

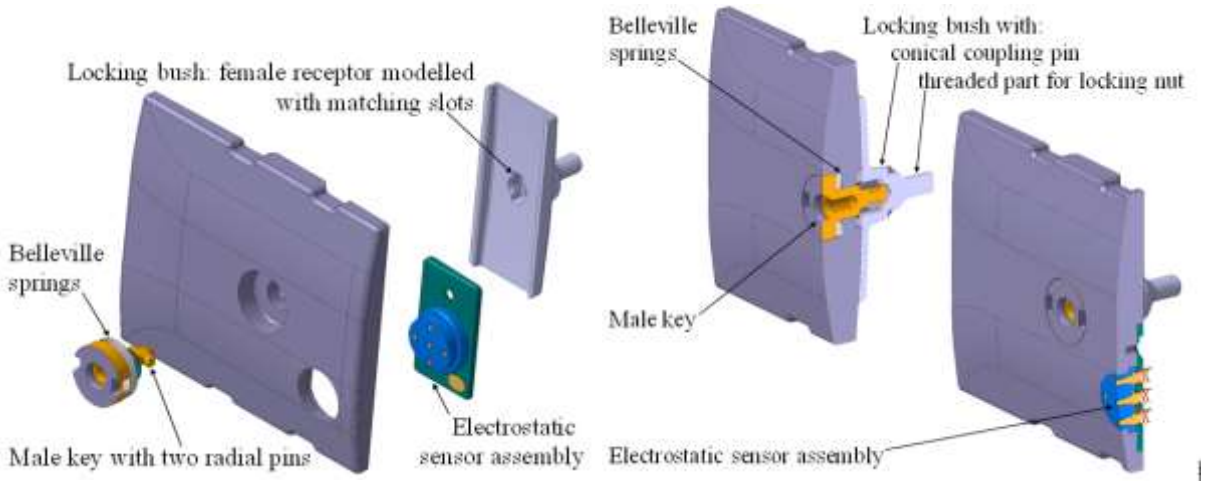

Fig. 3.7 (Left): Bayonet mount fastening a first wall tile. (Right): Cross sections of the RFX-mod2 with bayonet mount fastening and electrostatic sensors

3.1.2.4. Development of components made by additive manufacturing

In the framework of the MIAIVO project, a specific task is devoted to the development and characterization of in-vessel components made by means of additive manufacturing. First prototypes of locking bush (made of Stainless Steel) and antennas for RF diagnostics (made of Cu alloy) have been manufactured in collaboration with the industrial partner SISMA and are presently under test for proper characterization.

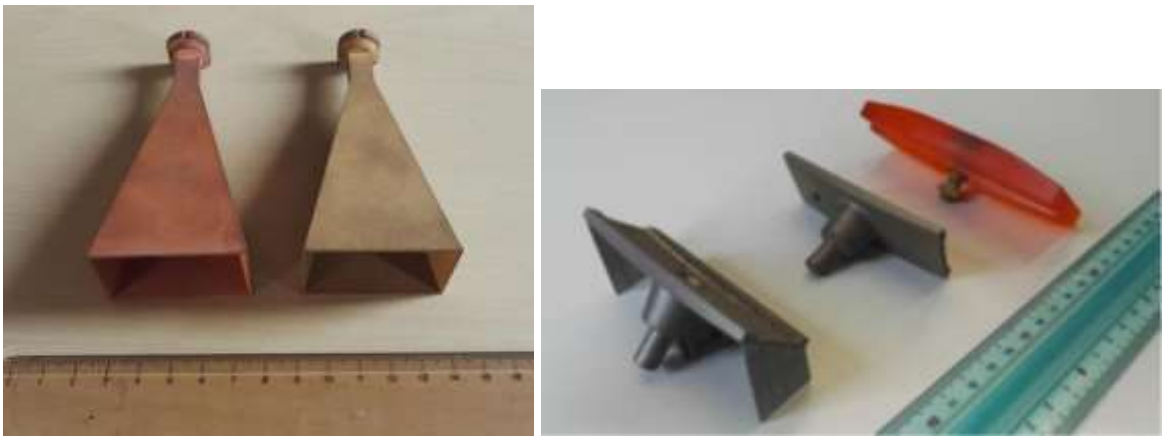

Fig. 3.8 First prototypes of in-vessel components made by additive manufacturing. (Left): antennas for reflectometer diagnostics (made of Cu and CuSn10). (Right): "locking bush" (made of AISI 316L)

3.1.3. ***Preparation of the RFX-mod2 scientific programme***

In 2019, a discussion has been promoted on the main research topics for RFX-mod2 and the scientific issues to be explored in its first experimental campaigns[33]. The former have been grouped in five areas

Extension of explored scenarios: this area develops along several lines. The first concerns the MHD control techniques, and includes the optimization of the feedback control parameters at different current levels, the assessment of the reduction of the LCMS achieved with the new magnetic front-end, and the characterization of the effect of high conductivity shell on the current threshold for spontaneous mode rotation, both in hydrogen and deuterium. The reduction of PWI related to the reduced LCMS deformation is expected to improve the density control, and the assessment of the maximum achievable density at medium/high current is considered as one of the most relevant topics. Of course a crucial issue, though presumably not explored in the first campaigns for prudence reasons in increasing plasma current, will be the characterization of the high current scenarios in the upgraded device, in particular with relation to the effect of a reduced PWI on the confinement properties and on QSH/SHAx performance. Though with lower priority, PPCD/OPCD experiments are also planned in RFX-mod2 : indeed the amplitude of m=0 modes is expected to be reduced, basically due to the reduction of m=1, and this could substantially improve the effect of PPCD/OPCD with respect to RFX-mod.

Energy and particle transport: the characterization of transport and confinement in a fusion device relies on adequate measurements of kinetic profiles. In particular, a reliable evaluation of the ion temperature, which was not available in RFX-mod, will be crucial in RFX-mod2, in order to relate the electron temperature internal barriers to the ion behavior. The role of residual magnetic chaos in driving energy and particle transport will be assessed in RFX-mod2, where a lower stochasticity is expected with respect to RFX-mod. On the other hand, the reduction of magnetic chaos will also allow to better discriminate the effect of microturbulence. Specific transient experiments, including pellet and impurity injection, will be planned since the first campaigns to study main gas and impurity transport. In addition, new insertable probes (including FARM, see sec.) are expected to provide current and flow profiles at the edge for momentum transport studies. An issue still not fully assessed for the RFP is the isotopic effect: first indications from RFX-mod indicate a positive isotopic effect with Deuterium, but these studies are to be deepened because at high current deuterium experiments in RFX-mod were suffering the failure of some saddle coils and the plasma

[33] L. Carraro et al., “Basis for the discussions of the first RFX-mod2 experiments”, internal note RFXmod2-TN-022

discharges were not fully optimized. In past years, RFPs (in particular MST) reported that fast ions are better confined with respect to thermal ions, which is interesting in the fusion perspective. This has to be confirmed in RFX-mod2, though the AIST 1MW neutral beam will not be available in the first operational phase.

Edge and SOL physics: an important topic to be addressed since the first campaigns is the exploration of the new density operational range, in particular to understand if, with an improved PWI, the operation at high current is compatible with higher densities: in RFX-mod a large part of the power exhaust and plasma-wall interaction, and an important part of edge transport is governed by the presence of m=0 magnetic islands and by the magnetic shift of the dominant m=1/n=7 mode. This was related to a severe localised PWI, with consequent uncontrolled release of deuterium and impurities. In RFX-mod2 the expected reduction by a factor ~ 2 of m=0 mode amplitude should widen the operative space, by increasing the operating density, and also reduce the detrimental, localized losses at φlock due to the residual phase locking of the secondary modes, at the same time increasing the strength of the stochastic layer in the helical edge. The effect on edge profiles and turbulence of the spontaneous rotation of modes at higher current than in RFX-mod will be a further field of investigation.

Tokamak plasmas: in principle, main aim for RFX-mod2 is the study of the potentialities of the RFP configuration. However, specific contributions to open issues in tokamak physics can be given by the operation as a low current Tokamak. The active control system (with the layout of magnetic sensors specifically upgraded to be more effective also for the tokamak experiments)will be exploited to apply in a controlled way magnetic perturbations and to study their effect on several instabilities, in particular on ELMs. To reconstruct magnetic equilibria the EFIT code will be used in addition to the tools developed for RFX-mod, and compared with reflectometric measurements.

Theory and modelling developments: in RFX-mod2 the experimental exploration of externally induced helical state will be still more strictly related to numerical modelling , since the reduced amplitude of magnetic fluctuations will favor the access to helical states. Even before new experiments, 3D visco-resistive codes are going to be advanced in order to simulate a resistive wall coupled to RFX-mod2 conducting structures and to characterize the interaction of plasma rotation and helical states. In the same codes, the solution of a self-consistent diffusion equation is going to be included. New experimental data will allow a better understanding of the role of Cantori structures in the formation of transport barriers and the study of the properties of plasmas with helicities different from the spontaneous one and produced by ad-hoc magnetic perturbations

3.1.4. ***Design/upgrade of new diagnostic systems for RFX-mod2***

New plasma position reflectometer: In 2019 the activity on the new reflectometry system for plasma position control has concerned the progress towards its final design. The system will involve 4 independent systems that will monitor the local position of the plasma in 4 different poloidal position. The activity has, thus, concerned the integration of the antennae in the RFXmod2 chamber (that is now at its detailed definition phase) and the analysis of the diagnostic system capabilities against the various possible RFXmod2 tokamak scenarios (with particular care to the DEMO-like equilibria). At the same time, a preliminary electromagnetic study for the antennae design has started and will continue in 2020.

Magnetic sensors layout: The main goal of magnetic measurement system of RFX-mod2 is to provide a detailed spatial and temporal resolution of plasma magnetic structure, with the aim to overcome the limitations found during the RFX-mod operation and scientific exploitation. The fundamental design criteria have been defined to fulfill the operation needs and to allow a detailed reconstruction of the magnetic plasma boundary in all the configuration accessible: RFP, tokamak and ultra low-q. The requirements had then to match the geometrical and the accessibility constrains given by the machine assembly. The main limitations found during the RFX-mod operation where due to the insufficient spatial resolution: for the high m modes in tokamak and ultra low-q operation, where the RFX-mod system had ($m_{max}=\pm4$); the presence of high order tearing modes (n>24) and lack of m=2 phase information on RFP configuration (resolution on RFX-mod: $n_{max}=\pm24$, $m_{max}=\pm2$); moreover the limited signal bandwidth (~10 kHz) for the pick-up measurements made difficult a detailed and comprehensive measurement of the spontaneous rotation of MHD modes and of the dynamic of magnetic reconnection.

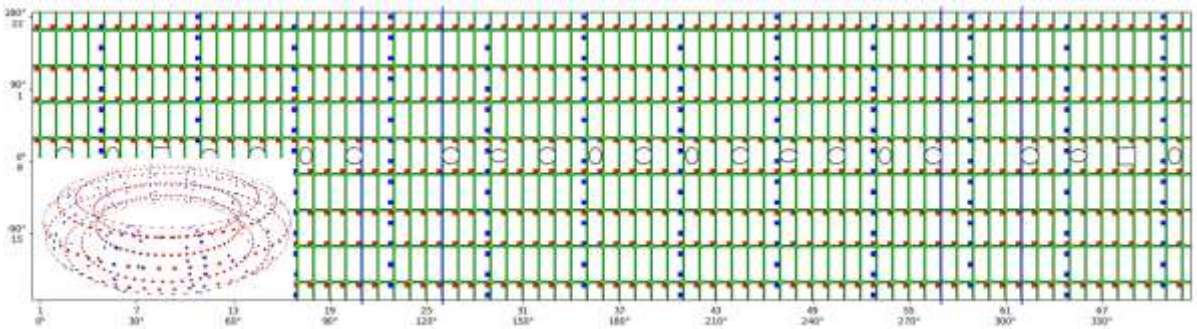

Fig. 3.9 Layout for the local magnetic field sensors on RFX-mod2: blue Bp, Bt, Br pick-up (12 pol by 14 tor), red Bt pick-up (8 pol by 72 tor), green Br saddle (8 pol by 72 tor). -

The current design (Tab. 1) will substantially increase the spatial resolution to ($m_{max}=\pm4$, $n_{max}=\pm36$) for the RFP and ($m_{max}=\pm14$, $n_{max}=\pm3$) for the tokamak, with an available analog bandwidth of 200 kHz.

Probe type	Measurement	Layout	Main use
Toroidal loops	Poloidal Vloop	8 + 8 equally spaced	Toroidal Loop Voltage Axisymmetric Poloidal flux
Poloidal loops	Toroidal Vloop	12 equally spaced	Toroidal flux
Three axes pick-up	Local magnetic field (B_p, B_t, B_r)	12 checkerboard shifted poloidal arrays of 14 probes: equivalent to 6 poloidal arrays of 28 probes.	Plasma current Shape reconstruction
Saddle loops	Averaged radial field (B_r)	8 along poloidal and 72 along toroidal direction, full coverage of the torus	Real time MHD control 3D boundary reconstruction
Single axis pick-up	Local toroidal field (B_t)	8 uniform toroidal arrays of 72 probes	Real time MHD control 3D boundary reconstruction MHD mode spontaneous rotation and reconnection dynamics
Three axes pick-up	External tangential magnetic field (B_p, B_t)	2 arrays of 14 probes	Shell current distribution
Shunt	Halo current	2 arrays of 14 probes	Halo current

Tab. 1: Magnetic sensor organization for RFX-mod2

This design has evolved from the previous one[34], since numeric simulation[35] highlighted that the measured Br component during RFP operation is severely affected by local eddy currents, which pollute the MHD spectrum with spurious harmonic. To get rid of this effect, it has been decided to measure the Br component by means of saddle coils, which average out the local field. Instead during tokamak operation, the effects of the higher harmonic of the shell eddy currents on the pick-up coil have been considered negligible, being the evolution of the field at slower time scales and the 3 axis pick-up coil design has been maintained.

Magnetic sensors; Digital Acquisition: The DAQ system for the magnetic measurement is under design with the aim to made all magnetic measurements available to the real-time control system, allowing the implement and test of advanced control algorithm for MHD mode, equilibrium and plasma shape control. The legacy system of RFX-mod, was based on analog integrators, and had separate systems for offline data transient recording and real-time. This architecture is quite complex and includes obsolete VME components. The new system is based on the recent System On Chip (SOC) technology, which integrates Field Programmable Gate Array (FPGA) logic and multicore processor technologies, together with a state of the art high-speed high-resolution ADC (20 bit, 1Msamples/sec). These two

[34] N. Marconato et al., "Design of the new electromagnetic measurement system for RFX-mod upgrade", Fus. Eng. and Des., vol. 146, 2019

[35] L. Marrelli et al, "Upgrades of the RFX-mod reversed field pinch and expected scenario improvements", Nucl. Fusion, vol. 59, 2019

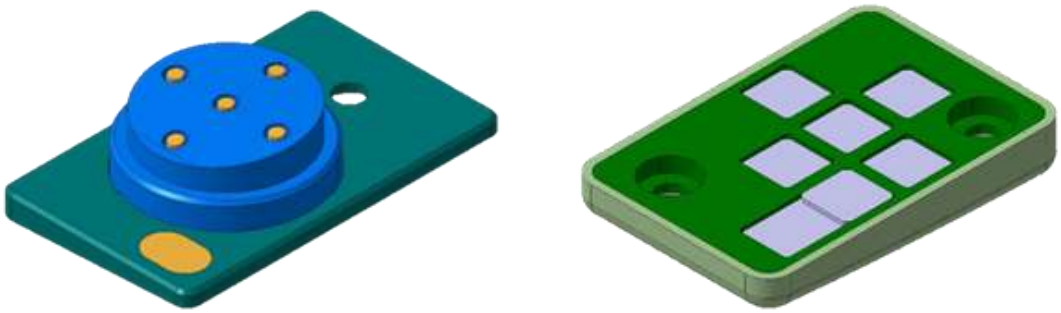

Fig. 3.10 Design of a 5-pin electrostatic sensor: on the left, the part of the sensor inserted in the graphite tile; on the right, the part to be fastened to the PSS

technologies allow the acquisition of the signal at full bandwidth (200 kHz) at high resolution, a direct numeric signal integration and provide the real time data stream for the plasma control system. In addition to the increased performances, the new system drastically simplifies the overall architecture, increases compactness and eases its deployment and maintenance.

Electrostatic sensors layout: RFX-mod2 will be equipped with poloidal and toroidal arrays of electrostatic probes, measuring plasma density and temperature T_e, plasma potential V_p, particle and energy fluxes and floating potential V_f fluctuations: two toroidal arrays of 72 probes each (one on the HFS and one on the LFS), along with four poloidal arrays of 28 elements (2 arrays of single probes and 2 arrays of 5-pin balanced triple probes). The design activity is almost finalized. The whole electrostatic sensors system has been presented in the poster session of the 3rd European Conference on Plasma Diagnostics (ECPD2019), which proceedings have been published in [36].

A first evaluation on the costs of the whole system started. To this end, a preliminary design of the electronics for the biasing and the acquisition that the system requires for the sensors operation, has begun. Regarding to the sensor design (Fig. 3.10), last optimizations are ongoing. In particular, a better way to fasten the insulated support of the sensor to the PSS is under study: the possibility to use peek rivets must be furthermore verified to be confirmed.

A modification of one of the poloidal array of single probes with one array of *ball-pen probes* has been proposed in the last part of the year: the method described in [37] allows to estimate

[36] Design of embedded electrostatic sensors for the RFX-mod2 device, S. Spagnolo, M. Spolaore, M. Bernardi, R. Cavazzana, S. Peruzzo, M. Dalla Palma, G. De Masi, G. Grenfell, N. Marconato, E. Martines, B. Momo, N. Vianello and M. Zuin JINST 14 C11014, 3rd European Conference on Plasma Diagnostics (ECPD2019), 6–10 May 2019 Lisbon, Portugal

[37] A novel approach to direct measurement of the plasma potential, J. Adamek et al., Czechoslovak Journal of Physics 54 (2004) C95

the electron temperature and plasma potential poloidal distributions, with high time resolution, and without biasing the probe set electrodes. The idea is to directly measure the plasma potential by using a pin retracted with respect to the tile, exploiting the difference between the electron and ion gyroradii in a magnetized plasma: in this condition, ions can reach the electrode, while electrons are mostly screened off. The principle consists of a reduction of the electron saturation current down to the level of the ion saturation one, so the parameter $\alpha = \ln(I_e/I_i) = 0$ in $V_p = V_f + \alpha T_e$, thus, $V_f(retracted) \approx V_p$. A second pin, measuring the floating potential at the tile level, allows the electron temperature estimation. The pin retraction h must be of the order of the ion gyroradius, that for RFX-mod2 is $\rho_i \approx 1mm$ both in tokamak and in 1 MA RFP discharges. The choice if pin retraction h allows to use these sensors for a wide range of magnetic configurations.

New Thomson Scattering: The new Thomson scattering diagnostic foreseen on RFX-mod2 has been designed almost completely. The new system integrates a back reflector, a cylindrical telescope which is aimed at the reduction of radiation load on the back reflector and a relay system to recycle the laser beam in the edge system. The launch optics for the telescope have been purchased. An alternative mirror system for collection optics have been designed, in order to reduce vignetting on the inner pipe; at the same time, the corresponding refractive lens is left free and can be moved on the ventral pipe if differential TS spectrum measurement is foreseen. Actually, differential measurements of TS spectrum is required in order to evaluate the non-thermal features of electron distribution; the preferred location is on the external pipes (upper and lower) in order to take advantage of higher solid angle and higher component of the scattering vector on the field lines. The new TS system is designed to host a new laser blow-off target holder, exploiting the lower target-plasma distance at the equatorial port.

Tracer impurity experiments in RFX-mod2[38]: With the aim of characterizing impurity transport in the region of internal transport barrier during RFX-mod2 helical states, Ni-tracer encapsulated solid pellet (Ni-TESPEL) experiments are foreseen. This will allow a more detailed analysis of the impurity transport inside the outward convection barrier, by placing the impurity source further inside the plasma. The solid pellet injector already used in RFX-mod to inject C and Li solid pellets, will be adapted to inject TESPEL in RFX-mod2 (0.7/0.9 mm polystyrene ball with Ni powder inside, injection velocity up to 200 m/s can be reached). A fine tuning of pneumatic actuators has been obtained for a smoother loading of the sabot

[38] L.Carraro, et al., "1-dim Collisional Radiative impurity transport code with internal particle source for TESPEL inject", 46th EPS Conference on Plasma Physics – Milan, July 8-12 2019

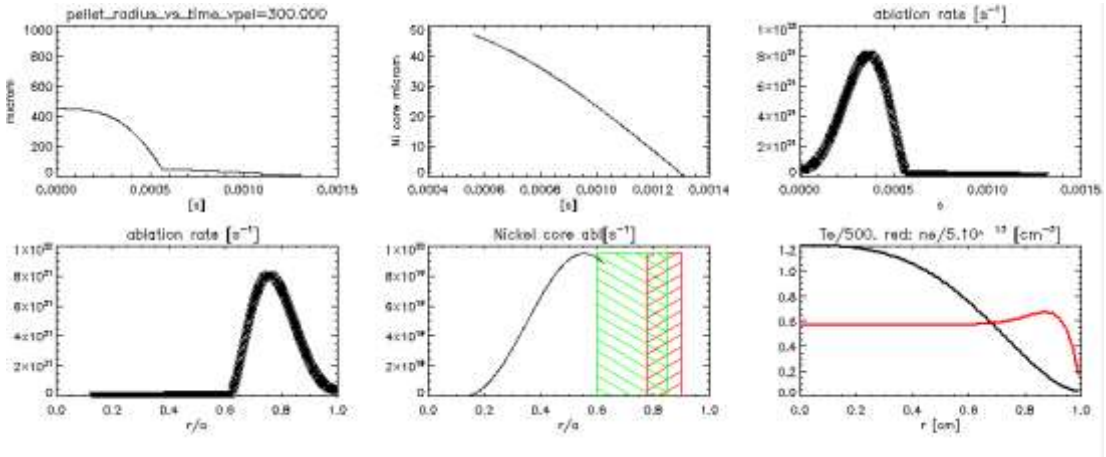

Fig. 3.11 Simulation of ablation of the polystyrene shell and of the Ni core of a TESPEL injected with a velocity of 300 m/s and 'typical' Te and ne in RFX-mod

in the injector; the diameter of the hole in the sabot hosting the TESPEL has been optimized to prevent TESPEL being lost when the sabot is stopped at the bumper.

The sensitivity of the two gate optical detectors used to measure the TESPEL speed will be increased by replacing the led light sources with stronger diode lasers. A higher speed at fixed pressure could be reached by reducing the sabot mass. It is foreseen to increase the speed up to about 300 m/s by drilling a hole on the back surface of the sabot, while maintaining the sabot material (light and resistant peek) and external shapes (compatible with the sabot loader and responding to stability requirements).

The available 1-dimensional, time dependent Ni Collisional Radiative code, used to reconstruct experimental Ni emissions in RFX-mod has been upgraded in preparation of such experiments in RFX-mod2 including the possibility of a Ni source (boundary condition) inside the plasma, placed in a time dependent position. The 900 μm polystyrene + 100 μm Ni ablation has been simulated in a typical scenario of T_e, n_e for RFX-mod and the results have been reported in Fig. 3.11: the polystyrene shell is completely ablated within r/a =1 and r/a=0.6,and Ni reaches about r/a=0.2. Ni is deposited inside the outward convection barrier (showed in figure: in red in the multiple Helicity scenario, in green in the Single Helicity one) and it will be possible to better probe the Ni transport in the central region.

3.1.5. *Mod Theory and modelling related to RFP helical states*

In 2019, nonlinear MHD modelling and data analysis tools improved in several respects. New boundary conditions, (resitive wall and vacuum layer), and ad-hoc momentum source have been implemented and tested in the visco-resistive 3Dnonlinear MHD SpeCyl code (semi-implicit, spectral code, cylindrical geometry). The more general 3D nonlinear MHD code "PIXIE3D" (fully implicit, finite-volume by L. Chacon LANL) including pressure equation has been installed and preliminary tested on the Marconi supercomputer at the Cineca

computing center. The T3D code (L. Chacon LANL) solving the temperature equation in a 3D magnetic field with anisotropic transport coefficients (lagrangian approach), has also been installed in Marconi and tested in some preliminary sample cases. The same cases have been analyzed to detect the Lagrangian Coherent Structures, LCS, which provide the "skeleton" of the magnetic patterns. Finally, a new version of the T3D code (able to deal with variation of |B| along the field line) has been tested and verified using the "*Method of Manufactured Solution*" during one month visit at LANL.

Some more details and highlights about the scientific results are detailed in the following paragraphs.

3D viscoresistive MHD modeling: Realistic Boundary Conditions. . New boundary conditions, (resistive wall and vacuum layer) have been implemented and tested in the visco-resistive 3D nonlinear MHD SpeCyl code (semi-implicit, spectral code, cylindrical geometry)The implementation of resistive shell and vacuum layer boundary conditions provided two main results. On the one hand, the decrease of secondary modes was observed by increasing the shell-plasma proximity. This is of interest in view of the upgraded RFX-mod2 device (starting operation in 2020), in which the shell-plasma proximity will change from b/a=1.11 to b/a=1.04[39]. On the other hand, with a proper choice for the resistivity of the thin shell at the plasma boundary, helical states are found to emerge in a self-consistent way, as in the experiment, even without the need to impose a fixed helical MP. This promising result[40],[41],[42],[43] is shown in Fig. 3.12.

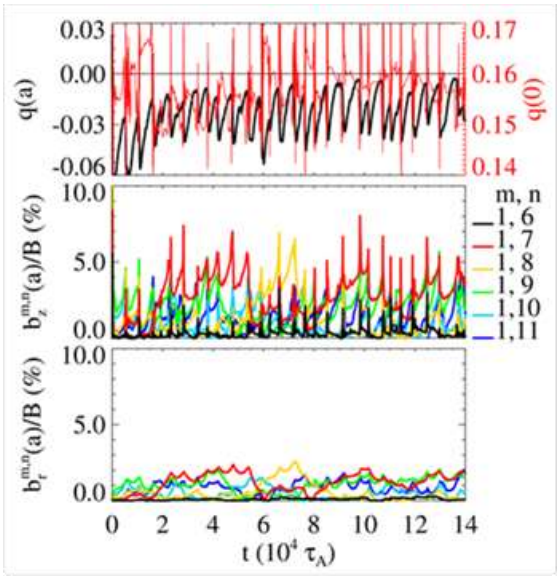

Fig. 3.12 Nonlinear RFP simulation with resistive wall at r=a (with $\tau_W/\tau_A=10^4$) and ideal wall at b/a=1.2, showing the self-consistent emergence of the m=1, n=7 mode as in RFX-mod.

3D viscoresistive MHD modeling: Effect of flow. A preliminary assessment of the interaction between a mean plasma flow and the helical self-organization process in RFPs

[39] Marrelli L. et al, 2019 Nucl. Fusion 59 076027

[40] Bonfiglio, invited presentation at 3th Asia-Pacific Conference on Plasma Physics, (2019), Hefei, China;

[41] Bonfiglio, EPS Conference 2019

[42] Bonfiglio et al. Poster contribution 18th EFTC conference (Ghent)

[43] Cappello invited talk 18th EFTC conference (Ghent);

has been performed with the SpeCyl code. It was observed that imparting an *ad hoc* axial flow (around $20 - 50$ km/s, which is a typical value of mean plasma flow measured in RFX-mod) leads to an enhancement of the helical state: a small increase of the energy of the dominant mode is associated with a clear decrease of the energy of secondary perturbations, independent on the direction of the mean flow[44].

Lagrangian Coherent Structures (LCS), Connection Length and Temperature/Pressure equation. The development of refined techniques to detect Lagrangian Coherent Structures started in 2018, and continued during 2019[45,46,47,48]. Several RFP numerical cases (obtained in 3D nonlinear MHD modelling) have been analysed see e.g Fig. 3.13. The LCS "quasi-surfaces" are proved to rule the chaotic transport of magnetic field lines and have been shown to match with the other transport related indicator "connection length". Furthemore, thanks to the collaboration with Luis Chacòn (Los Alamos National Laboratory), the T3D code for temperature transport equation has been used to obtain the temperature distribution consistent with the magnetic configuration for RFP numerical cases. The T3D tool gives results in agreement with the LCS, underlining the role of LCS in ruling the heat transport. A first step has been done concerning the application of such technique also to experimental data (RFX-mod magnetic field). These developments and results are described in [49], an example is shown in Fig. 3.13.

3D viscoresistive MHD modeling: PIXIE3D: The more general code (fully implicit, finite-volume by L. Chacon LANL) 3D nonlinear MHD code "PIXIE3D" including pressure equation has been installed and preliminary tested at the Marconi Compunting center. Significant work has been done using this code with the inclusion of the pressure equation. In fact, using PIXIE3D the anisotropy effects in the evolution of 2D RFP magnetic fields in helical symmetry has been studied.

---

[44] M. Veranda, D. Bonfiglio, S. Cappello, G. Di Giannatale, D.F. Escande , Nucl. Fusion **60** 016007 (2020) " Helically self-organized pinches: dynamical regimes and magnetic chaos healing"

[45] Pegoraro, Bonfiglio, Cappello, Di Giannatale, Falessi, Grasso, Veranda," Coherent magnetic structures in self organized plasmas" 044003, **61** PPCF (2019)

[46] S. Cappello, invited tutorial presentation Festival de Theorie Aix en Provence (2019)

[47] G. Di Giannatale et al " Lagrangian Coherent Structures as skeleton of transport in low collisionality and chaotic magnetic fields" poster presentation at 3th Asia-Pacific Conference on Plasma Physics, (2019), Hefei, China (Best Poster prize)

[48] M. Veranda, invited presentation Italian National Conference on the Physics of Matter, Catania, Italy, 30 September-4 October (2019)

[49] G. Di Giannatale PhD Thesis 2019 "Magnetic confinement properties of 3D equilibria for fusion plasmas: non linear MHD modelling and experimental comparisons"

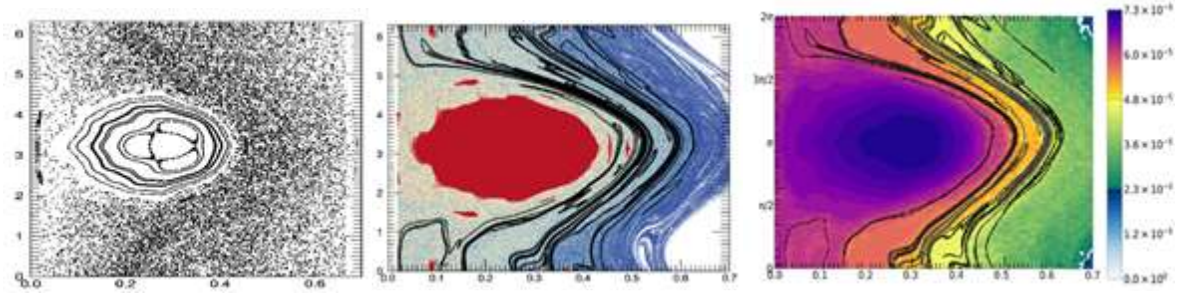

Fig. 3.13 Magnetic field lines confinement properties during an n=7 QSH state: Poincaré plot (left panel); LCS (Black stripes) and connection length (in color) (central panel); LCS and temperature (right panel).

3D viscoresistive MHD modeling: Alfven waves excitation by reconnection events in RFP and tokamak: The SpeCyl code was also used to perform a numerical characterization of Alfvén waves in tokamak and RFP plasmas in cylindrical geometry[50],[51]. Configurations with increasing level of complexity were analyzed. First, numerical solutions were compared with analytical ones in the most simple case of a uniform axial magnetic field. An excellent agreement was obtained for both the shear Alfvén wave (SAW) and the compressional Alfvén eigenmodes (CAEs). Then, the RFP configuration was studied by assuming perturbations with a given helical periodicity (m=1, n=0). Phenomena such as the phase mixing of the SAW, resonant absorption of CAEs and the appearance of the global Alfvén eigenmode (GAE) were observed. Finally, the fully 3D RFP case with realistic magnetic reconnection events was investigated, showing for the first time in nonlinear RFP simulations the excitation of Alfvén waves by magnetic reconnection. The typical spectrum of Alfvén eigenmodes excited by reconnection events in the RFP, shown in Fig. 3.14, is in reasonable quantitative agreement with experimental finding in the RFX-mod device.

A model of solar ion heating by low-frequency Alfvén waves has been published published[52] and presented as invited talk to the Asia Pacific Physical Society DPP 2019 Conference in Hefei-China [AAPPSD19][53]. The work has been recently started in order to apply the same formalism to interpret ion heating by waves in laboratory plasmas as well. The first step involves ion heating during reconnective processes, as

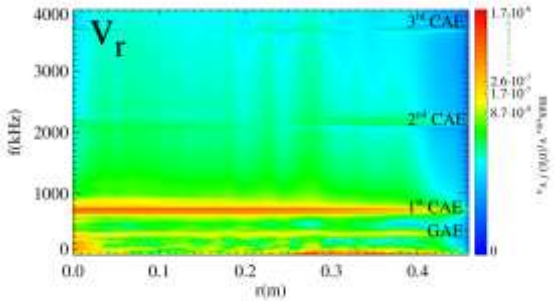

Fig. 3.14 Spectrum of Alfvén eigenmodes triggered by magnetic reconnection events in nonlinear RFP simulations of the RFP. Two main AEs are observed to be excited by magnetic reconnection, namely the GAE and the first CAE.

[50] A. Kryzhanovskyy et al., poster contribution 18th EFTC conference (Ghent) 2019

[51] D. Bonfiglio, et al., invited talk 2nd Trilateral Internat. Workshop Energetic Particle Physics (Seoul);

[52] DF Escande, V Gondret, F Sattin "Relevant heating of the quiet solar corona by Alfvén waves: a result of adiabaticity breakdown" Scientific Reports (2019)

[53] F. Sattin , invited presentation 3th Asia-Pacific Conference on Plasma Physics, (2019), Hefei, China

observed in RFPs.

Scaling laws of m=0 modes: 3D nonlinear MHD simulations vs RFX-mod data: A comprehensive study of the variation of m=0 amplitudes with Hartmann in the existing SpeCyl simulation database has been performed and compared to RFX-mod measurements. In the RFP, m=0,n=1 tearing mode (TM) islands resonating at the edge on the reversal surface q=0, have been shown to generate convective cells whose size is seen to increase as a function of the phenomenological Greenwald fraction, n/n_G with $n_G = I_p/\pi a^2$ the Greenwald density. These convective cells generate in turn MARFE-like, poloidal structures, which have already been identified as precursors of the RFP density limit[54]. From the theory point of view, 3D nonlinear visco-resistive MHD simulations with SpeCyl predict that the same TM's amplitudes scale with the Hartmann number $H = (\eta\nu)^{-1/2}$ (the inverse geometric mean of resistivity η and viscosity ν). During year 2019 a comprehensive study of the variation of m=0 amplitudes with Hartmann in the existing SpeCyl simulation database has been performed[55]: such amplitudes increase up to a critical Hartmann number $H_c \approx 3 \times 10^3$, and then they decrease as Hartmann is raised. Since low m=0 amplitudes correspond to QSH states, this behaviour separates two very different QSH basins: one at low H (high dissipation) and one at high H (low dissipation)[56]. By expressing the viscosity in the Hartmann definition with the Braginskii approach[57] it was possible to evaluate Hartmann within a large database of RFX-mod discharges, including the ones used for the density limit studies. The result is shown in Fig. 3.15: it is evident that in experiment only the low dissipation QSH branch can be seen, the density limit arising naturally as a value of Hartmann determining the critical size of the m=0,n=1 island as H decreases towards H_c. Moreover, the phenomenological n/n_G parameter seems to be nothing that Hartmann itself, and the high dissipation basin of the QSH, which was discussed in early papers[58], should be attained, in the upgraded RFX-mod2

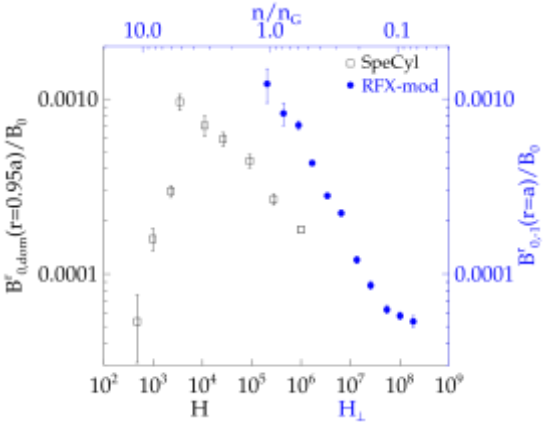

Fig. 3.15 Dependence of the m=0 Br fluctuation as a function of the Hartmann number in simulation (black) and experiment (blue).

[54] G.Spizzo, et al., Nucl. Fusion **55**, 043007 (2015)
[55] N. Vivenzi MS thesis (2019)
[56] Marco Veranda et al Nucl. Fusion **60**, 016007 (2020)
[57] J.A. Bittencourt, Fundamentals of Plasma Physics (New York: Springer, 2004)
[58] S.Cappello and D.F.Escande, Phys. Rev. Lett. 85, 3838 (2000)

device, in very high density discharges, with $n/n_G \geq 3$.

Helical Relaxed States Studies: The studies about the relaxed states dominated by a Single Helical (SH) mode have been pursued in 2019 along two lines. The first direction has regarded the comparison with the experimental results. In particular the data obtained in the low aspect ratio RELAX device has been considered, since in a previous paper[59] it was noted that at high values of the pinch parameter Θ the experimental curves deviate from the prediction of the SH relaxation theory. To reconcile the data and the model we consider the effect of the toroidal geometry, finding that the poloidal angle toroidal magnetic field modulation due to the effects of toroidicity shifts the equilibria in the F- Θ plane and therefore can explain why the experimental data differ from the theoretical predictions which are obtained assuming a cylindrical geometry. The deeper is the reversal of the magnetic field the higher is the deviation from the cylindrical predictions. The role of the toroidal geometry at low aspect ratio is therefore quite important and it can also explain why SH states are more difficult to be observed at high Θ (this is by the way true at all aspect ratios) due to the toroidal sidebands coupling and as consequence, in particular, the excitation of the m=0 mode.

Another line of research in 2019 was about the transport of helicity from the helical mode to the mean magnetic field. The SH dominated relaxation model assumes in fact the existence of a helicity invariant acting on the mean magnetic field scale related to the dominant mode. To explain the origin of this invariant we hypothesized a transport of helicity due to the dynamo electric field produced by the dominant mode. In this way it was possible to evaluate precisely the radial profile of this dynamo field in steady state. A 0-dimensional time dependent model of the helicity transport from the helical mode to the mean field was also formulated showing that the existence of a steady state solution is only allowed in presence of a sustainment (ohmic) electric field and other interesting oscillatory regimes of the dynamo and helicity content have been also discovered in absence or for moderate sustainment[60].

*Density limit across different configurations***.** A joint effort, coordinated by P. Zanca, D. Escande and F. Sattin, has advanced the understanding of density limits in tokamaks. The model developed in 2017 involving the different toroidal configurations (Tokamak, Stellataror and RFP) has been revised, in order to be more intuitive, and has been applied successfully

[59] R. Paccagnella, S. Masamune, A. Sanpei, Phys. of Plasmas 25 (2018) 072507.
[60] R. Paccagnella, New Journal of Physics **21** (2019) 093045.

to a larger tokamak experimental dataset. The results have been published in [61]

Participation in the Jorek team for SPI disruption mitigation in JET. First simulations of shattered pellet injection (SPI) in H-mode JET configurations have been obtained with the Jorek Code. The participation in the Jorek team provides a wondeful opportunity to learn best practices in large international (EUROfusion) numerical modelling teams.

3.1.6. *Edge physics*

Filament properties in L and H-mode regimes in the RFX-mod tokamak: The dynamics of turbulent filaments in L and ELM-free H-mode in the RFX-mod device operating as a tokamak was studied[62]. H-mode has been achieved recently in the RFX-mod with the aid of an external electrode biasing[63]. Through advanced statistical techniques, filaments were detected and tracked from the edge to the Scrape-Off Layer (SOL) in a two-dimension floating potential map associated with extreme events of a fixed ion saturation current signal in the SOL. While in L-mode filaments travel almost freely, during the ELM-free H-mode phase their motion is restricted to the near SOL. In this region, the background shear decorrelation time becomes shorter than the filament convective time, favoring its suppression. However, the experimental observation of a nearly 'trapped' monopole potential points rule out the possible role of the vortex selection mechanism. The sparse filamentary transport in the far SOL was further confirmed from the measurements of a poloidally symmetric electrostatic sensors array on the wall. While in L-mode a clear loss channel at outboard mid-plane is observed, in ELM-free H-mode, it virtually halts. Lastly, it was observed that filaments in L-mode better scale according to the sheath connected regime, where parallel dissipation towards the wall governs the potential depletion. The associated parallel current density, computed from magnetic field fluctuations measured with a 2D set of 3-axial coils installed in the probe head, is in qualitative agreement with that. In addition, the strong variation of the parallel connection length along the radial direction due to the plasma-wall proximity leads to a bifurcation, with filaments in the near SOL scaling differently from those further out (Fig. 3.17).

On the other hand, H-mode filaments near the edge exhibit a better match with the inertial regime, where parallel dissipation becomes less important. Such a result is consistent with the parallel current density measurement. The field line tracing code NEMATO has been used to compute the magnetic topology and the connection length coming from

[61] P. Zanca, F. Sattin , D.F. Escande and JET Contributors Nucl. Fusion **59** (2019) 126011

[62] G. Grenfell, PhD thesis, Padova Unversity, 2020. Paper in preparation

[63] Spolaore M. et al., *Nuclear Fusion* 57.11 (2017): 116039.

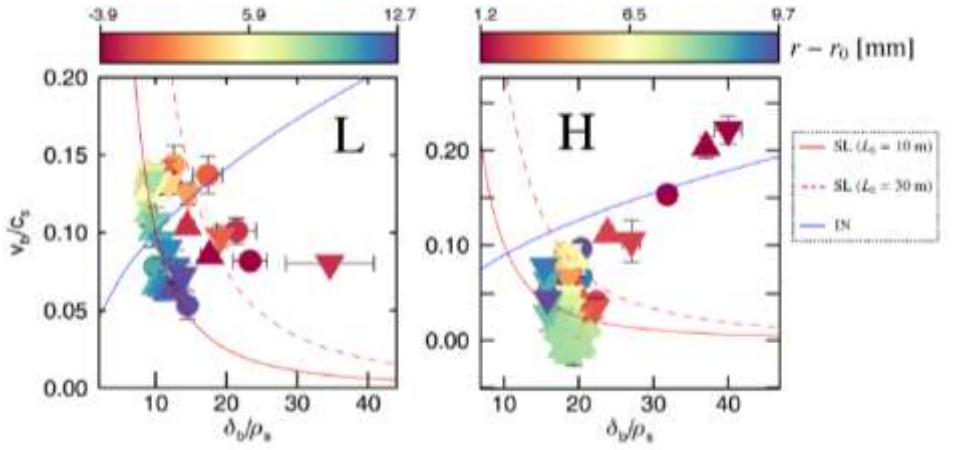

Fig. 3.17 Blob normalized velocity as function of normalized size in L (left) and H-mode (right). The symbols represent the 3 reference shots: circle (#39136), up-triangle (#39140), and down-triangle (#39143). The red lines stands for the sheath limited velocity scale (SL) at Lk = 10 m (full line) and Lk = 30 m (dashed line), the blue curve represents the inertial scale (IN). The colorbar refers to the position of the detected blob with respect to the separatrix in mm.

reconstruction of the magnetic field in RFX-mod tokamak discharges. Such cases were performed to study the dynamics of turbulent filaments observed at the edge. Two different edge regions were identified, one with higher and one with lower connection length, connected to different region of the vessel: this is important because it may influence the probes measuring the filament structures at the edge. Results were presented at the EFTSOMP 2019 Workshop in Padova[64].

Current carrying ELM fine structure in the SOL of RFX-mod tokamak: Similar statistical techniques were applied for the study of electromagnetic features of ELM events detected during the occurrence of H-mode regime, biasing induced, in RFX-mod. In particular detailed electrostatic and magnetic features analysis revealed a complex fragmented and radially extended filamentary structure within a single ELM. Strong peaks in parallel current density J_{tor} are observed to characterize the ELM bunch. Analogous features were observed in COMPASS[65] and RFX-mod ELM structures. Indications of ELM fragments of moving towards far SOL is always observed. The time evolution of near-SOL radial profiles (RFX-mod) allowed the reconstruction of a

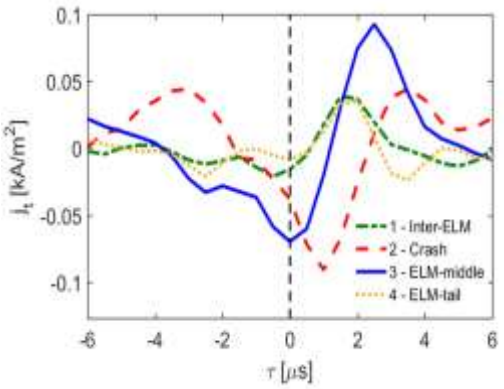

Fig. 3.16 Average parallel current density measured at different phase within the ELM bunch burst

[64] G. Grenfell, M. Spolaore et al. EFTSOMP 2019 Workshop, Padova, July 15-16

[65] M. Spolaore, et al. *Nuclear Materials and Energy* 12 (2017): 844-851.

sequence consistent with the cyclical establishment of strong edge gradients followed by the ejection of clusters of filamentary fragments (ELMs) with electromagnetic features (Fig. 3.16). This behavior is confirmed by the 2D potential map reconstruction. Within the ELM burst cycle (RFX-mod) the ejection phases were identified with the “crash” and “middle phase” where radial propagation of e.m. filaments recovers transiently the L-mode turbulent filament features. Results were presented as invited contribution [66] at the 3rd Asia-Pacific Conference on Plasma Physics 2019.

3.1.7. *Effect of RFP reconnections in global power balance*

Reconnection events related to transition from Quasi Single Helicity (QSH) to Multiple Helicity (MH) regimes represent an important power loss channel. A statistical analysis of the effect of dominant mode crashes on power balance during RFX-mod discharges has been performed by considering the associated variation of magnetic energy W_m. Such a quantity can decrease during a back transition event of about $\Delta W_m = -0.1/-0.3$ MJ, corresponding to a relative change between −1% and −5%. Given the number of reconnection events for second, the total power dissipated is $P_{rec} \approx 16–18$ MW, nearly half of the input power $P_{ohm} = V_{loop} I_p \approx 30–40$ MW. This result is similar to previous estimates done in the MST RFP[67]. An improved control of the helical states duration and of the frequency of back-transitions to MH regime, as expected in RFX-mod2[68], is expected to reduce this power loss channel.

3.1.8. *Studies of m=1 wall-locking in RFX-mod and RFX-mod2*

Study of wall-locked wall-unlocked transition of m=1 TM in RFX-mod: The transition between fast and slow MHD mode rotation branches under the application of magnetic feedback boundary conditions was experimentally characterized in RFX-mod and documented in [69] and the role of the main ion mass in determining the current threshold for such transition was shown in [68]. In such experiments fast (few kHz) mode rotation was obtained below a plasma current of about 90-100 kA, provided MHD feedback control was applied for higher current values. During the wall-unlock phase the MHD feedback system currents goes close to zero but this does not imply that it is not necessary to avoid wall locking. A systematic set of experiments with the active feedback control selectively switched on and off on specific

[66] M. Spolaore et al. 3rd Asia-Pacific Conference on Plasma Physics, November 4-8, 2019, Hefei, China, MF-I31, invited.
[67] Ji H. et al 1995 Phys. Rev. Lett. **74** 2945
[68] L. Marrelli et al 2019 Nucl. Fusion **59** 076027
[69] P. Innocente et al., Nucl. Fusion 54 (2014) 122001

modes during the discharge dynamics was performed and it has been recently reported in [70]. In particular, for the particular RFX-mod rotating discharge regime the lack of control of the m=1,n=11 mode was leading to wall locking while the same was not observed in a different discharge where the more internally resonant m=1,n=8 mode was left uncontrolled. This is related to the natural rotation frequency profile of the m=1 modes, shown in Fig. 3.18, which is tightly correlated with the plasma flow and in particular with it reversal near the edge. Without feedback action, the mode (1,11), which is naturally slowly rotating, penetrate the stabilizing shell and grow to a level sufficient to wall lock all other neighbor modes. On the contrary, when feedback is switched off on the (1,8) mode, no radial field penetration of the mode occur and wall locking does not occur. RFXLocking simulations aiming at reproducing this behavior, including diamagnetic effects are ongoing.

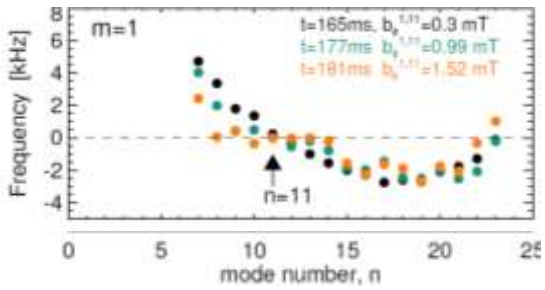

Fig. 3.18. Frequency spectrum for m=1, n modes. Different colors refer to different time instants, corresponding to different values of the increasing m=1,n=11 mode amplitude (indicated in the legend).

RFX-mod2 m=1 tearing modes wall locking threshold: Time dependent RFXLocking simulations with a simplified geometry have been performed in order to compare the wall locking threshold for RFX-mod2 and compare it with RFX-mod [71]. Experimental m = 1, n = 7–19 and m = 0, 1–12 TMs amplitudes at the resonant surface are taken as input, estimated from RFX-mod edge measurements and Newcomb's equation. In particular for RFX-mod2 the amplitude of tearing modes is conservatively assumed equal to RFX-mod. The simulated mode amplitudes grow linearly from zero at the beginning of the simulation up to the experimental value at 80 ms, in order to replicate the behavior during the start-up phase. The simulated tearing modes start in the fast rotation regime and eventually transit in the slow feedback controlled one when the mode amplitudes exceed the wall locking threshold, which occur at very different times for RFX-mod and RFX-mod2 (Fig. 3.19). In fact, wall locking in RFX-mod simulations occurs much earlier than in RFX-mod2, corresponding to a ratio of approximately 5 among locking thresholds in the two cases. This is consistent with previous estimates based on RFXLocking simulations with a simplified geometry (single mode, single conducting structure with thick shell model).

[70] T.Bolzonella, et al., "High-n tearing mode dynamics in fast rotating RFP plasmas" , 46th EPS Conference on Plasma Physics – Milan, July 8-12 2019

[71] Marrelli L. et al, 2019 Nucl. Fusion 59 076027

The increase of the TM locking current threshold could be spoiled by the presence of error field spectra due to the shell gap. RFXLocking simulations have been performed for the error field spectra computed for different choices of shell gaps, shown in activity report 2018 (Butt-joint, Overlapped, Separated Sleeve). A parametric study showed that, provided that MHD mode feedback system is operating, in the RFX-mod2 overlapped gap TMs lock to the wall only slightly earlier than the no-error simulation, *indicating that a localized error field feedback control system is not necessary.*

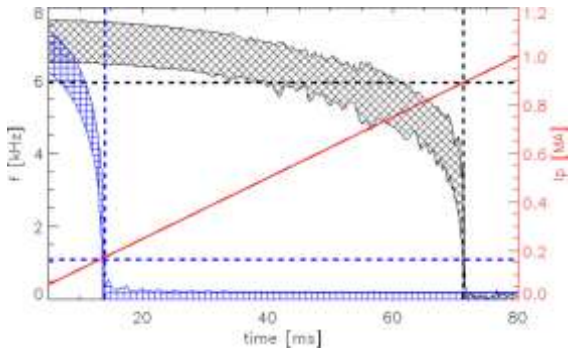

Fig. 3.19. Simulated time evolution of mode rotation frequencies with amplitude of tearing modes linearly increasing in time. The shaded areas enclose the time traces of m = 1, n = 7–19 mode rotation frequencies: Blue for RFX-mod; black for RFX-mod2. Red line: plasma current corresponding to the simulated tearing modes amplitude.

Error Fields due to reconnection events in RFX-mod2: The error fields due to faster phenomena, related to MHD modes dynamics, cannot be computed with the "thin shell" approximation used for the previous section. Due to the new RFX-mod2 boundary, fast phenomena similar to the ones observed in the Madison Symmetric Torus are expected. During a regular sawtooth activity, equilibrium current profiles slowly peak and suddenly flatten at the sawtooth crash, determining a fast inward displacement of the plasma column generating a large error field at the poloidal gap (which is a butt-joint in MST) finally leading to wall locking of m=1 tearing modes. A relative comparison of error fields between a butt joint gap (as in MST) and the overlapped shell design (as in RFX-mod2) has been performed[72] in order to determine if wall locking of tearing modes can occur.

The code CAFE-hVI[73] have been adopted, which implements an integral formulation to solve for eddy currents on a polyhedral mesh of generic topology (i.e. including an arbitrary number of cuts and holes) with a very efficient topological pre-processing algorithm. The determination of sawtooth-induced eddy currents adopts a simplified vacuum approach: the plasma is modelled with a thin sheet of current flowing along a toroidal surface inside the vessel. The time behaviour of the m=1,n=0 harmonic of b_r at plasma radius is chosen to increase in 0.25ms up to 1mT and then remains constant. Fig. 3.20b and c display the time evolution of the radial field at r=0.495 and θ =90° in a toroidal region around the shell edges

[72] Marrelli L., et al. "MHD Dynamics and Error Fields in the RFX-mod2 Reversed field Pinch", 46th EPS Conference on Plasma Physics – Milan, July 8-12 2019,

[73] Bettini P., et al., IEEE Trans. Mag. 53 (2017) 7204904

(at θ=0° for the butt joint, and 5° and 24° in the overlapped shell). A significant localized radial field enhancement takes place for the butt joint: a very high radial field (up to 150mT) is concentrated in toroidal region extending few degrees. Though qualitatively similar to the error field shape during the start-up phase, it affects a narrower toroidal region. Red dashed and dotted time traces in panel a represent the time behaviour of the field for two angles as depicted in panel c. A significant reduction (by a factor 10-20) of error field occurs in the overlapped concept (panel b). Interestingly, in the latter case, the error field evolves in two phases: initially (between 0.1 and 0.75ms), only one peak occurs, located at the inner edge of the copper shell; later on, a second lower peak, corresponding to the outer edge of the overlapped shell appear. At high frequency, i.e. on faster time scales, the difference between the overlapped and the butt joint scheme is even more dramatic than in the start-up case. Even though the error field is highly localized in the first phase, its amplitude is significantly reduced: this confirms that the overlapped gap design, which is under implementation in RFX-mod2, is considerably better for an RFP boundary.

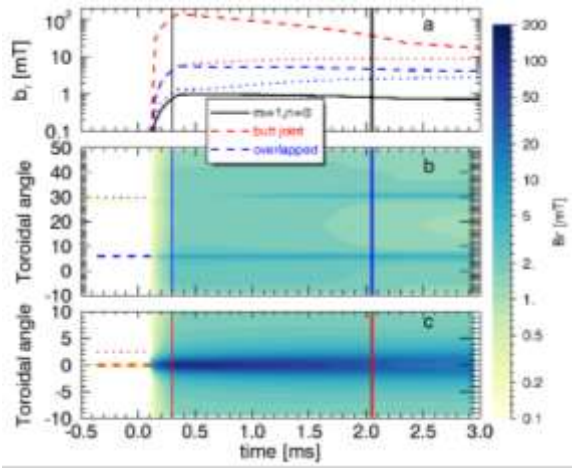

Fig. 3.20. ***Time evolution of radial error field during a reconnection event for overlapped (b) and butt joint (c) design. Panel a show time traces in selected locations and the m=1,n=0 harmonic***

3.1.9. *MHD equilibrium and control*

Studies on RFX-mod2 tokamak equilibria: A model-based approach has been used to define tokamak plasma equilibria with DEMO-like shape conditions (i.e. δ>0.3, κ>1.5)[74] including the possibility of either single or multiple X-points also with negative triangularity. The new shape conditions would allow achieving higher plasma current and plasma density values at the same toroidal magnetic field and safety factor limits of previous RFX-mod tokamak operations. The feasibility of the new equilibria has been explored in terms of coil current requirements and vertical stability analysis. The whole study is carried out with a model-

[74] G Federici, C Bachmann, L Barucca, W Biel, L Boccaccini, R Brown, C Bustreo, S Ciattaglia, F Cismondi, M Coleman, et al. Demo design activity in europe: Progress and updates. Fusion Engineering and Design, 136:729 - 741, 2018.

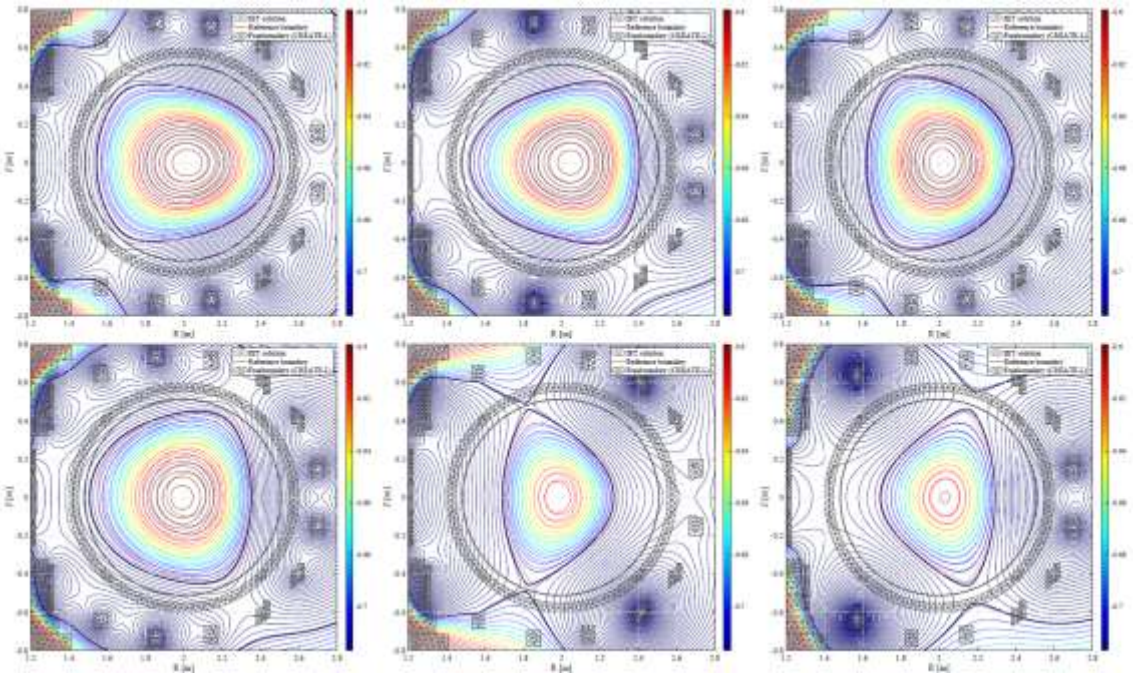

Fig. 3.21. ***Free boundary flux surfaces computed by CREATE-L code with the set of currents found by IET (solid lines); the inverse IET solution is also represented (dotted lines) in order to validate the reconstruction of RFX-mod2 plasma equilibrium.***

based approach by using the open source code Inverse Equilibrium Tool (IET)[75] to define the desired plasma equilibria satisfying engineering constraints on coil currents and the CREATE-L code for vertical stability analysis. The analyses confirm that RFX-mod2 is a very flexible device, able to perform DEMO-like shaped tokamak operations with low requirements on both magnitude and distribution of active coil currents exploring a wide range of shape parameters including negative triangularity conditions. Several examples of configurations that can be realized in terms of RFX-mod2 engineering constraint are shown in Fig. 3.21.

3.1.10. *Studies on RFP machine as Neutron Source*

D-T controlled nuclear fusion is of high interest, not only for its direct application as energy source, but also as large 14.1 MeV neutron source where high energy neutrons could be used in many applications, such as: energy production in Fusion-Fission Hybrid Reactors (FFHR), fertilization of nuclear fuel, nuclear waste transmutation and radio-pharmaceutical production. D-T fusion parameters for neutron source applications are less demanding with respect to fusion power plants: the fusion core of a FFHR could have a power of about 100 MW with $Q < 3 \div 5$, i.e. much less than a reactor like DEMO.

[75] D Abate and P Bettini. An inverse equilibrium tool to define axisymmetric plasma equilibria. Plasma Physics and Controlled Fusion, 61(10):105016, 2019

Specific features of the RFP configuration as a fusion neutron source are: ohmically heated plasma; toroidal field winding rated for a low magnetic field (one-two orders of magnitude lower than Tokamaks); very simple, robust and cheap construction; easy access for remote handling and maintenance. Quasi-continuous neutron production, as required in a hybrid reactor, is guaranteed by a continually pulsed operation without the need of additional current drive systems.

A first study[76], based on the experimental RFX-mod scalings (electron temperatures, plasma currents, loop voltages during flat top), has shown a significant neutron production from D-T reactions in a large RFP device (R=6m, a=1m) with 15–20 MA plasma current and ≈10–15 keV temperature. A neutron production rate in the range of 10^{19} n/s and a wall neutron load of 0.2 MW/m^2 is estimated.

In 2019 studies concentrated on the proposal of a pilot RFP neutron source in which a staged experimental approach[77], with increased complexity and investment, was utilized to tackle the existing issues related to scientific and technological aspects, and to test the D-T operation at reduced fusion power (P_fus ≈ 30 MW, Q ≈ 0.4). RFX-mod scalings indicate that a machine with R=4m and a = 0.8m is able to guarantee the Volt-second necessary to obtain up to 14 MA plasma current with a 8 s flat-top phase and a continuous pulsed operation.

In order to optimize the schedule, minimize investment and maintain some degree of flexibility, a three-staged approach has been identified, in which the experiment, built in a nuclear site, is gradually upgraded. The first phase is mainly devoted to improve the RFP physics understanding by extending scaling laws and plasma knowledge at higher plasma current values. A machine with the same layout and load assembly (vessel, copper toroidal field winding and saddle control coils) as the final device is considered, but with non-superconducting magnetizing and poloidal field windings, no blanket and D only operation. In this configuration, up to 8 MA with 4 s flat top could be reached in a single pulse, allowing the extrapolation of the plasma performances up to the full performance (14 MA).

In the second stage, the magnetizing and poloidal field windings are replaced by superconducting coils and the power supply system is upgraded in order to allow continual pulsed operation. The near unitary plasma heating system is obtained with the Magnetic

[76] R. Piovan et al. “A continuous pulsed Reversed Field Pinch core for an ohmically heated hybrid reactor”, *Fusion Eng. Des.*, vol. 136, pp. 1489–1493, 2018, doi: 10.1016/j.fusengdes.2018.05.040.

[77] R. Piovan et al. “Status and Perspectives of a Reversed Field Pinch as a Pilot Neutron Source”, *IEEE Trans. On Plasma Science*, in press

Energy Storage and Transfer (MEST), an innovative power supply system[78]. The technological issues at full plasma performances are tackled with operation in D.

Finally, in the third stage, the blanket is introduced, along with the systems required for tritium operation, allowing the full test of the pilot as neutron source.

3.2. *ITER Physics Work Packages*

3.2.1. *Introduction*

The diffused collaborations within the ITER Physics experiments (JET, AUG, TCV and Compass) have temptatively been oriented towards topics of interest to DTT, with an increased emphasys, among others, on divertor and edge physics, impurity transport, real time control issues, L-H transition, beam plasma interactions, disrutpion avoidance and runaway control. Also the works done for JT-60SA and W7-X have assumed the strong connotation of peparatory activity for DTT, with design of diagnostics in a supercontucting device with Electron Cyclotron Electron heating, modeling of divertor plasmas and scenarios preparation by means of integrated modeling tools. Activity specific to DTT have increased, with significant work on divertor scenarios integrated with pump modeling, diagnostic integration and design of the neutral beam injectors. A specifc preparatory workshop on DTT diagnostics has been organized at CFRX as part of the series of DTT Design Review Meetings in order to allow drafting diagnostics specifications with inputs from physics models. Several activities for DT have been caried out withing EUROfusion packages, DTT-ADC and PMI.

3.2.2. *MST1*

3.2.2.1. Topic 06 Disruption prediction and avoidance

Within the high-level topic T06 on ASDEX Upgrade (AUG), previous work aimed to reconstruct the eigenfunctions of the main tearing modes (TM) during the disruptive phase of a high–density discharge, showing that the m/n=2/1 island determines super-diffusive transport for electrons, which has an obvious impact on the thermal content of the plasma[79]. Nevertheless, passive structures surrounding the plasma, such as the vacuum vessel and the Poloidal Flux Loop (PSL), interact with the current produced by the TM, which possess frequencies in between 25 Hz and 10 kHz (1.7kHz in the case studied in[79]). These additional

[78] R. Piovan et al, “MEST: A new Magnetic Energy Storage and Transfer system for improving the power handling in fusion experiments”, *Fusion Eng. Des.*, vol.146, pp 2176-2179, 2019, doi: 10.1016/j.fusengdes.2019.03.146

[79] G.Spizzo, et al., Nucl. Fusion **59**, 016019 (2019)

currents pollute the signal of B_θ at the pick-up coils, which are used to constrain the values of the TM eigenfunctions at the edge. During 2019, a magneto quasi–static integral formulation[80] has been used to evaluate the response of AUG passive structures on each pick–up probe, which allows calculating the amplitude of each TM with periodicity m/n and given frequency. In the end, the *real* amplitude of each TM with periodicity m/n, cleaned of the contribution of the PSL and vacuum vessel, can be obtained as a simple, complex matrix inversion.

3.2.2.2. Topic 8- Runaway electron beam physics and MGI in support of ITER SPI

Experiments on runaway electrons (RE) have been performed during the year 2019 both in AUG, TCV and Compass devices, as highlighted in the following.

AUG

Few shots have been dedicated to investigate the effect of 3D magnetic perturbations (MP) externally applied before the disruption on RE beams. Indeed, it had already been shown that some kind of MP with toroidal number n=1 can reduce the final runaway current with an efficacy that depends on the MP poloidal spectrum[81]. The latter can be varied by changing the relative phasing ($\Delta\phi$) between the currents flowing in the upper and lower set of RMP coils. In the new 2019 experiments the role of intrinsic error field on RE mitigation has been investigated considering different RMP coils configuration (i.e. the absolute phase Φ) producing the same relative $\Delta\phi$. Varying the coils absolute phase has a partial impact both on the final RE current and on the pre-disruption electron temperature profile. Two discharges executed with the application of n=2 MP did not show the expected effect on the RE beam generation but only later it was discovered that one of the lower RMP coil had a wrong polarity The discharges will be repeated again during the 2020 campaign.

Modeling activity for the interpretation of past results is also in progress. In particular the hamiltonian guiding center code ORBIT (relativistic version[82]) has been adapted to RE discharges in AUG using as input for the MP the results provided by the code MARS-F.

TCV

In TCV, as in the previous years, the scenario for RE experiments has been characterized by 200kA low density ($<2\cdot10^{19}m^{-3}$) discharges with a toroidal magnetic field of 1.4T. Part of the campaign has been dedicated to investigate the RE beam stabilization by the control system. Many discharges have been performed to test the RE generation in different shapes

[80] P.Bettini, et al., IEEE Trans. Magn., vol. 53, no. 6, Jun.2017

[81] M. Gobbin et al 2018 Plasma Phys. Control. Fusion **60** 014036

[82] M. Gobbin et al Nucl. Fusion **57** (2017) 016014

of the plasma in particular varying the triangularity and the elongation. Finally, a fraction of the shots has been finalized to optimize RE generation following Ne injection (instead of Argon) and to test for the first time Krypton injection too. The collected data are implemented as inputs for reliable and robust physics modeling. The main results concerning both AUG and TCV RE experiments have been presented in an invited talk by G.Papp at the 46th EPS Conference on Plasma Physics (8-12July 2019, Milan).

COMPASS

In the framework of MST1 activity on complementary devices, runaway electrons mitigation experiments by Resonant Magnetic Perturbations (RMP) have been carried out in COMPASS too, in continuity with those already performed in 2017/2018[83]. For the first time, perturbations have been generated also by the high and low field side midplane error field correction coils. The amplitude of the current in the coils (I_{RMP}) has been varied (1-4kA) as well as the time of the MP application. Among the main results, it was found a reduction of about 35% in the RE beam duration for the most efficient midplane coil configuration when I_{RMP}=3.5kA. A modeling activity to reinforce the interpretation of the experimental results has recently begun using more numerical tools and will be continued next year. The experiments on RE mitigation in COMPASS have been presented [84] at the 46th EPS Conference on Plasma Physics (8-12 July 2019, Milan) and as an invited talk[85] at the 18th European Fusion Theory Conference (7-10 October 2019, Ghent).

3.2.2.3. Topic 9: Error field detection and control

A characterization of the intrinsic EF in AUG experiment has been performed. This study has been carried out by analysing data from multiple diagnostics, i.e. magnetics, rotation, density and temperature profiles, and vacuum modelling by means of the CAFE code. The framework for attempting the coupling between plasma response and vacuum modelling has been done by utilizing the codes CAFÉ and MARS-F. Two sets of experiments have been performed in AUG to experimentally identify the intrinsic EF by the use of the compass scan method, both in low and high beta plasma regimes. Unfortunately the experiments performed were compromised by a mistake on B5L coil polarity connection and consequently the data collected are not useful. Reports on these activities can be found in [86]:

---

[83] O. Ficker *et al* 2019 *Nucl. Fusion* **59** 096036

[84] E. Macusova , M.Gobbin et al. 46th EPS Conference on Plasma Physics P1.1057

[85] E. Macusova , O. Ficker, T. Markovic, M. Gobbin et al. talk I-09 European Fusion Theory Conference (7-10 October 2019, Ghent).

[86] https://users.euro-fusion.org/iterphysicswiki/index.php/WPMST1_2019:_Topic_9

A collaboration with IPP Prague has started with the target of modelling plasma response in COMPASS plasmas and investigate mode locking thresholds with the MARS-F code. A modelling strategy to calculate 3D plasma response has been implemented in the OMFIT modelling framework and applied to COMPASS equilibria(Fig. 3.22).

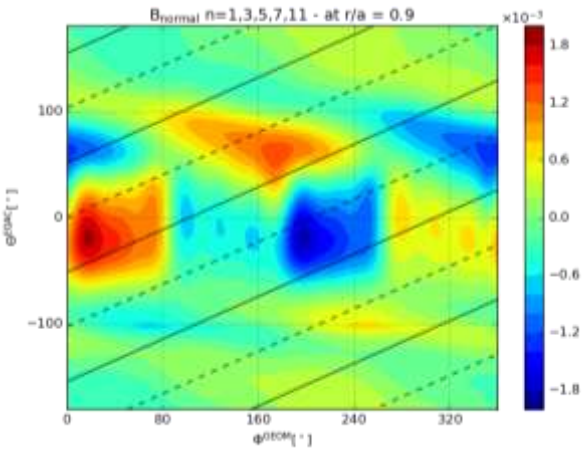

Fig. 3.22 3D plasma response map on q=2 surface. Calculated by inverse-Fourier transform with n=1,3,5,7,11.

3.2.2.4. Topic 16 Effect of filamentary transport on heat and particle loads

The investigation of filamentary transport in high density regimes in MST1 devices has continued during 2019. The experimental activity has been carried out on both ASDEX-upgrade and TCV both in L and H-Mode . In AUG experiment in ITER relevant power conditions has been perfomed with P/R ~ 6.4 MW/R and a reached Greenwald fraction of ~ 0.94. It has been clearly shown (Fig. 3.23) that in these condition the outer target is in partial detachment condition but the upstream density profile clearly exhibit a strong shoulder, i.e. flatter profiles. A strong dependence on the fueling levels has been observed with a more pronounced shoulder whenever puffing from the mid-plane suggesting a relationship to the midplane neutral density. Similar investigation has been carried out on TCV where for the first time H-Mode shoulder formation associated to small-ELM regime has been observed. On TCV the investigation has been performed in L-Mode as well where experiment of shoulder formation with the newly installed baffles have been performed.

3.2.2.5. Topic 03 ELM control and suppression towards ITER & DEMO and Topic 11 Fast ion confinement, transport and control under ITER relevant conditions

An investigation on AUG NBI fast ion losses due to non-axialsymmetric magnetic fields generated by Resonant Magnetic Perturbation (RMP) has started, in particular for shots aimed at ELM suppression/mitigation . The goal is to see if fast ion losses generates a non-balanced radial current[87], which affects the radial electric field[88]. This analys will be applied to shots of the new campaign to support the experiments. An evaluation of AUG experimental data has started to identify the best comparison cases to test the modelling tool, i.e. discharges with and without RMPs but with similar main plasma parameters. The investigation is carried out by means of ASCOT[89] Monte Carlo code for NB fast ion modelling in plasmas. At the moment, some candidate shots for testing this analysis have been identified, and the necessary modification of ASCOT code to calculate the radial current of fast ions have been implemented. The activity should continue in 2020.

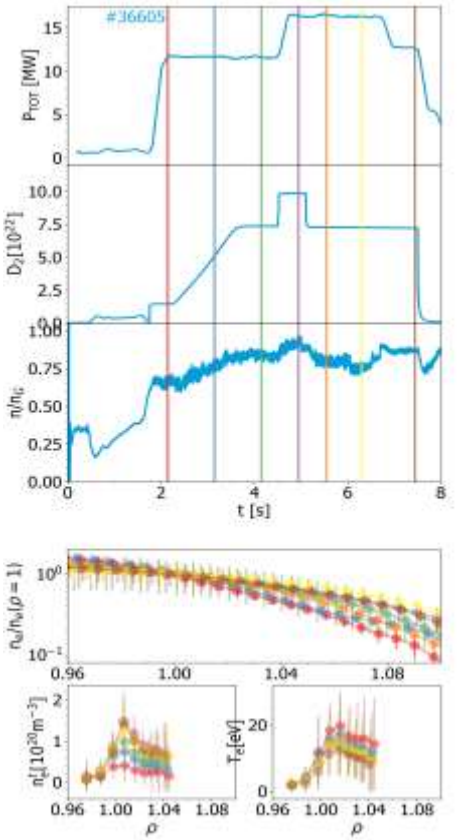

Fig. 3.23 AUG shot at high power. From top to bottom. Total power, total fuelling and Greenwald fraction as a function of time. The two bottom panels provide SOL density profile normalized to the density at the separatrix as well as density and temperature a the

3.2.3. *JET1*

3.2.3.1. T17-05 Equilibrium reconstruction

In the framework of deliverable D3 ("linear and non-linear gyrokinetic modelling of pedestal transport; assess whether results are consistent with inter-ELM evolution, pedestal structure, and limitations on pre-ELM pedestal pressure"), the activity related to the study of the isotope effect on pedestal micro-instabilities has further proceeded. Two couples of H/D discharges characterized by the same stored energy and the same input power have been compared, artificially changing the main ion mass (D to H, and vice versa) so as to

[87] Heikkinen J.A. et al., "Neoclassical Radial Current Balance in Tokamaks and Transition to the H Mode", PRL 84.3 2000

[88] T.E. Stringer 1995 Nucl. Fusion 35 1008

[89] E. Hirvijoki, et al., Comput. Phys. Commun. 185 (2014) 1310–1321.

disentangle isotope from profile effects. The analysis has been carried out with the gyrokinetic code GENE in the whole pedestal region, spanning from low-wavenumber KBM/ITG modes to high-wavenumber ETG instabilities. Mixing length transport estimates show only a moderate isotope effect across the steep gradient region, with higher conductivities in H than in D in gyro-Bohm units. Another activity in this task has been related to a benchmark among 3 different codes (GENE, GS2 and GKW) in the pedestal region of a single discharge. Very good agreement in the linear results has been found, both in the low and high wavenumber range, particularly showing an ETG dominance in the steep gradient region with the occurrence of both slab and toroidal ETG branches.

3.2.3.2. M18-06 Impact of inner leg flux geometry on W influx

The aim of the experiment, relying on 2 sessions, was to study the possibility to reduce the tungsten influx in the core of the plasma in the baseline and hybrid scenarios presently developped for the DT campain. The experiment was based on previous indications that showed a significan influx of tungsten from the inner vertical target and inner horizontal divertor top. In the experiment a reduction of the flux expansion at the inner leg and a stronger gas-puffing from the inner target were proposed. The aim of the flux expansion reduction (also, flux compression) was the mitigation of the interaction with the high field side of the divertor and a better screening toward the core of tungsten influx coming from the divertor. Before the experimental campain new equilibrium with flux compression was achieved by reproducing reference equilibria previously executed during relevant JET_ILW pulses with the CREATE-NL code[90]. Then, an optimization of the currents in the divertor coils was performed[91] to keep the plasma current and the plasma shape constant outside the divertor region where the flux compression was achieved. Taking also advantage from reversing the polarity of the divertor coil closest to the inner strike point (ID1), an experimental poloidal flux compression up to over 40% was achieved at the inner target and a poloidal flux compression of 8% on the inner strike point plane (with respect to equilibria performed with ID1 = 0). Due to failure of variuos JET components like NBI and RF heatings only a small subset of the planed configuratious have been tested, in particular flux compression scan on similarly heated discharges was achieved only for the baseline scenario. In this scenario the final effect of the flux compression was an increase of core radiation due to a corresponding growth of the tungsten content in the core. Indeed, preliminary data analysis show that, unexpectedly, tungsten influx increased far from strike points by about 10% and remained constant at the strike points. Data analys on the

[90] R. Albanese, et al., Fus. Eng. Des. 664-667 (2015) 96
[91] G. Calabrò, et al., Fus. Eng. Des. 115-119 (2018) 129

experimental measurements like spectroscopic and infrared camera is presently underway to better qualify the effect of the flux compression. Also edge modeling has started with the edge codes SOLEDGE2D[92] and EMC3[93] to understand the reason of experimental results.

Infrared camera measurements have been collected to evaluate heat flux deposition profiles in the different experimental conditions to assess heat load compatibility with the divertor material. Using the JUVIL software, the temperature profiles and heat flux profiles for the areas of interest inside the vessel have been analyzed and comparisons have been made for the considered discharges.

3.2.3.3. M18-41 Divertor geometry effect on detachment and SOL

The way different divertor configurations in different recycling conditions influence both the upstream SOL and the upstream Pedestal has been investigated. The experiment has been run with different levels of fuelling both in Horizontal Target (Tile 5 both Stack D and Stack C) and in Vertical Target configuration. The recycling condition has been determined both with target Langmuir probes and spectroscopically. Clear variation of the upstream SOL profile as well as pedestal properties have been observed (Fig. 3.24). Experiments exploring different recycling condition achieved through N_2 seeding have been performed as well. In this case even though high radiation and high recycling regime is obtained, the pedestal profile and height seem to be less degraded. The experiment will continue next year exploring the isotope effect of the described mechanisms during the T campaing.

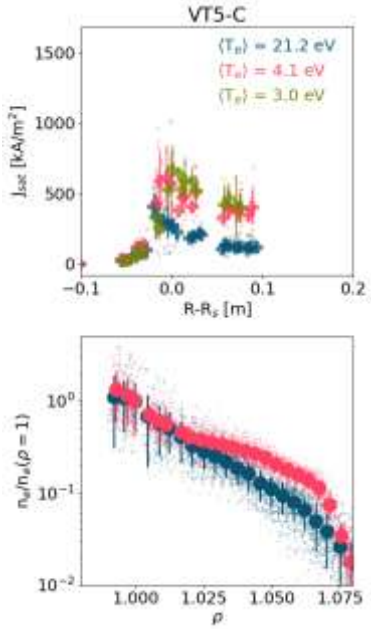

Fig. 3.24 Top Ion saturation current profile at the target at 3 density values and target temperature. From blue to green the plasma is moving towards high-recycling regime. In the bottom panel the SOL density normalized to the value at the separatrix exhibits a clear shoulder when the plasma enters a high-recycling regime

3.2.3.4. M18-09 WP: Prepare integrated RTC schemes for scenarios

The development of several real-time controllers and RAPTOR suites has been performed. The real-time controllers, which act for example on beta, plasma density, auxiliary heating, ELM frequency, once tested their robustness, have then been delivered for

[92] H. Bufferand, et al., J. Nucl. Mater. S445-S448 (2013) 438
[93] D. Harting, et al., J. Nucl. Mater. S540-S544 (2011) 415

exploitation during JET campaign. Such tools have been used for example to reach the target of the experimental proposal, to assess high plasma performance especially when exploring baseline, hybrid and advanced tokamak regimes, to protect the integrity of the device itself, for example injecting the desired Neon concentration content and avoiding excessive thermal loads on the first wall. Real-time controllers which will be relevant for next future DT campaigns, such as the dud detector and the isotope mixture controller, have been developed as well and tested successfully in real-time. Progress on adapting RAPTOR suite in JET device has been carried out in multiple front-ends, for example: MARTe2, real-time, data-interfacing improvement, equilibrium reconstruction, validation and benchmark of neutral rate estimation. The performed activities are reported in [94][95]

3.2.3.5. B18-19 WP: Locked mode avoidance by the use of EFCCs system

A characterization of the intrinsic EF in JET device has been investigated by analyzing a large database of baseline and hybrid discharges and ad-hoc experiments have been performed to identify the optimal Error Field Correction Coil Currents able to minimize this spurious magnetic field source. Such analyses have been carried out both on experimental and modeling sides and have been presented as invited talks in several conferences, i.e. 46 EPS conference, Milan, Italy, PPPL workshop on disruptions, Princeton, USA, ITPA MHD workshop, Garching, Germany.[96]

3.2.3.6. T17-07 isotpe studies (regarding M18-01, M18-02 , M18-19 and M18-23)

Modelling activity has been performed aiming to study the isotope effect (i.e. the anti-gyroBohm behavior where isotopes with higher mass show reduced transport properties) in JET discharges in view of the next high performance Deuterium, Tritium and DT JET campaign. The modeling has the primary goal to identify the operational regimes in terms of plasma current, magnetic field, NBI settings that maximize the neutron yield in Baseline and Hybrid scenarios. The main numerical tool has been TRANSP, both for interpretive and predictive analysis with the TGLF turbulence transport model. The main results are that increasing the plasma current above a threshold (that depends on the specific scenario) a roll-over of the performance can be observed. This is due to the stronger coupling of ions and electrons that result in a plasma with Ti~Te instead of Ti>Te observed at lower current. The fine identification of such threshold depends on the collisionality level at the top of the pedestal, which is still under investigation, with the buinding up of an appropriate database

---

[94] euro-fusion.org/tfwiki//M1809Prepare_integrated_RTC_schemes_for_scenarios

[95] Fusion Engineering and DesignVolume 146, Part A, September 2019, Pages 1364-1368

[96] euro-fusion.org/tfwiki//B18-19:_Locked_mode_avoidance_by_the_use_of_EFCCs_system

of recent high performance discharges. The main experiments and tasks involved in this studies are M18-01 (Baseline scenario development) and M18-02 (Hybrid scenario development)

Moreover, since the ExB sheared rotation (i.e. the toroidal rotation gradient) is a key factor to stabilize the plasma turbulence, a proper comparison among isotopes requires similar plasma rotation profiles when main gas progressively changes from Hydrogen, to Deuterium and to Tritium. The identification of the dependencies of rotation on beam injection geometry, energy and power has been perfomed, giving preliminary indication that the rotation shear is localized in a narrow region close to the top of the pedestal, more effective for higher mass isotopes. The modelling results have been cross-checked also with other numerical tools, in particular exploiting JETTO and ASCOT for interpretive simulation. The main experiments and tasks involved in this studies are M18-19 and M18-23.

3.2.3.7. M18-07 W transport control

Out of the 4 foreseen experimental sessions, only 2 of them have been actually performed, while. 2 sessions have been moved to early 2020, as the high power (>32 MW) required was made available only late in the year. The first 2 sessions have been dedicated to the detailed study of the effect of the ICRH on the W behaviour with a scan of the power deposition profile in mid power discharges - to avoid the overwhelming effects associated with strong rotation – and clear differences in the W distribution have been found. Analysis of the data is ongoing. The attempt to study the W radiation in the pedestal region and yield good reference radiation data for better atomic physics coefficients has been washed out by accidental impurity inflow from the divertor during the session. Next sessions will be dedicated to the study of the penetration of W in high power discharges hoping to reach or get close to the ITER conditions, where W repulsion at the H mode barrier is expected.

3.2.3.8. M18-14 L-H transition studies

One of the aim of this task is to investigate the physics of the existence of a minimum density for the L-H transition power in JET, and to evaluate the importance of the heating to the ion channel at the transition to H-mode. New experiments with NBI heating have been run, with now the ion temperature measurement available also in the plasma core, which is crucial to evaluate the ion-electron exhange power in the power balance. To complete the power balance analysis, interpretative simulations by JETTO[97] within JINTRAC have been run, using ASCOT[98] to model NBI-plasma interaction. The results of the last experiments are

[97] Cenacchi G. and Taroni A. 1988 Rapporto ENEA RT/TIB(88)5

[98] E. Hirvijoki, et al., Comput. Phys. Commun. 185 (2014) 1310–1321.

being analysed, while the analysis of shots from previous campaign has been completed. Results have been presented at the EPS Conference[99]. JET experiments seem to confirm the theory elaborated for AUG plasmas, for shots heated by NBI[100]. This activity should continue in 2020.

3.2.3.9. M18-32 Mitigation of the disruption thermal load with the SPI

The modelling study of JET experiments with shattered pellet injection (SPI) continued in 2019. For the first time, the nonlinear 3D-MHD code JOREK was used to model SPI experiments in a H-mode JET plasma. The simulated pulse is the reference pulse for Scenario 1 “high thermal energy” SPI experiments (JET#89800). Both pure neon pellets and mixed D_2/Ne pellets were considered for this modelling study, which is still ongoing.

Preliminary results show that the plasma thermal quench is obtained when the magnetic field becomes stochastic as a result of SPI-induced MHD modes, as shown in the example of Fig. 3.25, similarly to what was observed in the past with JOREK simulations of D_2 SPI in L-mode JET plasmas [101].

Numerical convergence issues, in particular with significant Ne content, have to be solved in order to complete the scan in impurity content.

3.2.3.10. T17-05 equilibrium reconstruction

Equilibrium reconstruction is a critical issue as it is required to assess several issues concerning both safety and control of the plasma configuration as well as being the starting point for any analysis. In particular its determination during disruptions has to face several specific issues linked to a very dynamical evolution where currents induced on machine structures can become important and non axi-symmetric features appear.

[99] P. Vincenzi et al., “Ion heat channel at the L-H transition in JET-ILW”, 46th EPS conf., P2.1081 , Milano, Italy 2019

[100] F. Ryter et al. 2014 Nucl. Fusion 54 083003

[101] D. Hu *et al.*, Nucl. Fusion **58,** 126025 (2018) https://doi.org/10.1088/1741-4326/aae614

The new EFTP scheme developed this year in collaboration to run EFIT++ on JET with the colleagues provides a pressure constrained equilibrium with an automatic procedure (useful for statistical analysis) fitting well both the pedestal and core regions. Still some issues are present and have to be solved, but the result is quite promising. In particular improvements linked to the polarimetry diagnostics and MSE are presently under study based on the correlation with MHD markers. This scheme was also tentatively applied to equilibrium reconstruction close to a disruption, though it can be used over a limited time evolution interval since at some point profile measurements are not available due to the small plasma size (see Fig. 3.26).

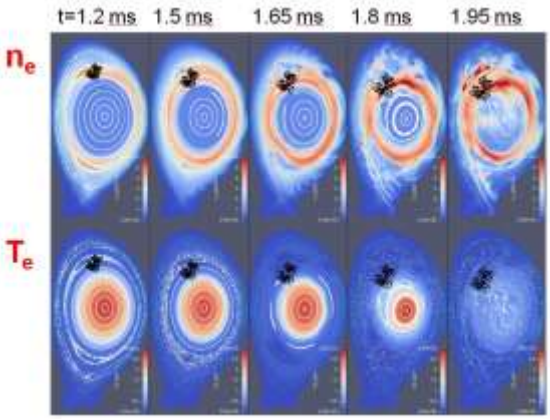

Fig. 3.25 JOREK simulation of thermal quench induced by neon SPI in JET. The position of the fragment cloud is given by the black dots. Poincaré plots (white dots) show that the thermal quench and subsequent density penetration in the core are obtained after the magnetic field becomes globally stochastic due to SPI-induced MHD modes

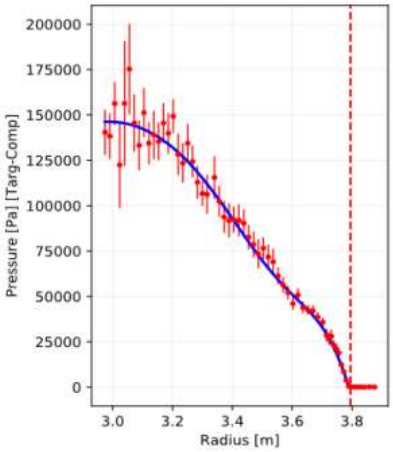

Fig. 3.26 Pressure profile: measurement from HRTS diagnostic (red points) and fitted profile from EFTP equilibrium (blue line).

Two approaches are being followed for JET: an axi-symmetric analysis using EFIT++ and a 3D approach using VMEC/V3FIT. As far as EFIT is concerned, as shown in Fig. 3.27, given the limited experimental measurements the best option is to consider simplified parametrization for internal profile in order to solve for the equilibrium.

Theoretical models for profiles are also being considered to improve the reconstruction in order to reduce the level of degeneracy of the solution due to limited diagnostics information.

As far as a full 3D solution with VMEC a benchmark was done, but induced currents become a critical aspect for the 3D evolution and to this end it is being analysed the possibility to merge VMEC and Cariddi codes to have a full 3D description of both plasma and passive structures. This is quite important as octant specific runs of EFIT (i.e. reconstructions obtained using only diagnostics information coming from a single octant), show that indeed in some case some level of asymmetry is observed. By a Montecarlo analysis it was found that some of these asymmetries can be accepted within the confidence region due to errors

in measurements, but 3D events are observed at JET and these cannot be modelled with a simple approach.

The Faraday angle measured by the polarimeter has been compared with the one yielded by the Stokes code based on the magnetic field is given by different equilibrium reconstruction codes EFTP and EFIT respectively. The result show clearly that the best fit of the experimental Faraday angle is obtained when EFTP is used.

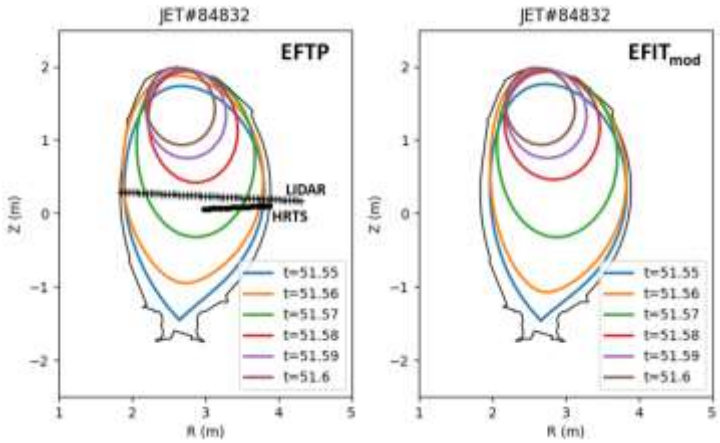

Fig. 3.27 equilibrium reconstruction during a VDE. Different profile parametrization are used: left spline; right: low order polynomial. LIDAR and HRTS view lines are also shown.

We note that the Faraday angle is only marginally disturbed by the Cotton-Mouton effect.

3.2.4. *DTT*

3.2.4.1. Edge modelling

The edge modelling of DTT single-null scenario was performed with the edge numerical code SOLEDGE2D-EIRENE.The main objectives of this activity were: providing scrape-off-layer and divertor plasma conditions in reasonable plasma regimes towards the designing phase of the pumping system; calculating plasma cooling with different seeded impurities and power loads to the divertor in such configuration. The chosen scenario was a medium density scenario ($n_{e,sep}$ = 5.0x10^{19} m^{-3}) with 45 MW of input power, the maximum predicted for the machine. Simulations were performed with no drifts.

Firstly, Deuterium-only simulations were performed, it was found that the maximum input power to obtain partial detachment at the outer divertor is 9 MW. Nitrogen, Neon and Argon were added as seeding impurities to investigate the cooling performances of each element. Nitrogen's cooling performances were studied even if the element is not relevant for DTT operation. Low and high puffing rate for both deuterium and the seeded impurities were fixed, and the simulations were performed by varying the albedo at the pump duct entrance in order to obtain the predicted density at the separatrix. It was found that, for the described scenario, the minimum $Z_{eff.}$ required to reduce the power to the divertor plates below the limit imposed by the tungsten divertor design increases with the increasing of the atomic number of the seeded impurity. It was found that for neon and argon seeding the minimum Z_{eff} is always > 4 in both high and low puffing rate cases. The outcome of the low and high puffing scenario with Neon seeding is being used at KIT as the plasma background for the

simulation of neutral transport in the subdivertor volume for pumps designing. A similar analysis was performed with SOLPS-ITER and a comparison between the two codes has been done. The comparison shows that the two codes return similar plasma parameters but different neutral density (factor 3 to 5) when using the same set of input parameters.

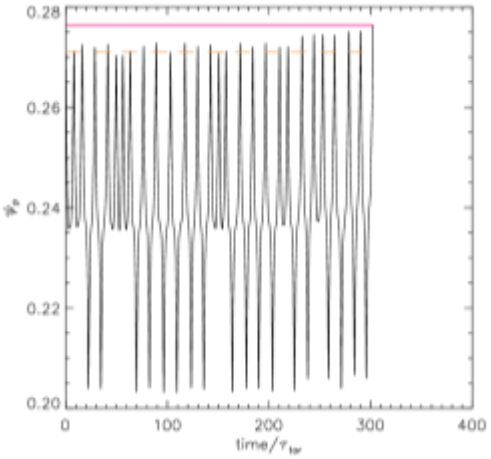

Fig. 3.28 Example of loss of a trapped, fast ion, through the mechanism of resonance with the ripple. The resonance number is n=4. Time is normalized to toroidal transits

3.2.4.2. Fast ions transport

Studies of fast-ion transport are ongoing on the DTT project: fast ions will be generated by the negative neutral beam (NNBI) system which is developed by Consorzio RFX[102]. An issue for DTT is that a Toroidal Field (TF) ripple with a maximum value of about ~0.42% (with respect to the on-axis B) is expected on the LFS[103], and this ripple interacts with fast ions through rather well-known phenomena of ripple-precession resonances[104]. In fact, TF ripple breaks the conservation of the toroidal canonical momentum, $P_\zeta = g\rho_\parallel - \psi_p$, where g is the covariant toroidal field, $\rho_\parallel = v_\parallel / B$ and ψ_p is the poloidal flux which serves as radial coordinate, in such a way that the decrease of the canonical momentum results in the increase of the radial positions of the particles, which are ultimately lost. Regarding the reference DTT configuration (the "Green Book"[103]), and with the parameters of the NNBI project, namely energy E=400 keV and injection angle of ~40° w.r.t. the first wall[102], it is possible to recognize at least four resonances of the type $\omega_b - nN\omega_d = 0$, ω_b and ω_d being the bounce and precession frequency, respectively, and N the ripple periodicity: those resonances are characterized by resonant numbers $3 \leq n \leq 6$. The resonances seem to be well spaced apart (Fig. 3.28), so that the possibility of stochastic overlapping is remote: this is consistent with the calculated contribution of ripple losses in DTT, which are of the order of less than 0.5%, as already published elsewhere[102]. A sensitivity study of the resonance overlap, as a function e.g. of ripple strength and trapped particle population (which depends on the inverse aspect ratio), is anyway ongoing work, since ripple-precession resonances are potentially disruptive for the fast ion trapped population[104]. This work has been

---

[102] P.Agostinetti, et al., Fus.Eng.Design **146**, 441—446 (2019)

[103] https://www.dtt-project.enea.it/downloads/DTT_IDR_2019_WEB.pdf, DTT Divertor Tokamak Test facility Interim Design Report, Edited by ENEA (ISBN 978-88-8286-378-4), April 2019 ("Green Book")

[104] R.B. White, Phys. Rev. E **58**, 1774—1779 (1998)

performed within the Enabling Research project AWP19-ENR-01-ENEA-05 : *Multi-scale Energetic particle Transport in fusion devices*, with principal investigator Fulvio Zonca (ENEA Frascati)[105]. This ER project will be continued during year 2020.

3.2.4.3. The DTT NBI system

Regarding the activities on the design of the DTT NBI system, the conceptual design has been developed considering as main guidelines the maximization of flexibility, feasibility, RAMI and efficiency, and the minimization of cost and weight. The main components of the injector, visible in Fig. 3.29, are: a beam source (composed of an ion source and an accelerator), three beam line components (BLC, i.e. a neutralizer, a residual ion dump and a calorimeter), an absolute gate valve and a duct to connect the injector to the vacuum vessel. As for the NBIs of JT60 and LHD, a design with an air-insulated beam source is proposed, to reduce the vacuum volume, increase the source accessibility and avoid the need of a single large bushing to connect the Transmission Line to the vacuum vessel.

A drawback of this solution is the required clearance between the ion source and the surrounding building structures (at least 2 m, to avoid electrical discharges). The DTT design differs from the Japanese scheme in the choice of the ion source: in fact, it is proposed to use the same Radio Frequency source concept adopted for ITER and developed by IPP Garching. BLC will be ITER-like too, while the vacuum vessel will be without large flanges (differently from ITER) to reduce cost and weight. Only small flanges are foreseen for pumping, diagnostics and BLC supplies, while the BLC maintenance is planned to be from behind, by removing the beam source. For the vacuum pumping, it is foreseen to have a system based on the Non-Evaporable Getter (NEG) pumps.

Also the design of the power supplies for DTT NBI have been developed. The NBI power supplies are composed of: Acceleration Grid Power Supply (AGPS, to feed the acceleration grids), Ion Source and Extraction Power Supply (ISEPS, to feed all the ion source loads) and Ground Related Power Supply (GRPS, to feed the Residual Ion Dump and the correction coils to compensate the stray fields, if any). The AGPS has to provide up to 400 kV on the two acceleration stages (200 kV each), with an output current up to about 60 A. A specific requirement for this application is the capability to switch-off the voltage generation in some tens of μs in case of grid voltage breakdown, to limit the energy delivered to the acceleration grids. For the AGPS, a solution similar to that adopted for the ITER NBI prototype, MITICA, could be envisaged. This would foresee one or two step-down transformers fed by MV network, an AC/DC rectifier, a DC-link capacitor bank and two DC/AC inverters (instead of

[105] Web page of the project: https://www.afs.enea.it/zonca/METproject/

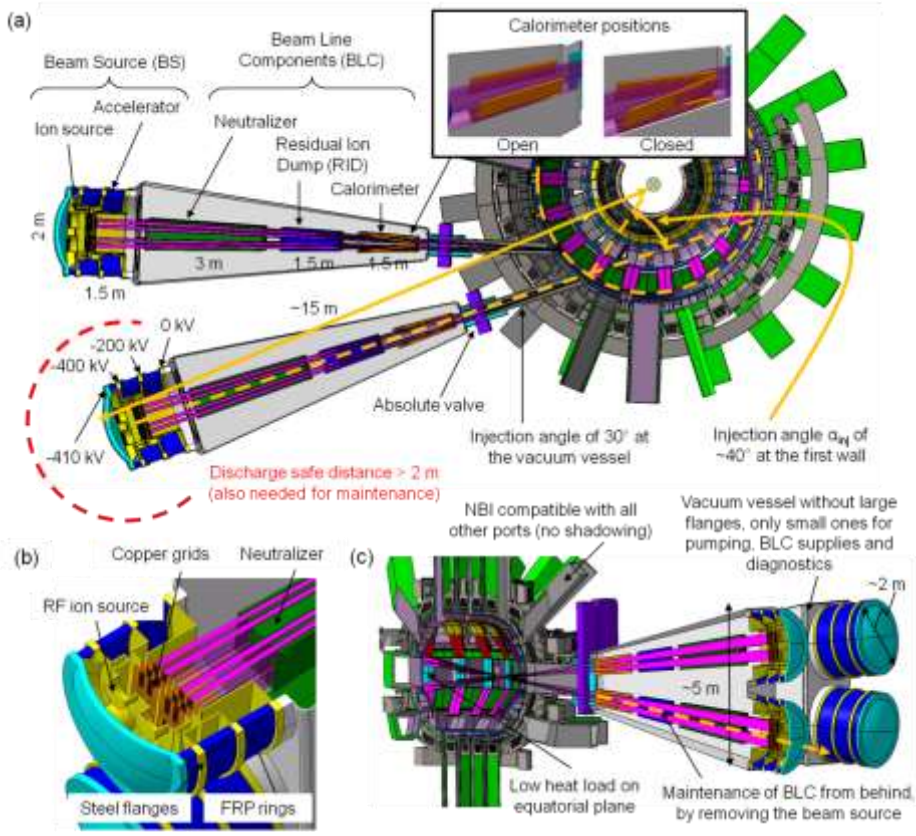

Fig. 3.29 Conceptual design of the DTT NBI conceptual design with main dimensions: (a) view from top; (b) horizontal section view; (c) vertical section view.

five installed in MITICA). Each inverter would fed a step-up transformer, to which is connected a High-Voltage (HV) full-bridge diode rectifier insulated with SF_6. These rectifiers are connected in series to provide the full voltage, and to a DC-filter tank containing HV resistors and capacitors to reduce the voltage ripple. Once filtered, the voltage is transmitted to the accelerator through a SF_6-insulated Transmission Line.

3.2.4.4. Interferometer/polarimeter system

A design of an interferometer/polarimeter system for DTT was presented at the conference LAser Plasma Diagnostics. Laser interferometer/polarimeter systems are used in magnetically confined fusion experiments for simultaneous measurements of the line-integrated electron density and of the poloidal magnetic field. They can also contribute to evaluate the plasma magnetic equilibrium and can provide the real time estimate of the q profile.

An interferometer/polarimeter optical design based on a 7+7 chords scheme was proposed, which is also compatible with a possible Double Null divertor configuration. For the same reason, an equatorial port was used. In the presented design, each chord employs a back reflecting mirror installed in the high field side inner wall close to the divertor, where some plasma-free space is available, and one retroreflector installed in the space behind the low

field side outer first wall. The proposed study had the main goal of demonstrating that a multi-chords interferometer/polarimeter can be accommodated inside the DTT vacuum vessel current design. The analysis of the laser beam propagation along the interferometer/polarimeter chords was firstly addressed and the feasibility of the design was assessed. All the analyses were carried out for different laser source wavelengths (118.8 μm, 50.0 μm, 10.6 μm), to get insight about the advantages and drawbacks of each of them. First estimates of the refractive effects on the probe laser beam were performed, which indicate that these effects are not negligible on the longer considered wavelength, i.e. 118.8 μm. Indeed the interferometric signal decreases to 64% of the unperturbed case. The interferometric and polarimetric signals were also evaluated, when assuming a reference plasma discharge scenario. Considering that a typical error on the Faraday rotation measurements is of order of 1-0.5 deg, the estimated values of the Faraday rotation are then well above the measurement error for the laser source at 118.8 μm. Therefore, we individuate this wavelength as the optimum choice, provided that the refractive effects can be controlled.

3.2.4.5. Divertor and core Thomson Scattering systems

Two different Thomson scattering (TS) systems have been considered, as indicated in the DTT Green Book, aimed to measure the Te and ne profiles in the plasma core and in the lower divertor region. For the latter one we have considered a conventional TS system based on a Nd:YAG laser source, a fiber optic based light collection system and a set of filter polychromators equipped with Si APD detectors [106]. The laser beam and the collection optics share a long and narrow aperture between adjacent cassettes of the lower divertor and the scattering signal is collected from the divertor region by a collection optics system located under the divertor dome. Fiber optic bundles carry the light to a set of filter polichromators, designed to measure T_e as low as 1 eV. Measurements in ~ 30 points with a spatial resolution of 10 mm are possible, with accuracy limited by the plasma n_e and the background light. For the core TS system, two options have been considered. The first option is a conventional system, with a layout similar to that designed for the ITER core TS. Here T_e and n_e are measured along a large fraction of a laser beam crossing the plasma near the equatorial plane and the detection system is again based on fiber optic coupled filter polychromators. The spatial resolution is 5 cm in the central region and 1 cm at the plasma edge. The second option is a TS system based on the LIDAR concept, previously

[106] L. Giudicotti, A. Fassina, R. Pasqualotto and P. Franz, "Design of Thomson scattering diagnostics for the Divertor Tokamak Test (DTT) facility", Proceedings of LAPD19, the 19th Symposium on Laser-Aided Plasma Diagnostics, Whitefish, MT, USA, 22-26 September, 2019, to be published in JINST

implemented in JET, and never adopted again.[107] The analysis of recent advancements in laser and detector technology showed that by the LIDAR approach in DTT it is possible to achieve a spatial resolution similar to that of a conventional system, but with a simpler and reliable experimental set-up.

3.2.4.6. PEX/DTT

Several activities have been launched by PPPT/WPPMI to investigate specific Power Exhaust issues in a Divertor Test Tokamak, and Consorzio RFX has been involved in :

- Divertor interfaces for different divertor options: mechanical connections, integration, remote maintenance
- Non-magnetic divertor diagnostics for control
- Neutrals and impurities model pumping
- In-vessel divertor coils: vertical and radial control; divertor coils(sweping) RWM coils; ELM coils
- Additional heating requirements and impact on plasma scenarios
- Divertor interfaces: pumps functional specifications and requirements

3.2.5. *WPSA*

3.2.5.1. Discharge simulator and Resistive Wall Modes stability

Preliminary numerical activities in the framework of WPSA discharge simulator research were set-up for the 4.2 Hybrid scenario of JT60-SA. Firstly, METIS simulations were performed. Then, static equilibria for the ramp-up and start of flat-top phases were designed with CREATE-EGENE code. In addition, CREATE-EGENE code was set-up and tested for RFX-mod device in order to verify the METIS-EGENE weak coupling in a circular simple case. In the framework of TRA-EEG.AWP18, progress has been made in studies on Resistive Wall Mode stability including drift-kinetic effects, with the self-consistent approach of the MARS-K code[108]. Resistive Wall Mode stability has been studied with toroidal flow consistent with the JT-60SA NBI geometry, for a Scenario-5-like plasma. In the full kinetic description the n=1 mode undergoes strong damping both at very slow and relatively fast

---

[107] P. Nielsen et al. "A LIDAR Thomson Scattering System for the Divertor Tokamak Test (DTT) facility", Proceedings of LAPD19, the 19th Symposium on Laser-Aided Plasma Diagnostics, Whitefish, MT, USA, 22-26 September, 2019, to be published by JINST

[108] L. Pigatto et al. Nucl. Fusion 59 (2019) 106028

toroidal flow. The results of a separate investigations with three damping mechanisms (precession drift, bounce and transit resonance) are summarized in Fig. 3.30. The effect of pressure on the drift-kinetic damping of RWMs has also been investigated. A collaboration framework with QST (Naka, Japan) has been set up for studies on RWM stability. Validation of numerical results with JT-60U experimental data is ongoing within this framework.

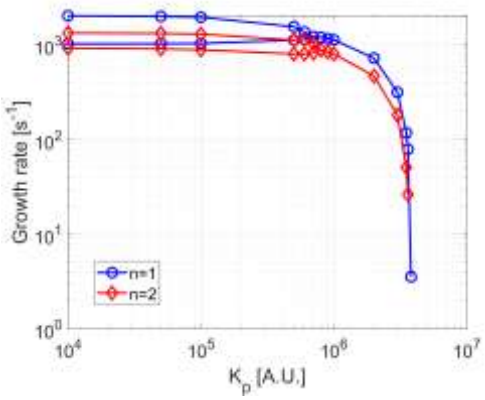

Fig. 3.30 Scan of proportional gain with simultaneous feedback on n=1,2 modes. Poloidal field component used as feedback variable.

A multi-modal version of the dynamic simulator for RWM feedback on JT-60SA has been developed with the CarMa code, as a progress of the work presented in [108]. With this tool, a proof-of-principle eigenvalue study for simultaneous control of n=1,2 RWMs has been carried out. The results in Fig. 3.31 show simultaneous stabilization of both modes is achieved with an ideal proportional controller[109]. A new approach to modelling RWM stability in presence of 3D structures has been developed[110] , in order to take non-ideal effects (plasma flow, kinetic effects) into account. This new approach, which represents an improved version of the CarMa coupling[111], has been applied to JT-60SA and the benchmark of results against MARS-K calculations has started.

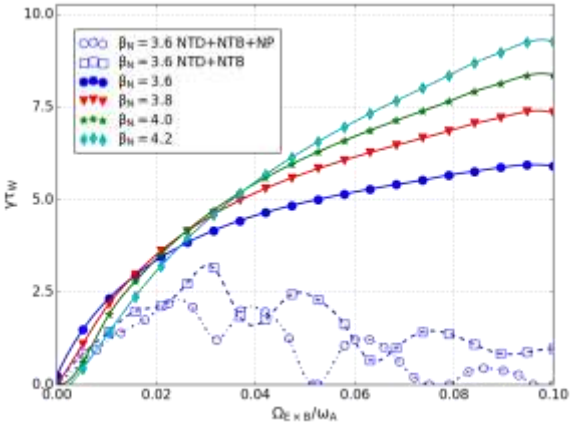

Fig. 3.31 Behavior of RWM eigenvalue with varying rotation magnitude

3.2.5.2. Edge Modelling

The edge modelling of JT-60SA ITER-like scenario (low density high input power scenario) with carbon wall was performed with the edge numerical code SOLEDGE2D-EIRENE

The outcome of edge simulations highly depends on input parameter such as cross field transport coefficients, their radial and poloidal shape and redisposition coefficients. For this

[109] L. Pigatto et al., 46th EPS Conference on Plasma Physics, P05.1002
[110] M. Bonotto et al., submitted to Plasma Physics and Controlled Fusion
[111] A. Portone et al., Plasma Physics and Controlled Fusion 50.8 (2008): 085004.

reason, a similar JET pulse with carbon wall was found to compare the experimental data to the outcome of the simulations of such pulse. A model, including the upper mention parameters, was found and validated with JET experimental data, then, it was used for JT-60SA ITER-like scenario simulations.

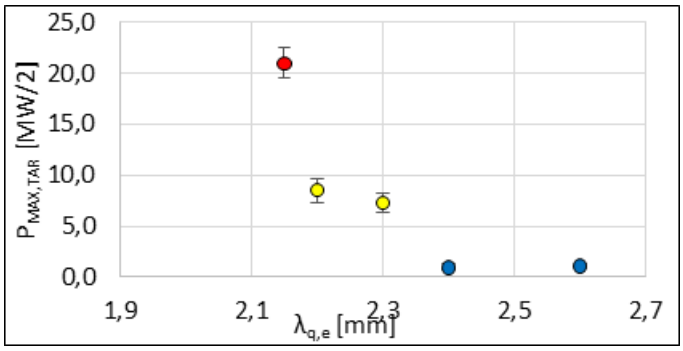

Fig. 3.32 Maximum power to the divertor plates as function of the radial heat decay length at the separatrix, calculated with $n_{e,sep}$ = 2.0x1019 m^{-3} and argon seeding.

In JT-60SA ITER-like scenario simulations, neon and argon were chosen as seeded impurities to compare the cooling performances of the two elements. It was found that in this scenario, argon is a more efficient seeded element, due to the temperature in the divertor region. It was found that the minimum density at the separatrix required to obtain partial detachment at the outer target (and so power flux to the divertor reduced below the technological limits) is 2.0x10^{19} m^{-3}. With this low density high $Z_{eff,sep}$ is required ($Z_{eff,sep}$≈4).

Using the transport parameter shape validated in the JET case, a scan on value at the separatrix of the heat transport coefficient was performed. The power peak to the divertor as a function of the heat decay length in this scan is shown in Fig. 3.32.

Results were presented in a poster at the *3rd IAEA technical meeting on divertor concepts, November 2019, Wien, Austria.*

3.2.5.3. Procurement of the Thomson Scattering diagnostic

Within the collaboration between EU and QST-Japan for the procurement of components for the JT-60SA experiment, Consorzio RFX is contributing to the design of the core and edge Thomson scattering diagnostics and to the in-kind procurement of four subsystems: the collection optics with their mechanical structure and the laser of edge TS system, the fibers and polychromators for both core and edge TS systems. Consorzio RFX has the project leadership of the EU contribution, partly funded by EUROfusion, partly procured directly by F4E, with a total budget for hardware of over 4 M€ in two years, and coordinates a project team comprising the Romanian Institute of Atomin Physics (IAP) and the Institute of Applied Physics IFAC-CNR.

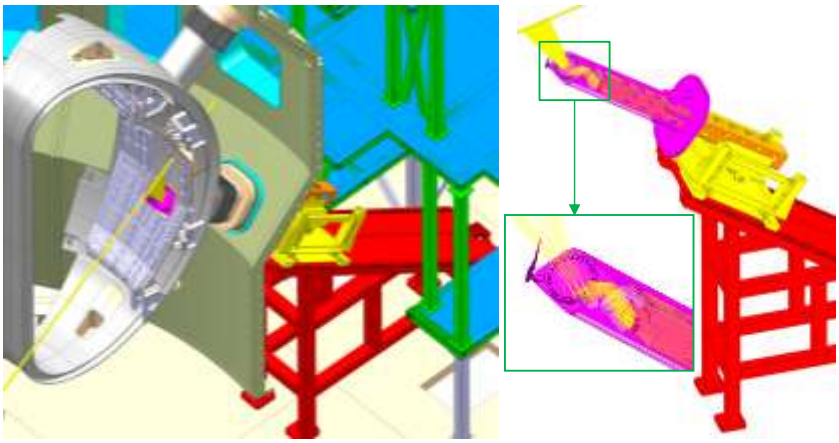

Fig. 3.33 Layout of the edge Thomson scattering diagnostic in JT60SA

In 2019 Consorzio RFX has completed the design of the edge TS diagnostic (Fig. 3.33).[112] The specification and the baseline optical design of the collection optics have been finalized by Consorzio RFX and IFAC, while the design of the mechanical structure has been performed by IAP (with the coordiantion of Consorzio RFX). FInally Consorzio RFX and IFAC have produced the specifications of the optical fibers and of the prolychromators, the former being already in the final phase of the tender process, the latter ready for tendering.

3.2.5.4. Procurement of the VUV imaging divertor spectrometer

Consorzio RFX is leading the procurement of a VUV divertor spectrometer fully funded by EUROfusion, and coordinating the contributions of UKAEA, IAP, IPPLM and ENEA Frascati. The design of the VUV divertor spectrometer has started with the definition of the main scientific objectives for the system, which led to the identification of the spectral range and wavelength resolution and to the decision to build an imaging system rather than just a survey spectrometer[113]. As a consequence, an optical relay system has been designed to bring the image of the divertor on to the entrance slit of the spectrometer 12 meters away. The spectrometer will be the revamped version of a TEXTOR double VUV spectrometer made available by FZJ, renewed in the gratings, designed by W Biel, and detectors, i.e modern CCD 2D arrays, and with additional modifications useful for its calibration. Bids for gratings, detectors, pumps and the sophisticated mechanical structure that will allow fine alignment of the entire vacuum spectrometer will be launched early in 2020. Assembly, test and calibration will be organized at ENEA Frascati in the second half of 2020.

3.2.6. ***WPS1***

---

[112] R.Pasqualotto et al, “Conceptual design of JT-60SA edge Thomson scattering diagnostic”, accepted on Journal of Instrumentation

[113] M Czernishova et al. 46th EPS Conf. 2019 Milan, P1.1012

3.2.6.1. Edge insertable probe

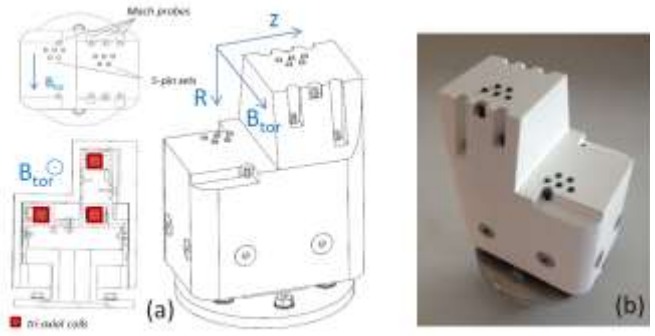

Fig. 3.34 Schematic sensor layout within the probe head (a); HRP probe head final assembly (b).

For the study of electrostatic and magnetic properties of filaments characterizing the edge region of the stellarator experiment W7-X, a specifically designed insertable probe head was constructed within the framework of EUROfusion WP.S1 work package in collaboration between Consorzio RFX, IPP Greifswald and Forschungszentrum Jülich. The probe head, shown in Fig. 3.34, named High Resolution Probe (HRP)[114],[115], was conceived to be installed on the mid-plane multi-purpose fast reciprocating manipulator on W7-X. Electromagnetic filamentary turbulent structures are found to characterize the edge region of different magnetic configurations including Reversed Field Pinch, stellarator and tokamak, where strong currents are associated also to ELM filamentary structures. The study of those phenomena in W7-X stellarator is of particular interest as the electromagnetic features of filaments are expected to become more relevant with the increase of the local plasma beta. In particular the aim is to provide information about the presence and the features of parallel current density associated to filamentary turbulent or ELM-like structures. Furthermore, the possibility to measure the time evolution of the flow radial profiles using the Mach probe array was considered as a further interesting part of the study, given the strong interplay expected between the turbulent fluctuation and the average flows. Further important information provided is the radial propagation of turbulent flux. The design development, the R&D studies and the applied solutions for the sensors embedded in the probe head were presented at the ECPD 2019 and EFTSOMP2019 conferences[116],[117]. In particular, the presence of 140 GHz ECRH plasma environment represents one of the main challenges for reliable magnetic fluctuation measurements [115]. First measurements were performed during the W7-X experimental campaign OP1.2b, where electromagnetic features of turbulence were measured with the

[114] P. Agostinetti et al.2018 *IEEE Transactions on Plasma Science* **46** 1306–1311
[115] M. Spolaore et al. 2019 JINST 14 C09035
[116] M. Spolaore et al. ECPD 2019, Lisbon, O4.1
[117] M. Spolaore et al. EFTSOMP 2019, Padova

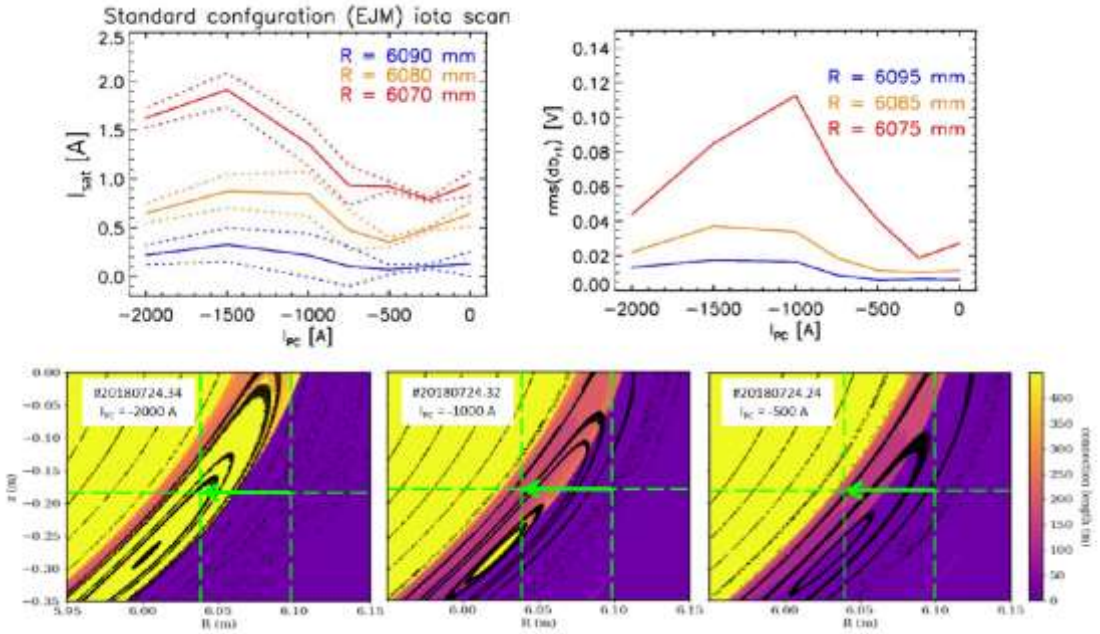

Fig. 3.35 Top panels: profiles of I_{sat} as a function of W7-X planar coil currents, I_{PC}, for three different radial positions analogous measurements for the δb_r . Bottom panels: Poincarè reconstruction of the magnetic topology at the manipulator toroidal section, color scale indicates the local magnetic connection length map, green arrows indicates the range explored by the probe plunge. Data are shown for three different I_{PC} values.

probe, at different magnetic configurations, an example is shown in Fig. 3.35. More details are given in [118].

3.2.6.2. Dual Laser Thomson Scattering

In 2019 the collaboration stared in 2018 with the Thomson scattering team of W7-X has continued ad a study has been carried out and completed for the modification of the TS system of W7-X in order to include the possibility of Dual laser TS experiments in the next experimental campaign. A performance analysis of the TS system has been carried out in order to calculate the expected measurement errors on Te, ne and the relative channel sensitivity factors with the dual laser technique. The analysis has indicateed that the dual laser technique is effective in improving the performances of the W7-X TS system for Te > 5 keV and is also suitable for self-calibrating TS.

3.2.7. ***WPISA***

The activity has been carried out in the context of the Universal Data Layer (UAL) component if the ITER Integrated Modeling (IMAS). In particular, support for data storage using MDSplus data system and memory caching has been provided during the final

[118] S. Lazerson et al. Nucl. Fusion 59 (2019) 126004

debugging phase and the initial releases. Moreover, several optimizations have been carried out, driven by practical use cases, enhancing the performance of the system.

3.2.8. *Collaborations: Interfacing VMEC and Cariddi to study dymnamic plasma equilibria (F4E OPE0951)*

In the context of the studies of plasmas close to critical regimes (e.g. VDE, disruption phases, etc) 3D effects come into play both due to intrinsically non-axisymmetric features of the machine load assembly as well as in terms of plasma response to growing instabilities leading to a global 3D structure of the plasma column.

In this work, carried out within the F4E OPE0951 contract, the 3D equilibrium code VMEC has been coupled to the 3D electromagnetic code Cariddi in order to provide a better representation of the plasma response to 3D fields produced by eddy currents flowing in the passive structure. The coupling procedure takes into account two integration levels: 1) an equilibrum computation with the vacuum field due to eddy currents induced by the plasma equilibirum; 2) a time evolution of the configuration for computing equilibria at different time steps. The first level was implemented in a soft link scheme by taking into account a control surface that manages the link between plasma fields towards Cariddi and vacuum fields due to eddy currents towards VMEC: all the matrices computed by Cariddi are made available to VMEC and a first test case for an axi-symmetric thermal quench (modelled through a plasma β drop) has been done for an axi-symmetric configuration. For the second level, a flow diagram has been devised and pre-processing and post-processing routines along with data management and data sharing schemes are being developed for later integration into VMEC.

3.3. *ITER NBI Physics activities and accompanying program*

3.3.1. *NIO1 Experiment*

The NIO1 experiment hosts an RF negative ion source, with the aims to optimize negative ion production and extraction, and to support the experimentation on SPIDER (eg. tests of materials, devices and diagnostics). The main target for 2019 was to perform experimental campaigns with evaporation of Cs in the source, in order to boost the production of negative ions by surface reactions and reduce the amount of co-extracted electrons. This was not possibile, because a leakage on one of the components of the Cs oven was detected during the tests at INFN – LNL Legnaro. After three failed attempts to fix the component, this was entirely remanufactured. The Cs oven will be installed in NIO1 in Dec. 2019 –January 2020. Due to Cs unavailability, the experimental campaigns in 2019 were in any case conceived in

view of favouring Cs operation: maximize the extracted ion current, improve the high voltage holding of the system and suppress the slow but relevant fluctuations of plasma conditions.

The first months of 2019 were dedicated to improve HV holding by reducing the current of co-extracted electrons impinging on the Extraction Grid (EG). This was done by adding a set of external permanent magnets on top and bottom of the source, just upstream the Plasma Grid (PG) position. The peak magnetic filter field intensity was increased from 5 mT to 9 mT (±4 mT added by the filter current on the PG). A second set of magnets was also installed, adding 2 mT to the peak filter field intensity. Fig. 3.36 shows the co-extracted electron current as function of the extraction voltage before and with the consecutive installation of the magnets. The increased magnetic filter field resulted to be effective in reducing the electron current.

In 2018 the plasma produced in NIO1 suffered from slow but relevant variations of its visible luminosity, strongly correlated with huge variations (one order of magnitude) of the extracted current, thus limiting performances and reproducibility of the source. It was already understood in 2018 that this behavior is due to the conditions of the inner surface of the pyrex cylinder, used as dielectric shield between plasma and RF coil. In 2019 it has been discovered that operating the source with O_2+5% Ar can beneficially condition the pyrex surfaces, leading to dramatically improved plasma long term stability and extracted current in hydrogen operation. Fig. 3.37 shows the accelerated current collected by a CFC tile used as beam dump, as function of the total acceleration voltage. It was possible to increase both the accelerated current and the maximum acceleration voltages reachable without incurring in arcs. The two trends visible in the plot refer to two pumping regimes, with active cryopump (10^{-2} Pa in the vacuum vessel) and without (10^{-1} Pa). The higher currents obtained without the cryopump are partly due to secondary electrons generated by the beam.

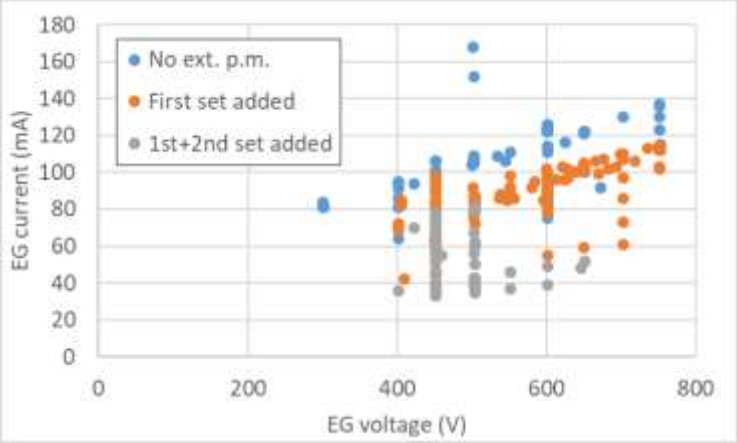

Fig. 3.36 Co-extracted electron current collected on the EG as function of extraction voltage before and after the introduction of the two sets of external magnets. Datasets have been filtered to show only cases with 0.75 Pa source pressure, RF power >1000 W and PG filter current 400 A.

In order to maintain these performances, it was necessary conditioning the source with about 7 h O_2+5%Ar operation every about 14 h of operation in hydrogen. While this is not an issue in pure volume operation, it is absolutely not recommended to use oxygen in a cesiated source, as NIO1 should be in future. Designing, manufacturing and installing a Faraday shield for the pyrex cylinder would be a conceptually easy solution (and is under evaluation in the long term perspective), but it would have been impossible to have it ready before the installation of the Cs oven. It was then decided to conduct a experimental campaign in which, every week, the source was conditioned for 6.5 h with the plasma of a test gas and then the perfomances in hydrogen were probed for 7 h. Noble and chemically reactive gases were used and compared, also in order to understand the nature of the modifications on the pyrex walls: in chronological sequence, Ar, N_2, O_2+5%Ar and Xe were tested. The campaign was performed in november 2019; collected data are under analysis and the results will be subsequently published. A preliminar inspection of data indicated that conditioning in O_2+5%Ar gives the best results, but also the other gases don' lead to much poorer performances.

During 2019 the HV capability of the acceleration system was further improved first by moving the CFC tile farther from the grids, in order to prevent the acceleration and production of secondary charges between grid and tiles. In a subsequent step the vacuum vessel was also opened to remove the probes, the retarding field analyzer and a mirror of the tomographic system that were installed around the beam path, in order to minimize the presence of sharp metal corners and then stray electric fields.

Other secondary activities in 2019 regarded the procurement of the Laser Absorption

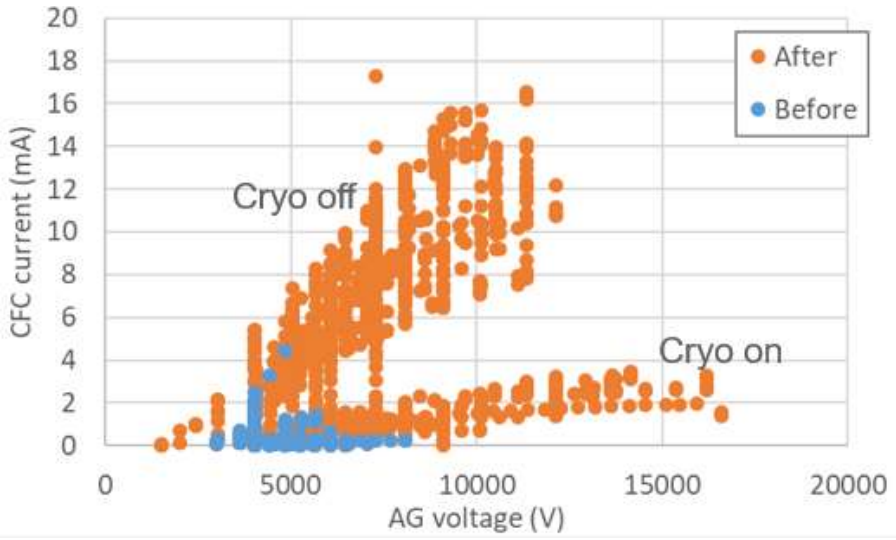

Fig. 3.37 Accelerated current collected on the CFC tile as function of total acceleration voltage before and after the conditioning with O_2+5%Ar. Datasets have been filtered to show only cases with 0.75 Pa source pressure and PG filter current 400 A.

Spectroscopy (LAS) diagnostic, which will be the only one capable to measure Cs density in the source. During 2019 the technical design of the components of the Cavity Ring Down Spectroscopy diagnostic (CRDS), required to measure the density of produced negative ions, was completed and the first components have been procured.

Between December 2019 and January 2020 NIO1 will be in a shutdown phase, required to install the Cs oven and its control system; the cooling system is also being modified in order to let the PG temperature reach 100 °C; PG temperature is indeed relevant to maximize negative ion production[119]. The LAS diagnostic and part of the CRDS diagnostic are also going to be installed. The NIO1 operation in 2020 will be mainly dedicated to learning how to manage Cs evaporation and to characterize the cesiated source performances.

3.3.2. *NBI Complex system and controllability*

In the context of the theory of complex network controllability, the network of processes affecting generation, extraction and acceleration of negative ions in ion beam sources has been considered. A model has therefore been developed and tested for the negative ion beam source NIO1. Preliminary results have shown good agreement between model predictions and experimental behavior of the source. Indeed despite the linear approximation, the system has been found reliable in a sense that the main trend of the source behaviour is found coherent with the model predictions for a simple system with only volume generation of negative ions as in the case of the ion source NIO1. A subset of driver processes which in principle allow the system to be controlled has been identified. One of the driver processes, namely the beam deflection between the extraction grid and the plasma grid which is related to the meniscus formation has been found to play a key role in the global controllability of the system.

3.3.3. *RAID*

From January to June 2019, Consorzio RFX has collaborated with SPC in Lausanne developing the design of a negative ion extraction system for the ion source RAID. RAID is a RF helicon antenna source where during experiments in Hydrogen, a pronounced peak in density of negative hydrogen ions has been detected in the outer part of the plasma column. In the context of the collaboration, electromagnetic and particle tracing simulations have been carried out and two extractor prototypes have been outlined. The first one provides extraction along the radial direction of the plasma column, taking advantage of RAID intrinsic axial magnetic field to suppress the co-extracted electrons. The second one has been

[119] R. Riedl and U. Fantz, AIP Conf. Proc. 1655, 020004 (2015)

designed to extract negative ions along the axis of the plasma column with the support of ferromagnetic electrodes and permanent magnets. Fig. 3.38 shows the final configuration of the radial extractor. The components are already manufactured and the first experimental campaign will start on Febrauray 2020. Fig. 3.39 shows the axial configuration accepted by the SPC technical office and that has still to be optimized.

3.4. *PPPT Projects*

3.4.1. *WPBoP - Balance of Plant - DEMO Plant Electrical System (PES)*

In the EU DEMOnstration power plant, the Plant Electrical System (PES) is one of the largest systems; its scope covers the electrical power generation and the Power Supply (PS) systems necessary for supplying all the plant loads; a block scheme, indicating the different subsystems is shown in Fig. 3.40 Block scheme of the EU DEMO Plant Electrical system.

The studies on the EU DEMO Plant Electrical system (PES) are presently addressed to understand on the one hand the specific design challenges with respect to an equivalent system for a fission power plant of similar size and on the other hand the additional issues with respect to the ITER electrical system. Results from first analyses highlighted that the design solutions adopted in the last decades in the main fusion experiments need to be

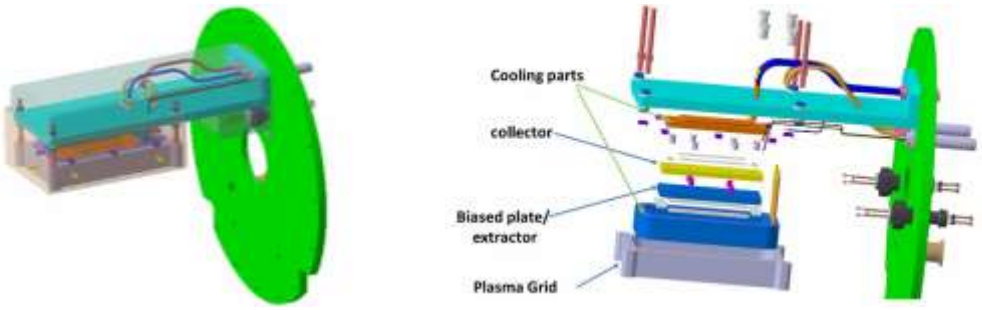

(a) (b)

Fig. 3.38 a) 3D view of the radial extraction configuration. b) Exploded view of the final configuration

(a) (b)

Fig. 3.39. a) SolidWorks 3D CAD of the final prototype. b) Exploded view of the axial extractor.

reconsidered. In fact, the requirements for DEMO are more demanding, because the power peaks envisaged are significantly higher than in ITER and the handling of the generated and recirculated power poses problems not experienced in previous experimental devices, requiring R&D to be solved[120].

The activities in 2019 have been concentrated to start outlining a first conceptual design of key subsystems of the PES, according to an ITER-like approach, where applicable. The TF, CS and TF circuit topologies have been drawn similarly to the ITER ones. The base converters to supply the superconducting coils have been based on the thyristor technology[121], and also for the Switching Network Units and the TF Fast Discharge Units an ITER-like approach have been studied to understand the issues when scaled to the DEMO size and to perform a first estimation of the overall dimensions to evaluate the impact on the plant layout.

In parallel, the studies proceeded to explore innovative design solutions capable to solve the identified problems in terms of too high power peak and reactive power demand; in particular, the work was concentrated on the MEST, a new Magnetic Energy Storage and Transfer system. This new scheme was conceived and its application to a Reversed Field Pinch as a Pilot Neutron Source was studied first[122]. This year, the application of this concept to the European DEMO has been studied, starting from the assumed circuit configuration and from the current and voltage scenario under consideration for the plasma breakdown and ramp-up. The results showed that the dynamic requirements during these

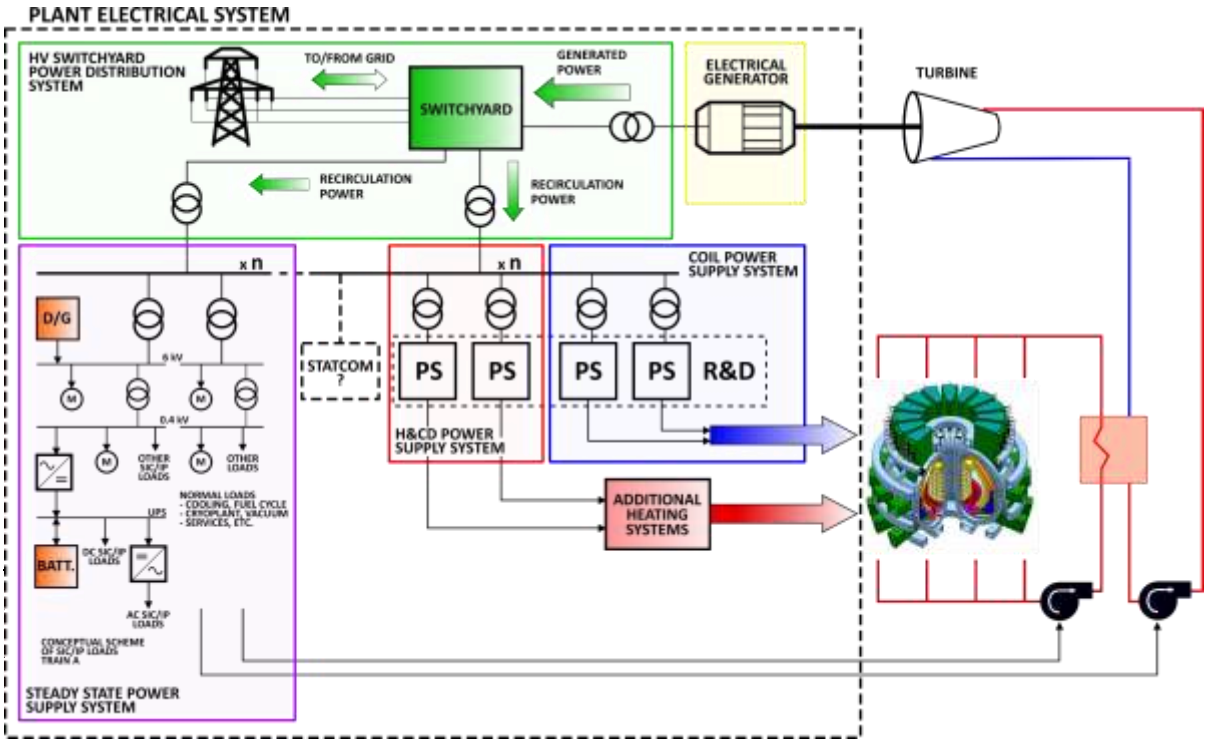

Fig. 3.40 Block scheme of the EU DEMO Plant Electrical system

phases of the pulse can be satisfied with reasonable values of the switching frequency of the MEST switches and that potentially the MEST could smartly solve both the issues related to high power peaks and huge reactive power demand associated to the adoption of the traditional design solution based on thyristor converters[123]. However, the first rating estimation indicates levels far beyond the most powerful industrial applications, thus a long R&D program, foreseeing a strict collaboration with the industry, is necessary to evaluate the scheme applicability at the power level required for DEMO. This work was object of a poster presentation at the last ISFNT-14, resulted winner of the FED student award.

3.4.2. *WPBoP - Balance of Plant - Thermal-Hydraulic Design of DEMO PHTS+BOP and Aux System*

The European DEMO is considered the nearest-term fusion reactor with the aim to generate several hundred MWs of net electricity, operate with a closed tritium fuel-cycle (achieving the tritium self-sufficiency) and qualify technological solutions for a Fusion Power Plant.

The heat exhaust in the fusion power plant will involve the first wall with the breeding blanket, the divertor and the vacuum vessel. The design of these components for EU DEMO is not yet finalized, but configurations and operation parameters have been identified. Different Breeding Blanket (BB) concepts are under investigation and two of them, relying on different coolants and breeding technologies, are considered for the EU DEMO baseline design: the Helium Cooled Pebble Bed BB (HCPB) and the Water Cooled Lithium Lead BB (WCLL).

The selection of the BB type is a key factor for the development of the whole DEMO plant including the Balance of Plant (BoP) system and, in particular, its sub-systems having the responsibility to remove thermal power generated by the plasma, its conversion in mechanical and finally electrical energy.

Preliminary thermo-mechanical design of the main heat exchangers and steam generator components were carried out during the 2019, in particular for the intermediate heat exchanger helium/molten salt of the HCPB concept (Fig. 3.41) and for the steam generator of the WCLL concept (Fig. 3.42).

FEM analyses were carried out to verify the sizing and identify the local discontinuities needed to satisfy the requirements in the most stressed regions. Stresses resulting from analyses were verified applying Section III of ASME Boiler and Pressure Vessel Code (Rules for Construction of Nuclear Facility).

---

[123] F. Lunardon, et al., poster presentation at ISFNT-14 – Winner of the FED student award – submitted to FED

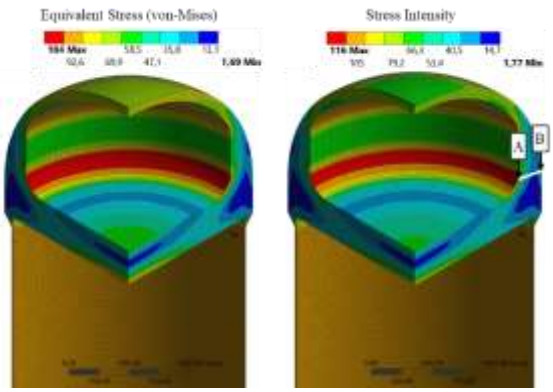

Fig. 3.41 HCPB Intermediate heat exchanger helium/molten: equivalent stress (von-Mises) [MPa] and Stress Intensity [MPa]

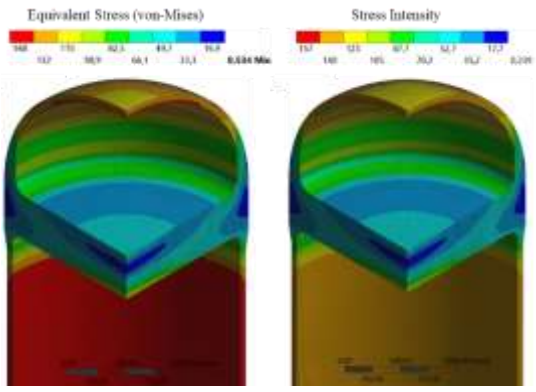

Fig. 3.42 WCLL Steam generator: equivalent stress (von-Mises) [MPa] and stress intensity [MPa]

3.4.3. *WPHCD – Heating and Current Drive systems*

The injection of high energy neutral beams is one of the main tools to heat the DEMO plasma up to fusion conditions. A conceptual design of the Neutral Beam Injector (NBI) for the DEMO fusion reactor is currently being developed by Consorzio RFX in collaboration with other European research institutes. High injector efficiency and RAMI (Reliability, Availability, Maintainability and Inspectability), which are fundamental requirements for the success of DEMO, must be taken into special consideration for the DEMO NBI.

A novel design of the beam source for the DEMO NBI is being developed featuring multiple sub-sources, following a modular design concept, capable of increasing the reliability and availability of the DEMO NBI. During 2019, the DEMO NBI conceptual design has been discussed with the interested working groups of EUROfusion, working on the main related issues (physics, integration, breeding blanket, remote maintenance, neutronics). Moreover, an External Design Review Panel has been organized in June 2019, which has given a feedback on the proposed design solutions. Based on the feedback received by the Review Panel, the following activities have been carried out in 2019 in collaboration with the EUROfusion groups working on the heating and current drive systems:

- Improvement of the RAMI analysis to evalaute also the error bars
- Improving the models (optics, particle reactions, thermo-mechanics) by developing a n integrated model of the beamline able to study various important process, i.e. vacuum pumping, beam transmission, stripping, neutralization, re-ionization.
- Studies on the possibility to use a plasma neutralizer instead of a gas neutralizer

Photoneutralization is regarded as one of the most interesting alternatives to stripping neutralizers in NBI systems. R&D activity on photoneutralization at Consorzio RFX involves the construction and test of a non-resonant cavity for second laser harmonic trapping, fed by a pulsed Nd-Yag laser RING concept

The RING Cavity mockup for photo-neutralization studies have been improved and operated, obtaining an enhancement factor of 25 on a target of 100. Major losses have been identified on mirrors, and a complete new mirror set with enhanced reflectivity (99.95 instead of 99.5) is under purchase. The numerical model of beam propagation inside the cavity has been validated and applied to the NIO1 negative ion beam injector, defining the laser requirements for application on NIO1. Parallel activity involved the dimensioning of a multipass optical resonator tailored on NIO1 beam characteristics. Thermal issues determination is a crucial point and will be addressed in the next year with a dedicated experiment.

3.4.4. *WPFTV - Tritium, Fuelling and Vacuum Pumping Systems*

Consorzio RFX is involved in the development and characterization of a large vacuum pump based on Non-Evaporable Getter technology within the WP-TFV.

In March 2019 the power supply and control systems have been completed and tested by SAES Getter.

In the end of June 2019 the NEG pump mock-up (NEG cartridges and support structure) and the power supply and control system have been shipped to Karlsruhe Institute for Technology (KIT), for the following installation in the TIMO facility (Fig. 3.43).

In the end of July 2019, the NEG pump mock-up has been installed into TIMO vessel, it has been mounted on the main flange of the vacuum vessel and inserted. The commissioning the power supply and control system has been carried out with the direct support of the SAES Getter technicians.

A first adsorption test was performed in the end of September 2019. The measured pumping speed for H_2 after the initial phase was 25.7 m^3/s, with a pressure in the vessel of 2E-2 Pa and a temperature of the NEG disks of about 130°C. This value remained stable and constant for the entire duration of the test (7 hours) and close to the value estimated by the results of single cartridge tests.

In the meanwhile numerical simulations have been carried out in order to define a global description of the pump, to study large modular NEG pumps (such as the NEG pump mock-up), where a scaling approach is needed to reduce the computational effort. This work has been presented at the ICIS conference 2019 with the name “Numerical simulation of

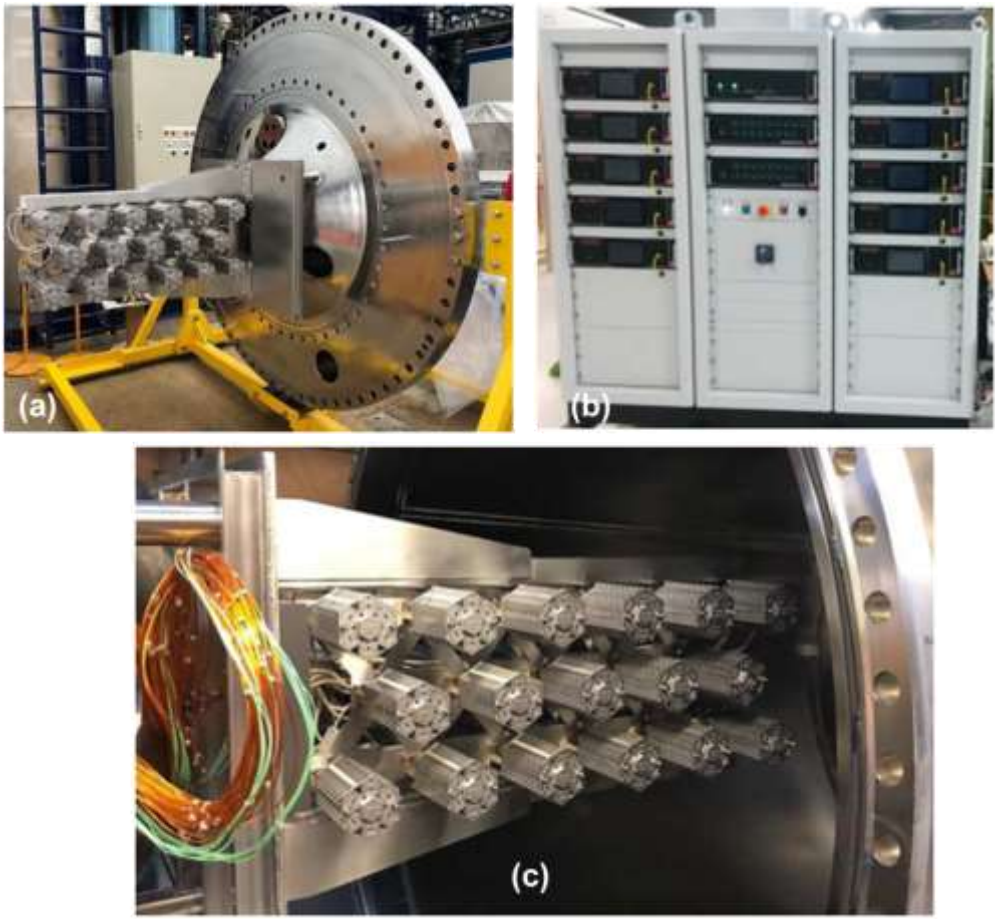

Fig. 3.43 Pictures of the mock-up pump in TIMO facility: (a) NEG pump mounted on the TIMO main flange; (b) mock-up power supply; (c) insertion of the pump into the TIMO vessel

experimental tests performed on ZAO® Non-Evaporable-Getter pump designed for Neutral Beam Injector applications".

3.4.5. *WPMAG – Magnet System: Quench Protection Circuit Studies*

The studies in 2019 have been addressed to further explore the possibility to reduce the number of TF coil sectors from 16 to 8, thus the number of cryostat penetrations and burbars in the tokamak building. The reduction is hindered by the need to respect the limits fixed for the voltage across the TF coils and the voltage at the coil terminals versus ground.

Analyses were performed to evaluate the voltages across the TF coils and of the coil terminals versus ground during the FDU intervention[124]; this year, further ones were made with the updated value of the time constant of the discharge set at 35 s and different values of coil current and inductance. The analysis ITER-like topology of the TF circuit and of the FDU have been assumed. A constant value for the discharge resistance was assumed first,

[124] A. Maistrello, et al., FED, 146 (2019) 539–542

then, an analysis with temperature dependent resistors, like those selected for the ITER FDU, has been done for the 16 and 8 sectors cases, with $\tau = 35\ s$. The constraint is keeping the I^2t in the coil at the end of the FDU intervention under 150 GA^2s. The material considered for the resistor is the same used for ITER: mild steel, which has a temperature coefficient of $6.6 \cdot 10^{-3}\ \left[\frac{\Omega}{K}\right]$. The results showed that, with some set of data under consideration and the adoption of temperature dependent resistors, the 8 sectors case comply with the assumed voltage limits. These analyses have been performed with the assumption that the entire energy stored in the TF coils is dissipated in the discharge resistors, neglecting the fraction of energy dissipated on the passive structures (coils mechanical supports and vessel). This assumption is probably too conservative, but at the moment not sufficient data are available to estimate a correct fraction of energy; this aspect will be object of next step studies.

The evaluation of the transient voltages during the fast current dump have been further improved estimating the impact of the stray inductances of the power connection; as a result a not negligible additional fast overvoltages have been calculated, which however can be damped by suitably designed clamping circuits.

3.5. *Socio Economic Studies (SES) and DEMO*

3.5.1. *Fusion power plant economic assessment*

The FRESCO code has been used for further assessments of the economics of a fusion power plant under different assumptions, without relevant improvements of the FRESCO routines. The resulting investment, operating and maintenance costs and availability were used for the economic characterization of a future fusion power plant which was simulated in a number of long term scenario.

3.5.2. *The role of fusion in long term energy scenarios*

The resources allocated on the EUROfusion Work Package on Socio Economic Studies encompass both project management and research activities.

Within the research activities, Consorzio RFX contributed to the development of new scenarios aimed at assessing how much fusion penetration would be affected by policies in favour (or not) of nuclear fission; by the availability (or not) of carbon capture and storage technologies coupled to fossil fuelled power plants; by fusion investment costs possibly ranging from 7 to 9 billion dollars and the inclusion of external costs. The viability of a full renewable scenario has been also assessed. On these bases, 24 scenarios have been produced per each storyline (Harmony, Paternalism, Fragmentation that models a global temperature increase <2°C, ~1.5°C and >2°C, respectively).

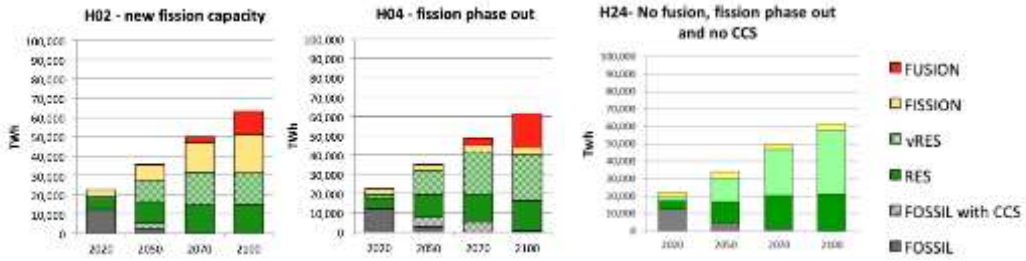

Fig. 3.44: Fusion penetration in Harmony scenarios assuming policies in favor of either new nuclear fission capacity (H02) or a progressive fission phase out (H04), compared to a 100% renewable scenario (H20).

The Harmony scenarios delineate alternative pathways towards the achievement of the Paris Agreement Goal (see Fig. 3.44) Although equally feasible from a modeling perspective, each corresponds to different power system configuration and management, requiring deep changes in the electric transmission grid especially when more than 50% of the electricity is generated by intermittent renewables. In this regard, Consorzio RFX has collaborated with ENEA and the Joint Research Centre (JRC) in the analysis of the dispatch model of a European power system based on the SES Harmony scenarios. The results show the key role of the flexible capacity and the proper geographical location of nuclear power plants to prevent transmission grid congestions.

Within EUROfusion activities dealing with the design of the new Fusion Expo, Consorzio RFX has provided support in the selection of the scientific content of the exhibition related to energy scenarios.

Besides, new studies have been carried out with the COMESE code (*COsto MEdio del Sistema Elettrico*) on European scale. The study presented at the 28th IEEE Symposium on Fusion Engineering investigates to what extent the integration of fusion power in European RES-based electricity generation mix might affect the power system affordability and

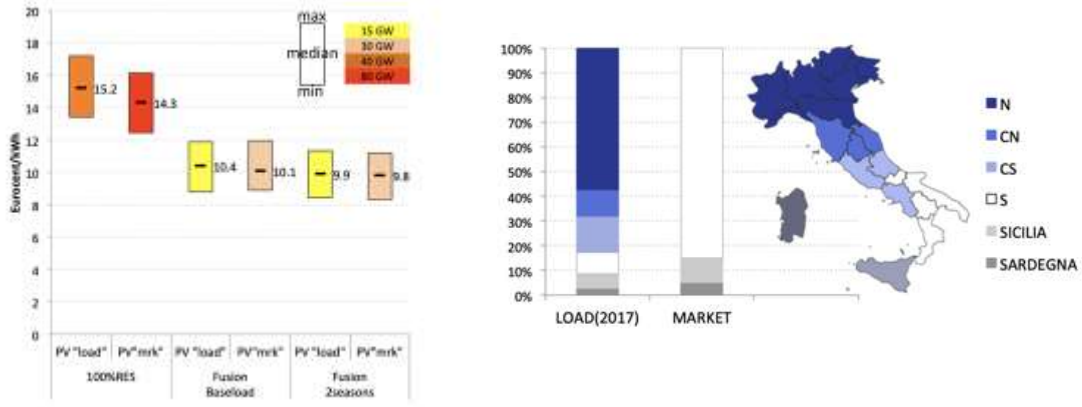

Fig. 3.45: LCOTE ranges and power flows (on the left) among Italian market zones under different assumptions of solar power stations geographical location (on the right), namely proportional to the zonal electricity demand ("load") or to the solar irradiation ("market")

reliability as compared to full-RES power mix by the last two decades of this century. As shown in Fig. 3.45 100% RES scenarios are more expensive than scenarios with fusion power, operating continuously over the whole year or with seasonal modulation - pretending the cost of fusion electricity is 6 cEur/kWh.

Nevertheless, because of the electric grid enhancements required in case of distributed generation, the levelled cost of timely electricity of 100%RES scenarios would be even higher. Additional transmission grid capacity could be limited by increasing the zonal generation capacity proportionally to the corresponding electricity demand (see Fig. 3.45)

3.6. *Education and Training*

In 2017 the Universities of Padua (UNIPD) and Gent (UGENT), on the basis of the successful experience in running two international leading programmes (the so called “Padua-Lisbon-Munich” initiative and the “Erasmus Mundus Fusion Doctoral College”), have implemented a Joint Doctorate Programme in “Fusion Science and Engineering” aiming at the continued formation of a suitable number of doctoral students at the highest level of excellence. In this framework, fifteen PhD students have been enrolled in the last three academic years:

- Academic year 2017/18 (XXXIII cycle): four
- Academic year 2018/19 (XXXIV cycle): four
- Academic year 2019/20 (XXXV cycle): seven

It is to be emphasized that a larger number of PhD students have been enrolled in academic year 2019/20, thanks to the additional fellowships funded by private companies and public research institutions: CARIPARO, ENEA, ENI, OCEM Power Electronics and Synecom.

Moreover, in 2019 ten PhD students (nine under the former international agreement between the Universities of Padua, Lisbon and Naples “Federico II”, and one under a co-tutelle agreement between UNIPD and Universidad Carlos III de Madrid - UC3M), completed their 3-years research programs and have been admitted to the PhD Defense (to be held early 2020). Overall, in 2019 twenty-five PhD students have been operating at Consorzio RFX and partners’ premises, under the tutoring of members of the PhD Academic Council and Consorzio RFX’s researchers.

3.7. *Scientific Conferences and Meetings*

In 2019 the Consorzio RFX Scientific Secretariat has organized and managed several Conferences and Workshops held in Padova. In particular:

- **2nd JT-60SA Technical Coordination Meeting .** 6-7 March 2019, Padova – Consorzio RFX, 44 participants, local chair Elena Gaio
- **MARTe2 Users Meeting** 8-9-10 May 2019 Padova - Consorzio RFX, 34 participants, local chair: Gabriele Manduchi
- **EFSTOMP 2019** - Workshop on Electric Fields, Turbulence and Self-Organization in Magnetized Plasmas - satellite meeting of EPS Conference 15-16 July 2019 Padova - Consorzio RFX, 31 participants, local chair Monica Spolaore, Emilio Martines
- **8th International Workshop on Mechanisms of Vacuum Arcs (MeVArc19)** September 16-19 2019 Padova – Orto Botanico, 80 participants, local chair Antonio De Lorenzi
- **DRM04 – DTT meeting** 28-29 October 2019 Padova - Consorzio RFX, 40 participants, local chair Marco Valisa

3.8. *Communication and outreach*

The Communication Office, in collaboration with ITER IO and F4E communication offices and Eurofusion Public Information network, worked along the two main lines:

- production of information content;
- outreach and communication initiatives.

Concerning the media, there was an increased coverage with a interviews and TV shootings. On September 11th, Walt Disney Italia published on the comic magazine *Topolino* n. 3329 the *episode Topolino e il Padrone del Buio* (*Mickey Mouse and the owner of the dark*), a story on SPIDER-NBTF, followed by a 6-pages article highlighting the NBTF research.

A great effort was spent in organizing of events, both in national and international contest, inclusive of visits at a high political level, such as the President of the Italian Senate Maria Elisabetta Alberti Casellati and deputy Ministers from Japan, China and Australia.

Finally, strong commitment was devoted to tours and visits by general public and secondary school students. Fig. 3.46 shows the number of visitors in the last 12 years, peaking to 2537 visitors in 2019, 2184 of them under direct scientific guide.

Interviews:

- prof. Giuseppe Zollino for TV7 Match August 8th
- Dr. Fulvio Auriemma for CaffèTV24 August 12th
- Dr. Matteo Agostinetti for TEDx Match August 21st
- Dr. Vanni Antoni for Focus Live Match October 19th
- Dr. Matteo Zuin for Radio 24 - Smart City December 24th

TV coverage:

- RAI Futuro 24 – an entire episode dedicated to Consorzio RFX
- *Fusion Nucleare: dal CNR di Padova i primi risultati concreti*, RAI3 national news May 24th, about first SPIDER operation.
- *Un Progetto Italiano* video tg5 mediasetplay

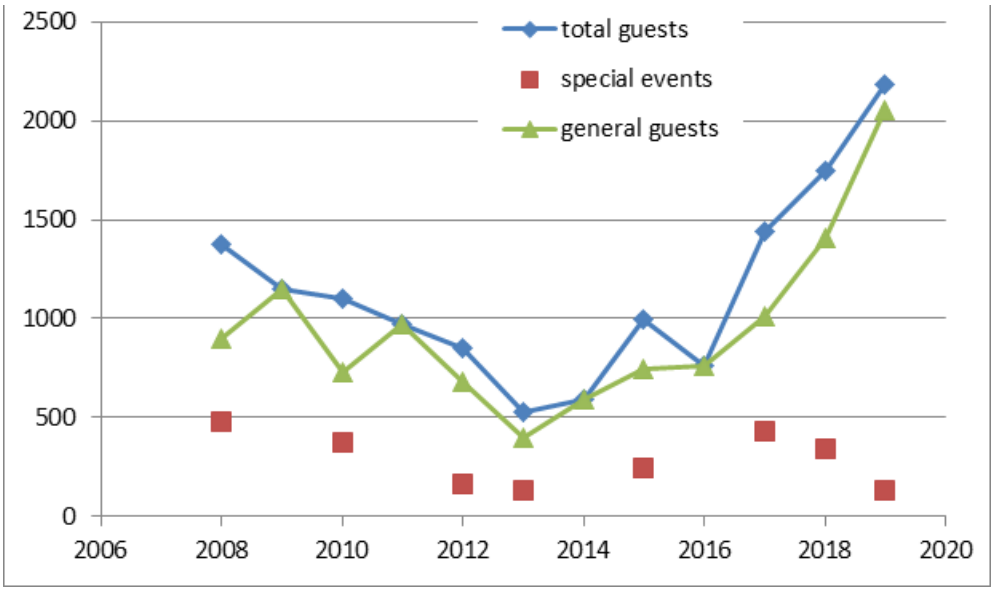

Fig. 3.46 Number of visitors to Consorzio RFX

Events:

- *Faccia da STEM* (February 1st). Secondary school students Skype interviews to Consorzio RFX scientists on Science, Technology, Engineering and Mathematics;
- *Le sfide dell'innovazione. Il viaggio nell'Italia che investe nel futuro*, in collaboration with the Gedi Italian publishing group (*Il Mattino* and *la Stampa* newspapers)

- *From Leonardo da Vinci to ITER* (Consorzio RFX Communication Office participation ITER Cadarache April 15th) in the frame of Leonardo da Vinci 500 year anniversary.
- *Visit SPIDER and learn how to make a sun on Earth* video conference organized by Consorzio RFX, CNR and the Energy Change Institute of Australian National University, in the framework of the Italian Research Day in the World.
- *European Night of Researchers, Veneto Night 2019* (Padova September 27th, participation with: a promo video on NBTF projected at Cinema Porto Astra from 19 September 19th to October 3rd; a stand in the city centre; projections of videos on NBTF in the Bo' palace of University of Padua, guided visits to NBTF).

VIPS visits:

- **Maria Elisabetta Alberti Casellati,** President of the Senate of the Republic . 8th February, event covered by print and television RAI3 - TGR Veneto.
- **Keiko Nagaoka**, Japanese Minister of Education, Culture, Sports, Science and Technology, May 3rd.
- **Huang Wei**, Chinese Deputy Minister of Science and Technology June 21th.
- **Yasuhiro Itakura** Executive Director of QST, **Kenichi Kurihara**, Director General of Naka Fusion Institute, and **Takashi Inoue**, Deputy Director of JADA Department of ITER Project, November 15th to see the Japanese components of MITCA 1 MV PS.
- **Keith Nugent,** Vice-Chancellor for Research and Innovation of the Australian National University, December 10th, to discuss collaborations in research and PhD education.

4. Broader Approach

4.1. *Contribution to the JT-60SA PS Combination Tests preliminary to the Integrated Commissioning*

The mission of Power Supply (PS) Combination Tests is to confirm that the PS components: SuperConducting Magnet Power Supply system (SCMPS), Switching Network Units (SNU) and Quench Protection Circuits (QPC) can properly work all together on a dummy load, under the control of the PS Supervising Computer (PS-SC) via the Reflective Memory (RM) networks. Besides the combined operation till the nominal performance, the tests are addressed to verify the correctness of the signal data acquisition, the protection sequences both at individual and system level, the absence of interferences among different components, etc. The correct PS joint operation has to be checked for 10 poloidal circuits and one toroidal circuit, before the start of the integrated commissioning.

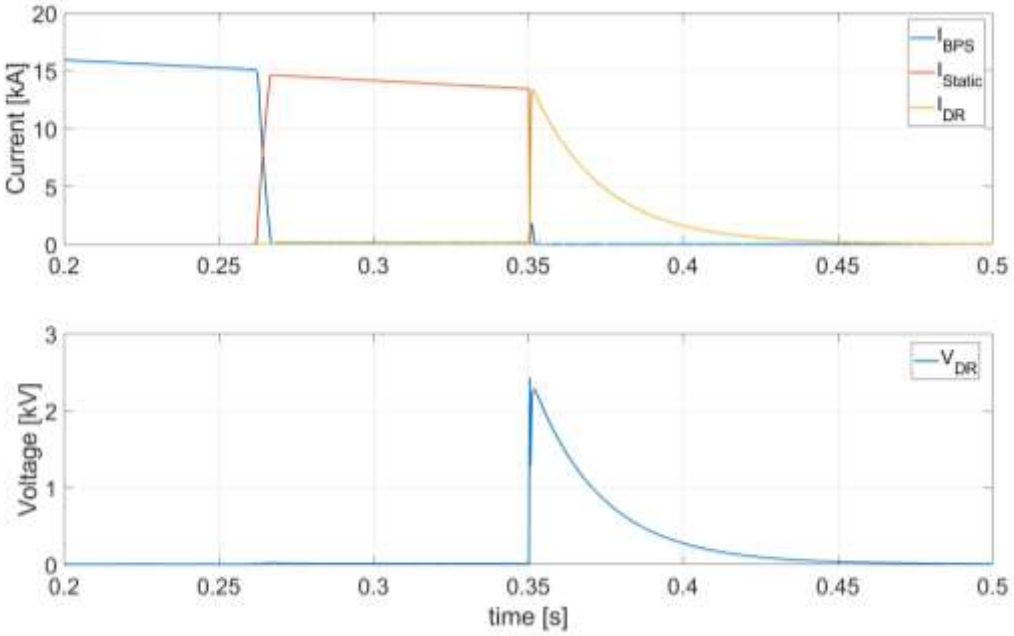

Fig. 4.1 Intervention of the Quench protection Circuit at the nominal current of 20 kA

Including the preparation, these test campaigns lasted all the year; the test execution started end of June 2019 and will proceed till next late spring 2020, even if not continuously.

Consorzio RFX is participating in the whole activity, but with particular attention to the Quench Protection Circuits. A challenge task was the identification of safe circuital condition for the QPC components, during the tests on dummy load without the pyrobreaker, which will be tested later. Other issues were found related to noises on current transducers due to magnetic flux variations during the high power pulses. Further improvements in the cables layout and transducers relative position have been introduced. Fig. 4.1 shows an example of intervention of the QPC of the CS3 central solenoid circuit, during a test at the nominal current. The current is initially risen up to the value of 20 kA by the SCMPS; then, an intervention command is sent to the QPC and the protection sequence starts. In the plot on the top, the current circulating in the Bypass Switch (blue curve) is commutated first in the Static Circuit Breaker (red curve) and then in the dump resistor (yellow curve). The top on the bottom shows the voltage acroos the dump resistor.

4.2. *Power supplies for in-vessel sector coils for RWM control*

It is recalled that during the unpacking of the components, arrived in Naka in September 2018, it was descovered that a cabinet including 9 inverters (PCC-B) sustained severe damages during the transportation. The reason and the time when the damages occurred was never found.

The Transportation was shared by EU (for the packaging the sea transportation from Italy to Yokohama) and JP (ground transportation from Yokohama to Naka) according to the agreement signed in Procurement Arrangement. For this reason, it was necesasry to open two independent insurance claims from EU and JP. The reimbursement claimed to the insurances includes rebuilding, factory tests and direct delivery to Naka of damaged cubicle. The clarification process among the insurance companies, in progress since October 2018 was concluded only one year later. For the reason that the damage responsibility remained unclear, the EU insurance refunded less than 50% while JP insurance nothing. Even if the refunded amount is not sufficient, the company E.E.I accepted anyway to perform the manufacturing and testing of the new cabinet. The delivery to Naka and disposal of damaged cubicle will be performed by F4E/QST, instead.

The contractual activities, suspended after the discovery of the damage wull restart beginning of the next year; the plan for the manufacturing and testing of the new cabinet will be confirmed after the verification of the delivery time for the puchase of key components.

5. Industrial and non-fusion related collaborations

5.1. *Design of Vacuum Interrupters with the Voltage Holding Prediction Model (VHPM)*

In 2019 the collaboration wih Siemens AG for the assessment of the VHPM applicability for the optimization of Siemens Vacuum Circuit Breakers (VCBs) continued. In particular during this year the activity focused on experimental campaigns on SIEMENS VCBs at the HV Test Laboratory of the University of Padova Industrial Engineering Department (DII). In these campaign, 5 new VSG36 and 1 VSG24 (already tested in 2018) VCBs were tested at DII.

The activity program agreed at beginning 2019 for the two years activity consisted in:

- Conclusion of 2018 campaign on VSG24 tubes;
- Tube equivalence verification on new VSG36 tubes;
- Correlation between the breakdown (BD) voltage distribution curves obtained with the different voltage application methods proposed (the Up-and-Down UD method, the Multi Level Method ML and the much more efficient Always BreakDown AwBD method);
- Verification of the effect of voltage derivative and/or the Breakdown energy on the berakdown voltages voltge distribution curve;
- Memory test to verify if the final BD voltage distribution is affected by the history of the tube itself (conditioning first with long gap and then short and viceversa).

The experimental effort carried out so far has allowed to fully examine the first 3 points. The main result was to establish the equivalence of the AwBD method with respect to the UD method: this means that the testing time can be greatly reduced to obtain the same voltage breakdown distribution. ML method has shown to be not effective in obtaining consistent statistical information regarding the Voltage Holding cabability ot the VCBs. Another important finding was that the voltage conditioning depends also by the electrostatic configuration (e.g. gap length).

The voltage derivative and the energy effects have been analytically studied on the basis of some assumption and simple models. Further work will be addressed to analyse in detail with ad hoc experimenatal campaigns thes two parameters: to this purpose, a modification of the experimental set up (Marx generator reconfiguration) is required to limit the energy involved in the BD arc when higher HV is applied. This will be done with the reduction of the overall capacitance by limiting the generator stage number and/or the insertion in series of dump resistors will be implemented. Arc current measurement will be introduced in order to better estimate the energy involved in the process.

The voltage holding degradation for long gaps campaigns will be numerically investigated with the VHPM 3D formulation, in particular to evaluate the role of other VCB components, such as the floating shield, in the BD occurrance. Further experimental campain will also carried out with new interrupters with very similar geometry, but grounded shield.

This activity is funded by Siemens because of its interest in customizing the VHPM as a design tool to reduce the developing effort of the new Vacuum Interrupters. On the other hand, the scientific return for the Consorzio RFX is to validate the effectiveness of the VHPM in a different operating condition (pulsed voltage instead of dc voltage application) and in a pure 3D formulation.

5.2. *Biomedical plasma applications*

The three-year project “A novel Plasma Medicine tool for accelerated hemostasis”, which has been awarded funding by the “Fondazione con il Sud” through a competitive selection named Brain2South, and is being carried out in collaboration with in collaboration with the Department of Medical and Surgical Sciences of the University of Catanzaro, has arrived at its last year. The project aimed at the development of a cold atmospheric plasma source for fast blood coagulation. Following the good results obtained in 2017 and 2018, the activity in 2019 has concerned two main topics: investigation of the physical properties of the plasma produced by the source and further biomedical tests in the view of a possible application on human patients.

The analysis of the plasma properties allowed a deeper understanding of the mechanisms of plasma generation and propagation. In particular, fast camera analysis revealed the presence of ultrasonic streamers (Fig. 5.1) traveling towards the plasma target [125]. A modeling activity, also in collaboration with the Engineering Department of the University of Bologna, has started to explain the experimental observations. Moreover, two other crucial activities have been carried out: calorimetric analysis and study of the thermal effects associated to the plasma action [126] and analysis of the UV emission (also this activity is being carried out in collaboration with the Engineering Department of the University of Bologna).

Biomedical tests were carried out at the University of Catanzaro. They concerned the analysis of the blood samples treated by the plasma source through different techniques: Western Blot analysis and Mass spectrometry in particular, revealed the activation of different proteins as a result of the plasma action. This activity is crucial for understandings the mechanisms of interaction of the plasma with living matter. On the other side, in a very preliminary way, tests on human patients affected by psoriasis (a dermatologic disease) have been successfully conducted. This very encouraging result has suggested a possible investigation in a clinical trial to be performed at University of Catanzaro in 2020.

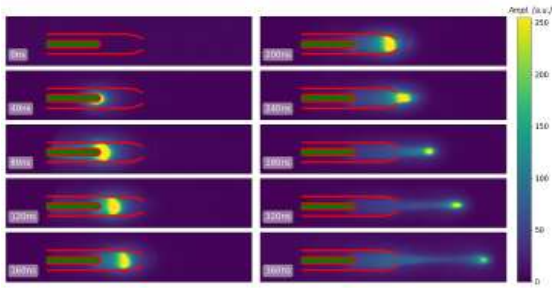

Fig. 5.1: Streamers generation and propagation at ultrasonic speed (v~100km/s) within the plasma source

5.3. *Plasma study for GALILEO Passive Hydrogen Maser*

This activity is covered by a contract of Leonardo with Consorzio RFX and Nanotech-Bari to investigate the malfunctioning of the Hydrogen Dissociator in the space Passive Hydrogen Maser (PHM), the master clock on the Galileo navigation payload manufactured by Leonardo-Finmeccanica and SpectraTime. After completion of the failure investigation review in 2018, this year Consorzio RFX has supported Nanotech in the development of a plasma and electromagnetic model of the Dissociator, in particular proposing a measurement procedure of the electromagnetic coupling in support of the model. RFX has also prepared the last phase of the contract: spectroscopic measRFXR$FXurements of the

[125] L. Cordaro et.al.,"On the Electrical and Optical Features of the Plasma Coagulation Controller Low Temperature Atmospheric Plasma Jet", Plasma, 2, 156 (2019).

[126] L. Cordaro et al., "The Role of Thermal Effects in Plasma Medical Applications: Biological and Calorimetric Analysis", Applied Sciences, in press (2019)

hydrogen plasma in a Dissociator test unit. Experimental procedure and layout have been defined and the experimental campaign will be executed at beginning of 2020. After spectroscopic data analysis with a collisional radiative model, contributing to the understanding of the Dissociator operational mode (capacitive or inductive RF coupling), the contrac

Publication list 2019

Journal papers submitted by a Consorzio RFX first author

Journal papers submitted by a Consorzio RFX first author

R.1. Grenfell G., Van Milligen G., Losada B. Ph., Ting W., Liu B., Silva C., Spolaore M., Hidalgo C., and the TJ-II Team: "Measurement and control of turbulence spreading in the scrape-off layer of TJ-II stellarator", NUCL. FUSION **59** Issue: 1, 016018 (JAN 2019)

R.2. Spizzo G., White R., Maraschek M., ASDEX Upgrade Team: "Nonlocal transport in toroidal plasma devices", NUCL. FUSION 59 Issue: 1, 016019 (JAN 2019)

R.3. Kudlacek O, Marchiori G., Finotto C., et al.: "Cleaning of the Eddy Current Effects From Magnetic Diagnostics", IEEE TRANS. ON PLASMA SCI. 47 Issue: 1, 858-863 Part: 3 (JAN 2019)

R.4. Gambetta G., Agostinetti P., Sonato P., Fedele L., Bobbo S., Cabaleiro D.: "Numerical analyses and tests for optimized and enhanced heat transfersolutions in DEMO", Fus Eng and Design, 146, Part B, 2692-2697 (Sep 2019)

R.5. Vincenzi, P., Varje, J., Agostinetti P., et al.: "Estimate of 3D power wall loads due to Neutral Beam Injection in EU DEMO ramp-up phase", NUCLEAR MATERIALS AND ENERGY 18, 188-192 (JAN 2019)

R.6. Fassina, A., Bilkova, P., Bohm, P., et al.: "Sensitivity of Thomson Scattering Measurements on Electron Distribution Modeling in Low-Density RFP Plasmas", IEEE TRANS. ON PLASMA SCI. 47 Issue: 3, 1605-1610 (MAR 2019)

R.7. Murari A., Peluso E., Cianfrani F., et al.: "On the Use of Entropy to Improve Model Selection Criteria", ENTROPY 21 Issue: 4, 394 (APR 2019)

R.8. Spada E., De Lorenzi A., Pilan N., et al.: "Theoretical Basis and Experimental Validation of the Breakdown Induced by Rupture of Dielectric Layer Model", IEEE TRANS. ON PLASMA SCI. 47 Issue: 5, 2759-2764 Part: 4 (MAY 2019)

R.9. Canton A., Cavazzana R., Grando L., et al.: "Designing high efficiency glow discharge cleaning systems", NUCLEAR MATERIALS AND ENERGY 19, 468-472 (MAY 2019)

R.10. Predebon I., Xanthopoulos P., Gobbin M.: "Electron temperature gradient driven instabilities in helical reversed-field pinch plasmas", PLASMA PHYS. CONTROL. FUSION 61 Issue: 5, 055011 (MAY 2019)

R.11. Abate D., Marchiori G., Villone F.: "Plasma shape effect on the n=0 stability of RFX-mod-shaped tokamak plasmas", NUCL. FUSION **59** Issue: 6, 066027 (JUN 2019)

R.12. Antoni V., Taccogna F., Agostinetti P., et al.: "Negative ion beam source as a complex system: identification of main processes and key interdependence", RENDICONTI LINCEI-SCIENZE FISICHE E NATURALI **30** Issue: 2, 277-285 (JUN 2019)

R.13. Marrelli, L., Cavazzana R., Bonfiglio, D., et al., RFX-Mod Team: "Upgrades of the RFX-mod reversed field pinch and expected scenario improvements", NUCL. FUSION **59** Issue: 7, UNSP 076027 (JUL 2019)

R.14. Montani G, Cianfrani F, Carlevaro N: "Quasi-linear model for the beam-plasma instability: analysis of the self-consistent evolution", PLASMA PHYS. CONTROL. FUSION **61** Issue: 7, 075018 (JUL 2019)

R.15. Scarin P., Agostini M., Spizzo G., et al., RFX-Mod Team: "Helical plasma-wall interaction in the RFX-mod: effects of high-n mode locking", NUCL. FUSION **59** Issue: 8, 086008 (AUG 2019)

R.16. Murari A., Lungaroni M., Gelfusa M., et al., JET Contributors: “Adaptive learning for disruption prediction in non-stationary conditions”, NUCL. FUSION **59** Issue: 8, 086037 (AUG 2019*)*

R.17. Toigo V, Dal Bello S., Bigi M., et al.: “Progress in the ITER neutral beam test facility”, NUCL. FUSION **59** Issue: 8, 086058 (AUG 2019)

R.18. Spolaore M., Agostinetti P., Killer C., et al., W7-X Team: “High Resolution Probe for filament transport and current density study at the edge region of W7-X”, JOURNAL OF INSTRUMENTATION **14** C09035 (SEP 2019)

R.19. Siragusa M., Sonato P., Visentin M., et al.: “Conceptual design of scalable vacuum pump to validate sintered getter technology for future NBI application”, FUS ENG AND DESIGN **146** Special Issue, 87-90 Part: A (SEP 2019)

R.20. Abate D, Marchiori G., Villone F.: “Modelling and experimental validation of RFX-mod Tokamak shaped discharges”, FUS ENG AND DESIGN **146** Special Issue, 135-138 Part: A (SEP 2019)

R.21. Zaupa M, Dalla Palma M., Sartori E., et al.: “Thermo-hydraulic analyses and fatigue verification of the Electrostatic Residual Ion Dump for the ITER HNB” , FUS ENG AND DESIGN **146** Special Issue, 182-186 Part: A (SEP 2019)

R.22. Dal Bello S., Battistella M., Grando L., et al.: “Safety systems in the ITER neutral beam test facility”, FUS ENG AND DESIGN **146** Special Issue, 246-249 Part: A (SEP 2019)

R.23. Manduchi G., Luchetta A., Taliercio C., et al.: “The timing system of the ITER full size neutral beam injector prototype”, FUS ENG AND DESIGN **146** Special Issue, 281-284 Part: A (SEP 2019)

R.24. Bettini P., Chiariello A.G., Formisano A., et al.: “Real time assessment of the magnetic diagnostic system in RFX-mod”, FUS ENG AND DESIGN **146** Special Issue, 426-429 Part: A (SEP 2019)

R.25. Agostinetti P., Bolzonella, T., Gobbin, M., et al.: “Conceptual design of a neutral beam heating & current drive system for DTT”, FUS ENG AND DESIGN **146** Special Issue, 441-446 Part: A (SEP 2019)

R.26. Luchetta A., Toigo V., Dal Bello S., et al.: “SPIDER integrated commissioning”, FUS ENG AND DESIGN **146** Special Issue, 500-504 Part: A (SEP 2019)

R.27. Maistrello A., Dan M., Corato V., et al.: “Preliminary studies on DEMO toroidal field circuit topology and overvoltage estimation”, FUS ENG AND DESIGN **146** Special Issue, 539-542 Part: A (SEP 2019)

R.28. Rizzolo A., Barbisan M. Bizzotto L., et al.: “Characterization of the SPIDER Cs oven prototype in the CAesium Test Stand for the ITER HNB negative ion sources”, FUS ENG AND DESIGN **146** Special Issue, 676-679 Part: A (SEP 2019)

R.29. Marrelli L., Marchiori G., Bettini P., et al.: “Optimization of RFX-mod2 gap configuration by estimating the magnetic error fields due to the passive structure currents”, FUS ENG AND DESIGN **146** Special Issue, 680-683 Part: A (SEP 2019)

R.30. Peruzzo S., Bernardi M., Berton G., et al.: “Technological challenges for the design of the RFX-mod2 experiment”, FUS ENG AND DESIGN **146** Special Issue, 692-696 Part: A (SEP 2019)

R.31. Pasqualotto R., Barbisan M., Lotto L., et al.: “Plasma light detection in the SPIDER beam source”, FUS ENG AND DESIGN **146** Special Issue, 709-713 Part: A (SEP 2019)

R.32. Pavei M., Marcuzzi D., Zaccaria P., et al.: “Spider beam source ready for operation”, FUS ENG AND DESIGN **146** Special Issue, 736-740 Part: A (SEP 2019)

R.33. Murari A., Bekris N., Figueiredo J., et al.,JET Contributors: “Implementation and exploitation of JET enhancements at different fuel mixtures in preparation for DT operation and next step devices”, FUS ENG AND DESIGN **146** Special Issue, 741-744 Part: A (SEP 2019)

R.34. Vallar M., Karpushov A. N., Agostini M., et al., TCV Team, EUROfusion Mst1 Team: “Status, scientific results and technical improvements of the NBH on TCV tokamak”, FUS ENG AND DESIGN **146** Special Issue, 773-777 Part: A (SEP 2019)

R.35. Chitarin G., Kojima A., Aprile D., et al.: “Improving a negative ion accelerator for next generation of neutral beam injectors: Results of QST-Consorzio RFX collaborative experiments”, FUS ENG AND DESIGN **146** Special Issue, 792-795 Part: A (SEP 2019)

R.36. Masiello A., Annino C., Busch M., Marcuzzi D., Pavei M., Zaccaria P. et al.: “The fabrication and assembly of the beam source for the SPIDER experiment”, FUS ENG AND DESIGN **146** Special Issue, 839-844 Part: A (SEP 2019)

R.37. Marconato N., Bettini P., Cavazzana R., et al.: “Design of the new electromagnetic measurement system for RFX-mod upgrade”, FUS ENG AND DESIGN **146** Special Issue, 906-909 Part: A (SEP 2019)

R.38. Fellin F., Boldrin M., Cucinotta E. S., et al.: “Simulation and verification of air cooling system for-1MVdc MITICA High Voltage hall in Padova”, FUS ENG AND DESIGN **146** Special Issue, 1069-1072 Part: A (SEP 2019)

R.39. Vincenzi P., Fassina A., Giudicotti L., et al.: “Design and mockup tests of the RING photo-neutralizer optical cavity for DEMO NBI”, FUS ENG AND DESIGN **146** Special Issue, 1360-1363 Part: A (SEP 2019)

R.40. Piron L., Challis C., Felton R., et al., JET Contributors: “The dud detector: An empirically-based real-time algorithm to save neutron and T budgets during JET DT operation”, FUS ENG AND DESIGN **146** Special Issue, 1364-1368 Part: A Published: SEP 2019

R.41. Dal Bello S., Fincato M., Breda M., et al.: “SPIDER gas injection and vacuum system: From design to commissioning”, FUS ENG AND DESIGN **146** Special Issue, 1485-1489 Part: B (SEP 2019)

R.42. Luchetta A., Pomaro, N., Manduchi G., et al.: “Progress in the design of MITICA control and interlock systems”, FUS ENG AND DESIGN **146** Special Issue, 1528-1532 Part: B (SEP 2019)

R.43. Tinti P., Fellin F.: “Conceptual design of Integrated Bivalent Auxiliary System (SABI) supporting the MITICA cooling plant and cryogenic plant”, FUS ENG AND DESIGN **146** Special Issue, 1694-1697 Part: B (SEP 2019)

R.44. Boldrin M., Simon M., Escudero G. G., et al.: “The High Voltage Deck 1 and Bushing for the ITER Neutral Beam Injector: Integrated design and installation in MITICA experiment”, FUS ENG AND DESIGN **146** Special Issue: 1895-1898 Part: B (SEP 2019)

R.45. Gasparini F., Recchia M., Bigi M., et al., “Investigation on stable operational regions for SPIDER RF oscillators”, FUS ENG AND DESIGN **146** Special Issue, 2172-2175 Part: B (SEP 2019)

R.46. Piovan R., Gaio E., Lunardon F., et al.: “MEST: A new Magnetic Energy Storage and Transfer system for improving the power handling in fusion experiments”, FUS ENG AND DESIGN **146** Special Issue, 2176-2179 Part: B (SEP 2019)

R.47. Bustreo C., Giuliani U., Maggio D., et al.: “How fusion power can contribute to a fully decarbonized European power mix after 2050”, FUS ENG AND DESIGN **146** Special Issue, 2189-2193 Part: B (SEP 2019)

R.48. Zanotto L., Dan M., Toigo V, et al.: “Acceleration grid power supply conversion system of the MITICA neutral beam injector: On site integration activities and tests”, FUS ENG AND DESIGN **146** Special Issue, 2238-2241 Part: B (SEP 2019)

R.49. Delogu R. S., Montisci A, Pimazzoni A., et al.: “Neural network based prediction of heat flux profiles on STRIKE”, FUS ENG AND DESIGN **146** Special Issue: 2307-2313 Part: B (SEP 2019)

R.50. Pimazzoni A., Cescon E., Dalla Palma M., et al.: “Thermo-mechanical analysis of unidirectional carbon-carbon composite for thermal imaging diagnostic of a particle beam”, FUS ENG AND DESIGN **146** Special Issue, 2457-2461 Part: B (SEP 2019)

R.51. Serianni G., Toigo V, Bigi M., et al.: “SPIDER in the roadmap of the ITER neutral beams”, FUS ENG AND DESIGN **146** Special Issue, 2539-2546 Part: B (SEP 2019)

R.52. Ferro A., Lunardon F., Ciattaglia S., et al.: “The reactive power demand in DEMO: Estimations and study of mitigation via a novel design approach for base converters”, FUS ENG AND DESIGN **146** Special Issue: 2687-2691 Part: B (SEP 2019)

R.53. Barbisan M., Pasqualotto R., Rizzolo A. : “Design and preliminary operation of a laser absorption diagnostic for the SPIDER RF source”, FUS ENG AND DESIGN **146** Special Issue: 2707-2711 Part: B (SEP 2019)

R.54. Bustreo C., Agostinetti P., Bettini P., et al.: “RFP based Fusion-Fission Hybrid reactor model for nuclear applications”, FUS ENG AND DESIGN **146** Special Issue: 2725-2728 Part: B (SEP 2019)

R.55. Paccagnella R. : “Helicity transport and dynamo sustainment for helical plasma states”, NEW JOURNAL OF PHYSICS Volume: 21 Article Number: 093045 Published: SEP 24 2019

R.56. Pigatto L., Aiba N., Bolzonella T., et al.: “Resistive wall mode physics and control challenges in JT-60SA high beta(N)scenarios”, NUCL. FUSION **59** Issue: 10 106028 (OCT 2019)

R.57. Abate D., Bettini P.: “An inverse equilibrium tool to define axisymmetric plasma equilibria”, PLASMA PHYS. CONTROL. FUSION **61** Issue: 10, 105016 (OCT 2019)

R.58. Escande D. F., Gondret V., Sattin F.: “Relevant heating of the quiet solar corona by Alfven waves: a result of adiabaticity breakdown: “SCIENTIFIC REPORTS **9** 14274 (OCT 3 2019)

R.59. Agostini M., Vianello N., Carraro L., et al., ASDEX Upgrade Team, EUROfusion MST1 Team: “Neutral density estimation in the ASDEX upgrade divertor from deuterium emissivity measurements during detachment and shoulder formation”, PLASMA PHYS. CONTROL. FUSION **61** Issue: 11, 115001 (NOV 2019)

R.60. Zamengo A.: “Operational and Performance Overview of the 50 kA-35 kV RFX-Mod DC-Current Interruption System”, IEEE TRANS. ON PLASMA SCI. **47** Issue: 11, 5198-5203 Part: 2 (NOV 2019)

R.61. Murari A., Lungaroni M., Peluso E., et al.: “A Model Falsification Approach to Learning in Non-Stationary Environments for Experimental Design”, SCIENTIFIC REPORTS **9**, 17880 (NOV 29 2019)

R.62. Zanca P., Sattin F., Escande D. F., et al., JET Contributors: “A power-balance model of the density limit in fusion plasmas: application to the L-mode tokamak”, NUCL. FUSION **59** Issue: 12, 126011 (DEC 2019)

R.63. Cordaro L., De Masi G., Fassina A., Gareri C. , Pimazzoni A., Desideri D., Indolfi C. and Martines E.: “The Role of Thermal Effects in Plasma Medical Applications: Biological and Calorimetric Analysis”, Appl. Sci. 9, 5560, doi:10.3390/app9245560 (2019)

R.64. Cordaro L., De Masi G., Fassina A., Mancini D. , Cavazzana R.., Desideri D., Sonato P., Zuin M., Zaniol B. and Martines E.: “On the Electrical and Optical Features of the Plasma

Coagulation Controller Low Temperature Atmospheric Plasma Jet", Plasma **2**, 156–167, doi:10.3390/plasma2020012 (2019)

R.65. Fellin F., Lama S., Viero L., Potente D.: "HVAC per i siti della ricerca scientifica applicata: il caso PRIMA-NBTF", Aicarr journal anno **10**,.44-49, (2019)

R.66. Barbisan M., Pasqualotto R., Rizzolo A.: "Laser absorption spectroscopy studies to characterize Cs oven performances for the negative ion source SPIDER", *JINST* **14** C12011 (2019)

R.67. Spagnolo S., Spolaore M., Bernardi M., Cavazzana R., Peruzzo S., Dalla Palma M., De Masi G., Grenfell G., Marconato N., Martines E., Momo B., Vianello N., Zuin M.: "Design of embedded electrostatic sensors for the RFX-mod2 device", JINST **14** C11014 (2019)

Journal papers with a Consorzio RFX co-author

R.68. Peluso E., Craciunescu T., Murari A., Carvalho P., Gelfusa M., and JET Contributors: "A comprehensive study of the uncertainties in bolometric tomography on JET using the maximum likelihood method", Rev. Sci. Instrum. 90, 123502 (2019)

R.69. Cristofaro S,, Fröschle M., Mimo A., Rizzolo A., De Muri M., Barbisan M. and Fantz U.: "Design and comparison of the Cs ovens for the test facilities ELISE and SPIDER", Rev. Sci. Instrum. 90, 113504 (2019)

R.70. Causa, F., Gospodarczyk, M., Buratti, P., Valisa M. et al. FTU Team: "Runaway electron imaging spectrometry (REIS) system", REV. SCI. INSTRUM. 90 Issue: 7, 073501 (2019)

R.71. Carnevale D., Ariola M., Artaserse G., Bagnato F., Bin W., Boncagni L., Bolzonella T., Bombarda F., Buratti P., L Calacci L., Causa F., Coda S., Cordella F., Decker J., De Tommasi G., Duva B., Esposito B., Ferrò G., Ficker O., Gabellieri L., Gabrielli A., Galeani S., Galperti C., Garavaglia S., Havranek A., Gobbin M. et al: "Runaway electron beam control", PLASMA PHYS. CONTROL. FUSION 61 Issue: 1, 014036 (JAN 2019)

R.72. Maurizio R., Tsui C. K., Duval B. P., Reimerdes H. , Theiler C. , Boedo J. , Labit B., Sheikh U. , Spolaore M., TCV Team and EUROfusion MST1 Team: "The effect of the secondary x-point on the scrape-off layer transport in the TCV snowflake minus divertor", NUCL. FUSION 59 Issue: 1, 016014 (JAN 2019)

R.73. Mlynar J., Ficker O., Macusova E., Gobbin M., COMPASS Team, EUROfusion MST1 Team: "Runaway electron experiments at COMPASS in support of the EUROfusion ITER physics research", PLASMA PHYS. CONTROL. FUSION 61 Issue: 1, 014010 (JAN 2019)

R.74. Yamanaka K., Nakanishi H., Ozeki T., Manduchi G. et al.: "High-performance data transfer for full data replication between iter and the remote experimentation centre", FUS ENG AND DESIGN 138 Special Issue, 202-209 (JAN 2019)

R.75. Sias G., Cannas B., Fanni A., Murari A. et al.: "A locked mode indicator for disruption prediction on JET and ASDEX upgrade", FUS ENG AND DESIGN 138 Special Issue, 254-266 (JAN 2019)

R.76. Vanini S., Calvini P., Checchia P., Garola Rigoni A. et al.: "Muography of different structures using muon scattering and absorption algorithms", PHILOSOPHICAL TRANSACTIONS OF THE ROYAL SOCIETY A-MATHEMATICAL PHYSICAL AND ENGINEERING SCIENCES 377 Issue: 2137, 0180051 (JAN 2019)

R.77. Muraro A., Croci G., Rebai M., Dalla Palma M., Fincato M., Pasqualotto R., Tollin M. et al.: "Directionality properties of the nGEM detector of the CNESM diagnostic system for SPIDER", NUCLEAR INSTR. & METHODS IN PHYSICS RESEARCH SECTION A-

ACCELERATORS SPECTROMETERS DETECTORS AND ASSOCIATED EQUIPMENT 916, 47-50 (FEB 2019)

R.78. Blanken T. C., Felici F., Galperti C., Martin P., Agostini M., Bettini P., Bolzonella T., Canton A., Cavazzana R., De Masi G., Delogu R.S., Gobbin M., Innocente P., Kudlaceck O., Marconato N., Marrelli L., Paccagnella R., Piovesan P., Piron C., Pedrebon I., Puiatti M.E., Spagnolo S., Spizzo G., Spolaore M., Terranova D., Valisa M., Vianello N., Zanca P., Zuin M. et al., EUROfusion MST1 Team, TCV Team: "Real-time plasma state monitoring and supervisory control on TCV", NUCL. FUSION 59 Issue: 2, 026017 (FEB 2019)

R.79. Finotti C., Gaio E., Benfatto I.e, et al.: "Continuous state space model of the ITER pulsed power electrical network for stability analysis", FUS ENG AND DESIGN 139, 62-73 (FEB 2019)

R.80. Bonofiglo P. J., Anderson J. K., Gobbin M., et al.: "Fast ion transport in the quasi-single helical reversed-field pinch", PHYS. PLASMAS 26 Issue: 2, 022502 (FEB 2019)

R.81. Abramovic I., Pavone A., Moseev D., Carraro L., Zuin M. et al., W7-X Team: "Forward modeling of collective Thomson scattering for Wendelstein 7-X plasmas: Electrostatic approximation", REV. SCI. INSTRUM. 90 Issue: 2, 023501 (FEB 2019)

R.82. Tierens W., Milanesio D., Urbanczyk G., Bolzonella T., Gobbin M., Martin P., Marrelli L., Piovesan P., Terranova D., Piron C., Valisa M., Vianello N., Agostini M., Bettini P., Canton A., Cavazzana R., De Masi G., Delogu R.S., Marconato N., Paccagnella R., Predebon I., Spagnolo S., Spizzo G., Zanca P., Zuin M. et al., ASDEX Upgrade Team, EUROfusion MST1 Team: "Validation of the ICRF antenna coupling code RAPLICASOL against TOPICA and experiments", NUCL. FUSION 59 Issue: 4, 046001 (APR 2019)

R.83. Dreni, A., Laguardi, L., McDermot, R., Bolzonella T., Delogu R.S., Gobbin M., Martin P., Piron C., Terranova D., Valisa M., Vianello N. et al., ASDEX-Upgrade Team, EUROfusion MST1 Team: "Evolution of nitrogen concentration and ammonia production in N-2-seeded H-mode discharges at ASDEX Upgrade", NUCL. FUSION 59 Issue: 4, 046010 (APR 2019)

R.84. Causa F., Buratti P., Alessi E., Carraro L., Puiatti M. E., Valisa M., Zaniol B. et al., FTU Team: "Analysis of runaway electron expulsion during tokamak instabilities detected by a single-channel Cherenkov probe in FTU", NUCL. FUSION 59 Issue: 4, 046013 (APR 2019)

R.85. Trier E., Wolfrum E., Willensdorfer M., Martin P., Agostini M., Bettini P., Bolzonella T., Canton A., Cavazzana R., De Masi G., Delogu R.S., Gobbin M., Innocente P., Kudlacek O., Marconato N., Marrelli L., Paccagnella R., Piovesan P., Piron C., Predebon I., Puiatti M. E., Spagnolo S., Spizzo G., Spolaore M., Terranova D., Trevisan G. L., Valisa M., Vianello N., Zanca P., Zuin M. et al., ASDEX Upgrade Team, EUROfusion MST1 Team: "ELM-induced cold pulse propagation in ASDEX Upgrade", PLASMA PHYS. CONTROL. FUSION 61 Issue: 4, 045003 (APR 2019)

R.86. Pegoraro F., Bonfiglio D., Cappello S., et al.: "Coherent magnetic structures in self-organized plasmas", PLASMA PHYS. CONTROL. FUSION Volume: 61 Issue: 4 Article Number: 044003 Published: APR 2019

R.87. Cannas B., Fanni A, Murari A., et al., JET Contributors: 2Recurrence Plots for Dynamic Analysis of Type-I ELMs at JET With a Carbon Wall", IEEE TRANS. ON PLASMA SCI. 47 Issue: 4, 1871-1877 (APR 2019)

R.88. Ionita C., Schneider B. S., Costea, S., Vianello N., Spolaore M. et al.: "Plasma potential probes for hot plasmas", EUROPEAN PHYSICAL JOURNAL D 73 Issue: 4, 73 (APR 2019)

R.89. Ho A., Citrin J., Auriemma F., et al., JET Contributors: "Application of Gaussian process regression to plasma turbulent transport model validation via integrated modelling", NUCL. FUSION Volume: 59 Issue: 5 Article Number: 056007 Published: MAY 2019

R.90. Schneider B. S., Ionita C., Costea S, Vasilovici O., Kovačič J, Gyergyek T., Končar B., Draksler M., Nem R. d., Naulin V,, Rasmussen J. J., Spolaore M., Vianello N., Stärz R., Herrmann A., Schrittwiese R.: "New diagnostic tools for transport measurements in the scrape-off layer (SOL) of medium-size tokamaks", PLASMA PHYS. CONTROL. FUSION 61 Issue: 5, 054004 (MAY 2019)

R.91. Wang N., Liang Y., Igochine V., Piovesan P. et al., ASDEX Upgrade Team, EUROfusion MST1 Team: "Impact of n=1 field on the non-axisymmetric magnetic perturbations associated with the edge localized mode crashes in the ASDEX Upgrade tokamak", NUCL. FUSION 59 Issue: 5, 054002 (MAY 2019)

R.92. Maurizio R., Duval B. P., Labit B., Vianello N., et al., TCV Team, EUROfusion MST1 Team: "Conduction-based model of the Scrape-Off Layer power sharing between inner and outer divertor in diverted low-density tokamak plasmas", NUCLEAR MATERIALS AND ENERGY 19, 372-377 (MAY 2019)

R.93. Federici G., Bachmann C., Barucca L., Gaio E., et al.: "Overview of the DEMO staged design approach in Europe", NUCL. FUSION 59 Issue: 6 Article UNSP 066013 (JUN 2019)

R.94. Huber V, Hubert A., Kinna D., Bustreo C., et al., JET Contributors : "The software and hardware architecture of the real-time protection of in-vessel components in JET-ILW", NUCL. FUSION 59 Issue: 7, 076016 (JUL 2019)

R.95. Maggi C. F., Weisen H., Casson F. J., Lorenzini R., et al., JET Contributors: "Isotope identity experiments in JET-ILW with H and D L-mode plasmas", NUCL. FUSION 59 Issue: 7, 076028 (JUL 2019)

R.96. Bonofiglo P. J., Anderson J. K., Boguski J. Gobbin M., et al.: "Fast Ion Transport in the Three-Dimensional Reversed-Field Pinch", PHYS. REV. LETT. 123 Issue: 5, 055001 (JUL 2019)

R.97. Labit B., Eich T., Harrer G. F., Agostini M. et al.: "Dependence on plasma shape and plasma fueling for small edge-localized mode regimes in TCV and ASDEX Upgrade", NUCL. FUSION Volume: 59 Issue: 8 Article Number: 086020 Published: AUG 2019

R.98. Nielsen A. H., Asztalos O., Olsen J., Vianello N. et al., EUROfusion MST1 Team, EUROfusion-IM Team, ASDEX Upgrade Team: "Synthetic edge and scrape-off layer diagnostics-a bridge between experiments and theory", NUCL. FUSION 59 Issue: 8, 086059 (AUG 2019)

R.99. Hernandez W. A., Guimaraes-Filho Z., Grenfell G., et al.: "Spatial inhomogeneity effects on burst temperature estimation using a triple probe configuration in Tokamak Chauffage Alfven Bresilien tokamak", J. OF PLASMA PHYSICS 85 Issue: 4, 905850407 (AUG 2019)

R.100. Da Silva F., Ferreira J., De Masi, G., et al.: "A first full wave simulation assessment of reflectometry for DTT", JOURNAL OF INSTRUMENTATION 14 C08011 (AUG 2019)

R.101. Craciunescu T., Murari A., Gelfusa M.: "Causality Detection Methods Applied to the Investigation of Malaria Epidemics", ENTROPY 21 Issue: 8, 784 (AUG 2019)

R.102. Li, J. C., Liu, S. F., Kong, W., S.C. Guo et al.: "Effects of trapped electrons and impurity ions on ITG modes in reversed-field pinch plasmas", EPL 127 Issue: 4, 45002 (AUG 2019)

R.103. Lungaroni M., Murari A., Peluso E., et al.: "Geodesic Distance on Gaussian Manifolds to Reduce the Statistical Errors in the Investigation of Complex Systems", COMPLEXITY 2019, 5986562 (AUG 18 2019)

R.104. Czarnecka A., Krawczyk N., Jacquet, P., Lerche E., Bobkov V., Challis C., Frigione D., Graves J., Lawson K.D., Mantsinen[7] M.J., Meneses L., Pawelec E., Pütterich T., M Sertoli M., Valisa M., Van Eester D. and JET Contributors,"Analysis of metallic impurity content by

means of VUV and SXR diagnostics in hybrid discharges with hot-spots on the JET-ITER-like wall poloidal limiter" Plasma Physics and Contr. Fusion 61(8), 085004 (2019)

R.105. Piron C., Garcia J., Agostini M., et al., TCV Team, EUROfusion MST1 Team: "Extension of the operating space of high-beta(N) fully non-inductive scenarios on TCV using neutral beam injection", NUCL. FUSION 59 Issue: 9, 096012 (SEP 2019)

R.106. Ficker O., Macusova E., Mlynar J., Gobbin M.et al., COMPASS Team, EUROfusion MST1 Team: "Runaway electron beam stability and decay in COMPASS", NUCL. FUSION 59 Issue: 9, 096036 (SEP 2019)

R.107. Albanese R., Crisanti F., Martin P., et al., DTT Team: "Design review for the Italian Divertor Tokamak Test facility", FUS ENG AND DESIGN 146 Special Issue, 194-197 Part: A (SEP 2019)

R.108. Biel W., Albanese R., Ambrosino R., Cavazzana R., Marchiori G., De Masi G. et al.: "Diagnostics for plasma control - From ITER to DEMO",FUS ENG AND DESIGN 146 Special Issue, 465-472 Part: A (SEP 2019)

R.109. Croci G., Muraro A., Cippo Perelli E., Grosso R., Pasqualotto R., Cavenago M., Cervaro V., Dalla Palma M., Feng S., Fincato M., Franchin, Gaicomelli L., Murtasc F., Nocente M., rebaiaf M., Tardocchia M., Tollin M., Gorini, G.: "The CNESM neutron imaging diagnostic for SPIDER beam source", FUS ENG AND DESIGN 146 Special Issue, 660-665 Part: A (SEP 2019)

R.110. Cavenago M., Serianni G., Baltador C., et al.: "Experimental experience and improvement of NIO1 H- ion source", FUS ENG AND DESIGN 146 Special Issue, 749-752 Part: A (SEP 2019)

R.111. Ambrosino R., Castaldo A., Ramogida G., Martin P. et al.: "Magnetic configurations and electromagnetic analysis of the Italian DTT device", FUS ENG AND DESIGN 146 Special Issue, 1246-1253 Part: A (SEP 2019)

R.112. Varje J., Kurki-Suonio T., Snicker A., Vincenzi P., Agostinetti P., Sonato P., et al.: "Sensitivity of fast ion losses to magnetic perturbations in the European DEMO", FUS ENG AND DESIGN 146 Special Issue, 1615-1619 Part: B (SEP 2019)

R.113. Franke T., Agostinetti P., Bachmann C., Sartori E., Sonato P.et al.: "Initial port integration concept for EC and NB systems in EU DEMO tokamak", FUS ENG AND DESIGN 146 Special Issue, 1642-1646 Part: B (SEP 2019)

R.114. Hatakeyama S., Shimada K., Yamauchi K., Novello L., Maistrello A., Ferro A., et al.: "Development of supervisory control system for magnet power supplies in JT-60SA", FUS ENG AND DESIGN 146 Special Issue, 1652-1656 Part: B (SEP 2019)

R.115. Siviero F., Caruso L., Porcelli T., Sartori E., Siragusa M., Sonato P. et al.: "Characterization of ZAO ®sintered getter material for use in fusion applications", FUS ENG AND DESIGN 146 Special Issue, 1729-1732 Part: B (SEP 2019)

R.116. Mazzotta C., Tudisco O., Galatola Teka G., et al.: "A two colour interferometer for PROTO-SPHERA experiment", FUS ENG AND DESIGN 146 Special Issue, 1801-1804 Part: B (SEP 2019)

R.117. Chiariello A. G., Formisano A., Ledda F., Murari A., Terranova D. et al., JET Contributors: "Plasma boundary reconstruction in JET by magnetic measurements", FUS ENG AND DESIGN 146 Special Issue, 2074-2077 Part: B (SEP 2019)

R.118. Yanovskiy V. V., Isernia N., Pustovitov V. D., Abate D., Bettini P., Paccagnella R., Peruzzo S. et al., COMPASS Team: "Comparison of approaches to the electromagnetic analysis of COMPASS-U vacuum vessel during fast transients", FUS ENG AND DESIGN 146 Special Issue, 2338-2342 Part: B (SEP 2019)

R.119. Ratta G. A., Vega J., Murari, A., JET Contributors: “A multidimensional linear model for disruption prediction in JET”, FUS ENG AND DESIGN 146 Special Issue, 2393-2396 Part: B (SEP 2019)

R.120. Chauvin N., Akagi T., Bellan L., Beauvais P.Y., Bolzon B., Cara P., Chel S., Comunian M. , Dzitko H., Fagotti E. , Gérardin F., Gex D., Gobin R. , Harrault F., Heidinger R. , Ichimiya R., Ihara A., Kasugai A., Kitano T., Knaster J. , Komata M., Kondo K. , Marqueta A., Nishiyama K., Okumura Y. , Pisent A. , Pruneri G., et al.: “Deuteron beam commissioning of the linear IFMIF prototype accelerator ion source and low energy beam transport”, NUCL. FUSION 59 Issue: 10, 106001 (OCT 2019)

R.121. Pau A., Fanni A., Carcangiu S., Murari A. et al., JET Contributors”, A machine learning approach based on generative topographic mapping for disruption prevention and avoidance at JET”, NUCL. FUSION 59 Issue: 10,106017 (OCT 2019)

R.122. Oliver H. J. C., Sharapov S. E., Breizman B. N, Terranova D. et al., JET Contributors: “Modification of the Alfven wave spectrum by pellet injection”, NUCL. FUSION Volume: 59 Issue: 10 Article Number: 106031 Published: OCT 2019

R.123. Strait E. J., Barr J. L., Baruzzo M., et al.: “Progress in disruption prevention for ITER”, NUCL. FUSION 59 Issue: 11, 112012 (NOV 2019)

R.124. Ascasibar E., Alba D., Alegre D., .., Momo B., et al., TJ-Team: “Overview of recent TJ-II stellarator results”, NUCL. FUSION 59 Issue: 11, 112019 (NOV 2019)

R.125. Coda S., Agostini M., Albanese R., et al., EUROfusion Mst1 Team: “Physics research on the TCV tokamak facility: from conventional to alternative scenarios and beyond”, NUCL. FUSION 59 Issue: 11, 112023 (NOV 2019)

R.126. Joffrin E., Abduallev S., Abhangi M., Baruzzo M. et al.: “Overview of the JET preparation for deuterium-tritium operation with the ITER like-wall”, NUCL. FUSION 59 Issue: 11, 112021 (NOV 2019)

R.127. Meyer H., Aguiam D., Angioni C., et al., AUG Team, EUROfusion Mst1 Team: “Overview of physics studies on ASDEX Upgrade”, NUCL. FUSION 59 Issue: 11, 112014 (NOV 2019)

R.128. Lazerson S. A., Gao Y., Hammond, K, Spolaore M. et al., W7-X Team: “Tuning of the rotational transform in Wendelstein 7-X”, NUCL. FUSION 59 Issue: 12 , 126004 (DEC 2019)

R.129. Verhaegh K., Lipschultz B., Duval B. P., ..,Vianello N. et al., TCV Team, EUROfusion MST1 Team: “An improved understanding of the roles of atomic processes and power balance in divertor target ion current loss during detachment”, NUCL. FUSION 59 Issue: 12, 126038 (DEC 2019)

R.130. Giruzzi G., Yoshida M., Aiba N., .., Bolzonella T., Bonotto M.,.. ,Giudicotti L., .., Marchiori G., .. ,Pasqualotto R., .., Pigatto L., .. ,Valisa M., Vallar M., et al. “Advances in the physics studies for the JT-60SA tokamak exploitation and research plan”, Plasma Phys. Control. Fusion 62, Number 1 Special Issue (2019)

R.131. Pucella, G., Alessi, E., Angelini, B., Apicella, M.L., Apruzzese, G., Artaserse, G., Baiocchi, B., Belli, F., Bin, W., Bombarda, F., Boncagni, L., Botrugno, A., Briguglio, S., Bruschi, A., Buratti, P., Calabro, G., Cappelli, M., Cardinali, A., Carnevale, D., Carraro, L., Castaldo, C., Causa, F., Ceccuzzi, S., Centioli, C., Cesario, R., Cianfarani, C., Claps, G., Cocilovo, V., Cordella, F., Crisanti, F., D'Arcangelo, O., De Angeli, M., Di Troia, C., Esposito, B., Fanale, F., Farina, D., Figini, L., Fogaccia, G., Frigione, D., Fusco, V., Gabellieri, L., Garavaglia, S., Giovannozzi, E., Gittini, G., Granucci, G., Grosso, G., Iafrati, M., Iannone, F., Laguardia, L., Lazzaro, E., Lontano, M., Maddaluno, G., Magagnino, S., Marinucci, M., Marocco, D., Mazzitelli, G., Mazzotta, C., Mellera, V., Milovanov, A., Minelli, D., Mirizzi, F.C., Moro, A., Nowak, S., Pacella, D., Pallotta, F., Panaccione, L., Panella, M., Pericoli-Ridolfini, V.,

Pizzuto, A., Podda, S., Puiatti, M.E., Ramogida, G., Ravera, G., Ricci, D., Romano, A., Simonetto, A., Sozzi, C., Tartari, U., Tuccillo, A.A., Tudisco, O., Valisa, M., Viola, B., Vitale, E., Vlad, G., Zaniol, B., et al.: "Overview of the FTU results", Nuclear Fusion 59 11 112015 (2019)

R.132. Peluso E., Craciunescu, T., Gelfusa, M., **Murari, A**., Carvalho, P.J., Gaudio, P. : "On the effects of missing chords and systematic errors on a new tomographic method for JET bolometry", Fusion Engineering and Design,146 (2019) 2124-2129

R.133. Mazzitelli G., Albanese R., Crisanti F., **Martin, P**., Pizzuto, A., Tuccillo A.A., Ambrosino, R., Appi, A., Di Gironimo, G., Di Zenobio, A., Frattolillo, A., Granucci, G., Innocente, P., Lampasi, A., Martone, R., Polli, G.M., Ramogida, G., Rossi, P., Sandri, S., Valisa, M., Villari, R., Vitale, V. : "Role of Italian DTT in the power exhaust implementation strategy", Fusion Engineering and Design, Volume 146, Part A, September 2019, Pages 932-936

R.134. Silva F., Ferreira J., De Masi G., Heuraux S., Ricardo E., Ribeiro T., Tudisco O., Cavazzana R., D'Arcangelo O., Silva A.: "A first full wave simulation assessment of reflectometry for DTT", Journal of Instrumentation (2019) 14 8 C08011

National and International Conferences (invited talks in red and oral communications in green,

papers submitted by other labs with Consorzio RFX co-athors in italic)

ISPlasma2019/IC-PLANTS2019, March 17-21 2019, Nagoya, Japan

P.1. De Masi G., Gareri C., Cordaro L., Fassina A., Cavazzana R., Martines E., Zaniol B., Zuin M.,et al. : "The Effect of an Atmospheric Plasma Source on Blood Coagulation", ISPlasma2020/IC-PLANTS2020, March 8-12 2019, Nagoya, Japan, invited

9th Workshop on Stochasticity in Fusion Plasmas , 8-10 April 2019, Bad Honnef Germany

P.2. Lorenzini R.: "Magnetic reconnection in 3D equilibria of RFX-mod", 9th Workshop on Stochasticity in Fusion Plasmas , 8-10 April 2019, Bad Honnef Germany, Invited

European Conference Plasma Diagnostics- ECPD, 6-9 May 2019, Lisbon Portugal

P.3. Franz P., Fassina A.,Trevisan L.: "Design Progress of new Thomson Scattering System in RFX-mod2", European Conference Plasma Diagnostics- ECPD, 6-9 May 2019, Lisbon Portugal

P.4. Cavazzana R., De Masi G., Cavazzana R., Bettini P., Marchiori G., M. Moresco, Peruzzo S., D. Voltolina, Bernardi M., A. Tiso: "Design of a new reflectometric system for real time plasma position control on the RFX-mod2 device", European Conference Plasma Diagnostics- ECPD, 6-9 May 2019, Lisbon Portugal

P.5. Spolaore M., Agostinetti P., Killer C., Brombin M., Cavazzana R., Ghirardelli R., Grenfell G., Grulke O., Moresco M., Martines E., Neubauer O., Nicolai D., Satheeswaran G., Schweer B., Vianello N.,Visentin M. and W7-X Team: "High Resolution Probe for filament transport and current density study at the edge region of W7-X", *JINST* **14** C09035 (2019)- Oral

P.6. Pasqualotto R., Hiroshi T., Fassina A., Giudicotti l., Nardino V., Naoyuki O., Pelli S., Raimond V.: "Conceptual design of JT-60SA edge Thomson scattering diagnostic", European Conference Plasma Diagnostics- ECPD, 6-9 May 2019, Lisbon Portugal

AIV XXIV Conferecnce, May 7-10, 2019, Giardini Naxos, Italy

P.7. Bustreo C., Giuliani U., Zollino G.: "Scenarios for power generation in Italy", AIV XXIV Conferecnce, May 7-10, 2019, Giardini Naxos, Italy

P.8. Polli G.M., Albanese R., Crisanti F., Martin P., Pizzuto A., Ambrosino R., A. Appi, Cucchiaro A., Di Gironimo G., Di Pace L., Di Zenobio A., Frattolillo A., Granucci G., Innocente P., Lampasi A., Martone R., Mazzitelli G., Ramogida G., Roccella S., Rossi P., Rydzy A., Sandri S., Tuccillo A., Valisa M., Villari R., Vitale V., the DTT Team: "DTT: Overview and Status of the Project", AIV XXIV Conferecnce, May 7-10, 2019, Giardini Naxos, Italy

P.9. De Lorenzi A.: "HV Holding in Vacuum, a Key Issue for the ITER Neutral Beam Injector The contribution of Consorzio RFX", AIV XXIV Conferecnce, May 7-10, 2019, Giardini Naxos, Italy

P.10. Marcuzzi D.,and the Consorzio RFX NBTF Team: "ITER Neutral Beam Test Facility status", AIV XXIV Conferecnce, May 7-10, 2019, Giardini Naxos, Italy

P.11. Barzon A., Degli Agostini F., Fasolo D., Franchin L., Tollin M., Lo Bue A, Semeraro L.: "Metrology for integration and installation activities at the PRIMA Test Facility", AIV XXIV Conferecnce, May 7-10, 2019, Giardini Naxos, Italy

P.12. Lotto L., De Lorenzi A., Pilan N., Tiso A., Rossetto F., Romanato L., Battistella M., Maniero M., Barbato P.,Cervaro V.: "The realization of the High Voltage Short Gap Test Facilty", AIV XXIV Conferecnce, May 7-10, 2019, Giardini Naxos, Italy

P.13. Maniero M., Pilan N., Lotto L., De Lorenzi A., Tiso A., Rossetto F., Romanato L., Cervaro V.: "Preparation of a double polarity dc experiment at the High Voltage Padova Test Facility", AIV XXIV Conferecnce, May 7-10, 2019, Giardini Naxos, Italy

P.14. Ravarottto D., Moro G., Serianni G.: "Proposal for upgrades of the control and data acquisition system of the Negative Ion Source NIO1", AIV XXIV Conferecnce, May 7-10, 2019, Giardini Naxos, Italy

P.15. Rizzieri R., Rizzolo A., Barbisan M., Capobianco R., De Muri M., Fadone M., Ghiraldelli R., Laterza B., Marchiori G., Marcuzzi D., Migliorato L., Molon F., Ravarottto D., Rossetto F., Sartori E., Serianni G.: "The CAesium Test Stand for the development of the caesium ovens for negative ion sources", AIV XXIV Conferecnce, May 7-10, 2019, Giardini Naxos, Italy

P.16. Siviero F., Mura M., Maccallini E., Manini P., Sartori E., Siragusa M. and Sonato P.: "LargeNon-evaporable Getter pumps for application in Nuclear Beam Injectors: from conceptual design to manufacturing", AIV XXIV Conferecnce, May 7-10, 2019, Giardini Naxos, Italy

IAEA TMC CODAS 2019, 13-17 May 2019, Daejeon, Republic of Korea

P.17. Luchetta A., Pomaro N., Taliercio C., Moressa M., Svensson L., Paolucci F,,,Labate C.: "Design of the Interlock System for MITICA", IAEA TMC CODAS 2019, 13-17 May 2019, Daejeon, Republic of Korea

P.18. Manduchi G., Moro G., Luchetta A., Rigoni A., Taliercio C.: "Web-based Streamed Waveform Display using MDSplus events and Node.js", IAEA TMC CODAS 2019, 13-17 May 2019, Daejeon, Republic of Korea

P.19. Manduchi G., Rigoni A., Fredian T.W., Stillerman J.A., Neto A., Sartori F.: "MARTe2 and MDSplus integration for a comprehensive Fast Control and Data Acquisition System", IAEA TMC CODAS 2019, 13-17 May 2019, Daejeon, Republic of Korea

The First International Conference on Innovative Fusion Approaches (ICIFA) will be held on May 26-28, 2019 in Xi'an, China

P.20. Zuin M. and the RFX-mod team: "Overview of the Fusion Science Activity in the RFX-mod Device towards RFX-mod2", The First International Conference on Innovative Fusion Approaches (ICIFA) will be held on May 26-28, 2019 in Xi'an, China

P.21. Cavazzana R., Piovan R., Bustreo C., Zuin M., Puiatti M. E., Valisa M., Bettini P., Zollino G., Casagrande R.: "Perspective of a Reversed Field Pinch as Fusion Core for Neutron Generation", The First International Conference on Innovative Fusion Approaches (ICIFA) will be held on May 26-28, 2019 in Xi'an, China

Giornata Nazionale Saldatura - GNS10, 30-31 May 2019, Genova, Italy

P.22. Manfrin S., Rossetto F., Valente M., Zaccaria P., Bolcato D., Parma A., Ruaro D., Zanotto M.,et al.: "Costruzione e ispezioni della camera da vuoto dell'iniettore di neutri per l'esperimento MITICA (progetto ITER)", Giornata Nazionale Saldatura - GNS10, 30-31 May 2019, Genova, Italy

28th IEEE Symposium on Fusion Engineering, 2 – 6 June, 2019, Florida, USA

P.23. Zaupa M., Dalla Palma M., Barucca L. , Ciattaglia S.: “Preliminary thermo-mechanical design of the once through steam generator and molten salt intermediate heat exchanger for EU DEMO”, 28th IEEE Symposium on Fusion Engineering, 2 – 6 June, 2019, Florida, USA

P.24. Aprile D., Patton T., Pilan N., Chitarin G.: “Design of a system for performing high voltage holding test campaigns on a mockup of MITICA negative ion source”, 28th IEEE Symposium on Fusion Engineering, 2 – 6 June, 2019, Florida, USA

P.25. Aprile D., Agostinetti P., Denizeau S., Chitarin G.: “Mapping of magnetic field of SPIDER by a three-axis automatic positioning system”, 28th IEEE Symposium on Fusion Engineering, 2 – 6 June, 2019, Florida, USA

P.26. Dan M., Zanotto L., Finotti C., Decamps H., Gutierrez D.: “Tests of Acceleration Grid Power Supply-Conversion System of the MITICA test facility”, 28th IEEE Symposium on Fusion Engineering, 2 – 6 June, 2019, Florida, USA

P.27. Agostinetti P., Franke T., Mantel N., Tran M. Q.: “RAMI Evaluation of the Beam Source for the DEMO Neutral Beam Injector”, 28th IEEE Symposium on Fusion Engineering, 2 – 6 June, 2019, Florida, USA

P.28. Ferro A., Zanotto L., Toigo V.: “Manufacturing, installation and commissioning of the residual ion dump power supply for MITICA experiment”, 28TH IEEE Symposium on Fusion Engineering, 2 – 6 June, 2019, Florida, USA, oral

P.29. Piovan R., Agostinetti P., Bettini P., Bustreo C., Cavazzana R., D. Escande, Gaio E., Maistrello A., Puiatti M. E., Valisa M., Zollino G., Zuin M.: “Status and Perspective of the Reversed Field Pinch as Fusion Core in a Fusion-Fission Hybrid Reactor”, 28th IEEE Symposium on Fusion Engineering, 2 – 6 June, 2019, Florida, USA, oral

2019 IEEE Pulsed Power and Plasma Science Conference (PPPS 2019), 23-18 June 2019, Orlando, Florida - USA

P.30. Recchia M., Jain P., Gaio E., Maistrello A., Serianni G., Zamengo A.: “Studies on power transfer efficiency in the drivers of the SPIDER inductively coupled RF ion source”, 2019 IEEE Pulsed Power and Plasma Science Conference (PPPS 2019), 23-18 June 2019, Orlando, Florida - USA

P.31. Gasparini F., Recchia M., Bigi M., Maistrello A., Zamengo A., Gaio E.: “An Eigenvalue Approach to Study SPIDER RF Oscillator Operating Space”, 2019 IEEE Pulsed Power and Plasma Science Conference (PPPS 2019), 23-18 June 2019, Orlando, Florida – USA

10th Festival de Théorie Aix en Provence, July 1-26, 2019

P.32. Cappello S.:Magnetic chaos healing and helical self-organization in plasma pinches" al 10th Festival de Théorie Aix en Provence, July 1-26, 2019 – Invited tutorial

EPS 2019 - 46th European Physical Society Conference on Plasma Physics, 8-12 July 2019, University Milano Bicocca, Milano – Italy

P.33. Bolzonella T., Cavazzana R., Innocente P., Zanca P., Zaniol B., Zuin M.: “High-n tearing mode dynamics in fast rotating RFP plasmas”, EPS 2019 - 46th European Physical Society Conference on Plasma Physics, 8-12 July 2019, University Milano Bicocca, Milano – Italy – P1.1048

P.34. Ferron N., Antoni V., Agostinetti P., Barbisan M., Cavenago M., Chitarin G., Delogu R. S., Minelli P., Pimazzoni A., Poggi C., Sartori E., Serianni G., Suweis S., Taccogna F., Ugoletti M., Veltri P.: “A real case of complex network controllability: the NIO1 ion beam source”, EPS 2019 - 46th European Physical Society Conference on Plasma Physics, 8-12 July 2019, University Milano Bicocca, Milano – Italy – P4.1072

P.35. Bettini P., Cavazzana R., Marchiori G., Marrelli L., Spizzo G., Voltolina D., Zanca P.: "MHD Dynamics and Error Fields in the RFX-mod2 Reversed field Pinch", EPS 2019 - 46th European Physical Society Conference on Plasma Physics, 8-12 July 2019, University Milano Bicocca, Milano – Italy - P4.1038

P.36. Cavazzana R.: "Electrical modelling of the Reversed Field Pinch configuration", EPS 2019 - 46th European Physical Society Conference on Plasma Physics, 8-12 July 2019, University Milano Bicocca, Milano – Italy – P1.1052

P.37. Vallar M., Bolzonella T., Garcia J., Kurki-Suonio T., Sarkimaki K., Varje J., Vincenzi P.: "Toroidal field ripple-induced NBIenergetic particle losses I nJT-60SA", EPS 2019 - 46th European Physical Society Conference on Plasma Physics, 8-12 July 2019, University Milano Bicocca, Milano – Italy – P5.1008

P.38. Veranda M., Scarin P., Agostini M., Bonfiglio D., Cappello S., Spizzo G., Zanca P.: " RFX-mod2: a reversed-field pinch device with edge transport optimization", EPS 2019 - 46th European Physical Society Conference on Plasma Physics, 8-12 July 2019, University Milano Bicocca, Milano – Italy – P2.1003

P.39. Voltolina D. Bettini P., Igochine V., Marrelli L., Pigatto L., Piron L., Zammuto I., the ASDEX Upgrade Team, and the EUROfusion MST1 Team: " Vacuum Estimation of Error Field Correctionon ASDEXU pgrade", EPS 2019 - 46th European Physical Society Conference on Plasma Physics, 8-12 July 2019, University Milano Bicocca, Milano – Italy – P4.1099

P.40. Spizzo G., White R.B., Maraschek M. Igochine V., Granucci G., the ASDEX Upgrade Team and the EUROfusion MST1 Team, " Nonlocal transport in toroidal plasma devices", EPS 2019 - 46th European Physical Society Conference on Plasma Physics, 8-12 July 2019, University Milano Bicocca, Milano – Italy –P2.1078

P.41. Vincenzi P., Delabie E., Solano E. R., Bourdelle C., Hillesheim J.C., Carvalho P., Chernyshova M. and JET contributors: "Ion heat channel at the L-H transition in JET-ILW", EPS 2019 - 46th European Physical Society Conference on Plasma Physics, 8-12 July 2019, University Milano Bicocca, Milano – Italy – P2.1081

P.42. Bonfiglio D., Cappello S., Escande D.F., Di Giannatale G. , Kryzhanovskyy A. , Veranda M., Marrelli L., Zanca P.: "Effect of a realistic boundary on the helical self-organization of the RFP", EPS 2019 - 46th European Physical Society Conference on Plasma Physics, 8-12 July 2019, University Milano Bicocca, Milano – Italy – P1.1049

P.43. Paccagnella R., Masamune S., Mizuguchi N., Predebon I., Sanpei A.: "Cylindrical vs toroidal Single Helical states in the low aspect ratio RELAX device", EPS 2019 - 46th European Physical Society Conference on Plasma Physics, 8-12 July 2019, University Milano Bicocca, Milano – Italy – P5.1103

P.44. Pigatto L., Bettini P., Bolzonella T., Bonotto M., Liu Y.Q., Marchiori G., Takechi M., Villone F.: "Modelling multi-modal Resistive Wall Mode feedback control in JT-60SA perspective high β scenarios", EPS 2019 - 46th European Physical Society Conference on Plasma Physics, 8-12 July 2019, University Milano Bicocca, Milano – Italy – P5-1002

P.45. Carraro L., Innocente P., Tamura N.: "1-dim Collisional Radiative impurity transport code with internal particle source for TESPEL inject", EPS 2019 - 46th European Physical Society Conference on Plasma Physics, 8-12 July 2019, University Milano Bicocca, Milano – Italy – P2.1084

P.46. Piron L., Hender T. C., Joffrin E., Auriemma F., Buratti P., Paccagnella R., Zanca P., Challis C., Gerasimov S., Henriques R. B., Marrelli L., Lomas P., Pucella G., Rimini F., Terranova D. and JET Contributors: "Experimental and modelling study of LM dynamics prior to disruptions in high performance JET", EPS 2019 - 46th European Physical Society

Conference on Plasma Physics, 8-12 July 2019, University Milano Bicocca, Milano – Italy – O4-109 Oral

P.47. Valisa M., Carraro L., Casson F. J., Citrin J., Frassinetti L., Koechl F., Romanelli M., Puiatti M.E., Coffey I., Delabie E., Giroud C., Menmuir S., O'Mullane M. , and JET, and JET contributors: "The role of the edge barrier in the penetration of impurities in the JET ELMy H-mode plasmas", EPS 2019 - 46th European Physical Society Conference on Plasma Physics, 8-12 July 2019, University Milano Bicocca, Milano – Italy – P5.1083

P.48. Fassina A., Franz P., Gobbin M., Marrelli L., Piovesan P., Spizzo G., Terranova D.: "Time evolution of electron temperature profiles in RFX-mod helical states", EPS 2019 - 46th European Physical Society Conference on Plasma Physics, 8-12 July 2019, University Milano Bicocca, Milano – Italy – P4.1061

P.49. Ugoletti M., Agostini M. , Brombin.., M., Pasqualotto R., Serianni G.: "Tomographic reconstruction of the visible emission of NIO1 negative ion beam", EPS 2019 - 46th European Physical Society Conference on Plasma Physics, 8-12 July 2019, University Milano Bicocca, Milano – Italy – P5.3012

P.50. Martines E.: "Atmospheric pressure helium plasma as a tool for interacting with cells and pathogens", oral, EPS 2019 - 46th European Physical Society Conference on Plasma Physics, 8-12 July 2019, University Milano Bicocca, Milano – Italy – I5.301 Invited

P.51. Varje J., Kurki-Suonio T., Vallar M., Sirén P., Särkimäki K., Garcia, Bolzonella T.: "ASCOT-AFSI simulations of fusion products for the main operatingscenarios in JT-60SA", 46th European Physical Society Conference on Plasma Physics, 8-12 July 2019, University Milano Bicocca, Milano – Italy – P2.1086

P.52. *Coelho R., Rodrigues P., Ferreira J., Vallar M., Särkimäki K., Garcia J.: "Interaction of energetic particles from neutral beam injection with Alfvén Eigenmodes in JT-60S", 46th European Physical Society Conference on Plasma Physics, 8-12 July 2019, University Milano Bicocca, Milano – Italy – P2.1031*

P.53. Nem R. D., Schneider B. S., Herrmann A., De Marne P., Naulin V., Rasmussen J. J., Sieglin B., Schrittwieser R. , Ionita C. , Costea S., Vianello N.,Spolaore M., Kovacic J. and MST1 team: "Comparison of Tokamak Plasma Midplane with Divertor Conditions", 46th European Physical Society Conference on Plasma Physics, 8-12 July 2019, University Milano Bicocca, Milano – Italy – P4.1050

P.54. Ayllon-Guerola J., Garcia-Munoz M., Davis S., Dibon M., Kurki-Suonio J., Nocente M., Perelli E., Snicker A., Sozzi C., Turnyanskiy M.,Vallar M., Wanner M., and the JT-60SA Team: "Feasibility study and physics performance of a fast-ion loss diagnostics for the JT-60SA tokamak", 46th European Physical Society Conference on Plasma Physics, 8-12 July 2019, University Milano Bicocca, Milano – Italy – P1.1009

P.55. Gerasimov N., Abreu P., Artaserse G., Buratti P., Carvalho I.S., De La Luna E., Hender,R.B. Henriques T.C., Lomas P.J., Matveeva E., Moradi S., Piron L., Rimini F.G., Szepesi G., Zakharov L.E., and JET Contributors: "Locked mode and disruption in JET-ILWS", 46th European Physical Society Conference on Plasma Physics, 8-12 July 2019, University Milano Bicocca, Milano – Italy – P1.1056

P.56. Valisa M., Chernyshova M., Biel W., Bombarda F., Carraro L., Coffey I., Czarski T., Davis S., Fassina A., Fornal T., Gabellieri L., Kowalska-Strzęciwilk E., Książek I., Lawson K., Malinowski K., Nakano T., Oyama N., Romano A., Puiatti M.E., Scully S., Soare S., Sozzi C.: "Physics requirements for the VUV survey spectrometer intended for the divertor radiation monitoring on JT-60SA", 46th European Physical Society Conference on Plasma Physics, 8-12 July 2019, University Milano Bicocca, Milano – Italy – P1.1012

P.57. Baruzzo M., Pironti A., Albanese R., Ambrosino R., Artaserse G., Castaldo A., Cavazzana R., Cianfarani C., Crisanti F., Marchiori G., Marconato N., Marrelli L., Martin P., Mele A.,

Peruzzo S., Ramogida G., Terranova D., Testa D., Zanca P., Zuin M.: "Conceptual design of DTT magnetic diagnostics", 46th European Physical Society Conference on Plasma Physics, 8-12 July 2019, University Milano Bicocca, Milano – Italy – P1.1010

P.58. Gobbin M., Macusova E., Ficker O., Markovic T., Bilkova P., Bohm P., Casolari A., Cerovsky J., Farnik M., Fassina A., Hron M., Mlynar J., Sos M., Valisa M., Weinzettl V., the COMPASS Team and the EUROfusion MST1 Team: "Runaway electron mitigation by n=1 and n=2 magnetic perturbations in COMPASS", EPS 2019 - 46th European Physical Society Conference on Plasma Physics, 8-12 July 2019, University Milano Bicocca, Milano – Italy

P.59. Albanese R., Ambrosino R., Baruzzo M., Bolzonella T., Crisanti F., Di Gironimo G., Di Zenobio A., Falessi M., Gobbin M., Granucci G., Innocente P., Mantica P., Martin P., Martone R., Mazzitelli G., Pironti A., Pizzuto A., Polli G., Ramogida G., Spizzo G., Tuccillo A., Valisa M., Vincenzi P., Zonca F. and the DTT team "The new Divertor Tokamak Test facility", EPS 2019 - 46th European Physical Society Conference on Plasma Physics, 8-12 July 2019, University Milano Bicocca, Milano – Italy – O2.102

P.60. Cavenago M., Barbisan M., Delogu R. S., Pimazzoni A., Poggi C., Antoni V., Balltador C., Cervaro V., Jain P., Laterza B., Maero G., Maniero M., Martini D., Minarello A., Ravarottto D., Recchia M., Romé M., Taccogna F., Ugoletti M., Variale V., Veltri P. and Serianni G.: "Experiments on negative ion sources at the NIO1 installation", EPS 2019 - 46th European Physical Society Conference on Plasma Physics, 8-12 July 2019, University Milano Bicocca, Milano – Italy – P1.1073

EFTSOMP - Workshop on Electric Fields, Turbulence and Self-Organization in Magnetized Plasmas, 15-16 July, Padova, Italy

P.61. Agostini M.., Vianello N., Carraro L., Carralero D., Cavedon M., Dux R., Lunt T., Naulin V., Spolaore M., Wolfrum E., the ASDEX-Upgrade Team, the EUROfusion MST1 Team: "Study of the role of divertor neutrals and SOL turbulence in the density shoulder formation and evolution in ASDEX-U", EFTSOMP - Workshop on Electric Fields, Turbulence and Self-Organization in Magnetized Plasmas, 15-16 July, Padova, Italy - invited

P.62. Grenfell G., Spolaore M., Abate D., Carraro L., Marrelli L., van Milligen B.Ph., Predebon I., Spagnolo S., Veranda M., Agostine, Cavazzana R., Cordaro L., De Masi G., Franz P., Martines E., Momo B., Puiatti M.E., Scarin P., Vianello N., Zaniol B., Zuin M. and the RFX-mod Team3: "3D filamentary transport and the role of edge sheared radial electric fields in the RFX-mod tokamak operation", EFTSOMP - Workshop on Electric Fields, Turbulence and Self-Organization in Magnetized Plasmas, 15-16 July, Padova, Italy - oral

P.63. Spolaore M., Agostinetti P., Killer C., Moresco M., Brombin M., Cavazzana R., Ghirardelli R., Grenfell G., Grulke O., Lazerson S., Martines E., Neubauer O., Nicolai D., Satheeswaran G., Schweer B., Vianello N. , Visentin M. and W7-X Team: "High Resolution Probe for filament transport and current density study at the edge region of W7-X", EFTSOMP - Workshop on Electric Fields, Turbulence and Self-Organization in Magnetized Plasmas, 15-16 July, Padova, Italy - oral

P.64. Momo B., Isliker H., Cavazzana R., Zuin M., Cordaro L. , Lopez Bruna D., Martines E., Spolaore M., Vlahos L.: "The phenomenology of fast reconnection events in the reversed field pinch", EFTSOMP - Workshop on Electric Fields, Turbulence and Self-Organization in Magnetized Plasmas, 15-16 July, Padova, Italy - oral

COMPUMAG 2019, July 15-19, 2019, Paris, Franc

P.65. **Voltolina D., Torchio R., Bettini P., Cavazzana R., and Moresco M.: " PEEC modeling of planar spiral resonators", 22nd International Conference on the Computation of Electromagnetic Fields**, COMPUMAG 2019, **July 15-19**, **2019, Paris**, **France – Pc-M1-1 to be published in** IEEE Transactions on Magnetics

P.66. Bonotto M., Villone F., Liu Y., Bettini P.: "Matrix Based Rational Interpolation for New Coupling Scheme Between MHD and Eddy Current Numerical Models", 22nd International Conference on the Computation of Electromagnetic Fields, COMPUMAG 2019, July 15-19, 2019, Paris, France – Pc-M2-6 to be published in IEEE Transactions on Magnetics

P.67. Bettini P., De Lorenzi A., Marconato N., Patton T., Pilan N., Specogna R.: "Residual-based error estimator with guaranteed error bounds for mixed-hybrid geometric formulations for electrostatics", 22nd International Conference on the Computation of Electromagnetic Fields, COMPUMAG 2019, July 15-19, 2019, Paris, France – PB-M3-14 to be published in IEEE Transactions on Magnetics

7th Annual Theory and Simulation of Disruptions Workshop, 5-7 August 2019, PPPL Princeton, New Jersey- USA

P.68. Piron L., Hender T. C., Joffrin E., Buratti P., Challis C., Gerasimov S., Henriques R., Marrelli L., Lomas P., Paccagnella R., Pucella G., Rimini F., Terranova D., Zanca P.: "Locked mode dynamics prior to disruptions in high performance JET plasmas", 7th Annual Theory and Simulation of Disruptions Workshop, 5-7 August 2019, PPPL Princeton, New Jersey- USA

5th Central and Eastern European Committee for Thermal Analysis and Calorimetry (CEEC-TAC5), 27-30 August 2019, Roma

P.69. Dalla Palma M., Gambetta G., Peruzzo S.: "Thermal analysis of the RFX-mod2 operating conditions for the design of the temperature measurement system", 5th Central and Eastern European Committee for Thermal Analysis and Calorimetry (CEEC-TAC5), 27-30 August 2019, Roma, OP1.12 oral

P.70. Dalla Palma M., Spolaore M.: "Modelling of fast response surface thermocouples for fusion plasma facing components", 5th Central and Eastern European Committee for Thermal Analysis and Calorimetry (CEEC-TAC5), 27-30 August 2019, Roma, PS1.078

18th International Conference on Ion Sources (ICIS'19), September 1-6 2019, Lanzhou, China

P.71. Fadone M., Barbisan M., Cristofaro S., De Muri M., Sartori E., Serianni G.: "Interpreting the dynamic equilibrium during evaporation in a Caesium environment". 18th International Conference on Ion Sources (ICIS'19), September 1-6 2019, Lanzhou, China –Rev. Sci. Instrum. **91**, (2020)

P.72. Sartori E., Candeloro V., Serianni G.: "Analysis of current voltage characteristics for Langmuir probes immersed in an ion beam", 18th International Conference on Ion Sources (ICIS'19), September 1-6 2019, Lanzhou, China – to be published in Rev. Sci. Instrum. **91**, (2020)

P.73. Serianni G., Toigo V., Boilson D., Rotti C., Bonicelli T., Paolucci F., Chakraborty A., Kashiwagi M., Fantz U., the NBTF team and the contributing Staff of IO, F4E, IPR, QST, IPP and other laboratories: "First operation in SPIDER and the path to complete MITICA", 18th International Conference on Ion Sources (ICIS'19), September 1-6 2019, Lanzhou, China – to be published in Rev. Sci. Instrum. **91**, (2020)

P.74. Zaniol B., Barbisan M., Bruno D., Pasqualotto R., Taliercio C., Ugoletti M.: " First measurements of Optical Emission Spectroscopy on SPIDER Negative Ion Source", 18th International Conference on Ion Sources (ICIS'19), September 1-6 2019, Lanzhou, China – to be published in Rev. Sci. Instrum. **91**, (2020)

P.75. Siragusa M., Sartori E., Bonomo F., Heinemann B., Orozco G., Serianni G.: "Simulation of the gas density distribution in the accelerator of the ELISE test facility", 18th International Conference on Ion Sources (ICIS'19), September 1-6 2019, Lanzhou, China – to be published in Rev. Sci. Instrum. **91**, (2020)

P.76. Poggi C., Sartori E., Zuin M., Brombin M., Fassina A., Fincato M., Siragusa M. and Serianni G.: " CRISP: a Compact RF Ion Source Prototype for emittance scanner testing", 18th International Conference on Ion Sources (ICIS'19), September 1-6 2019, Lanzhou, China – to be published in Rev. Sci. Instrum. **91**, (2020)

P.77. Pimazzoni A., Brombin M., Delogu R. S., Fasolo D., Franchin L., Laterza B., Pasqualotto R., Serianni G., Tollin M.: " Assessment of the SPIDER beam features by diagnostic calorimetry and thermography", 18th International Conference on Ion Sources (ICIS'19), September 1-6 2019, Lanzhou, China – to be published in Rev. Sci. Instrum. **91**, (2020)

P.78. Siragusa M., Sartori E., Siviero F., Mura M., Serianni G.: "Numerical simulation of experimental tests performed on ZAO® Non-EvaporableGetter pump designed for NBI applications", 18th International Conference on Ion Sources (ICIS'19), September 1-6 2019, Lanzhou, China – to be published in Rev. Sci. Instrum. **91**, (2020)

P.79. Poggi C., Sartori E., Tollin M., Brombin M., Fagotti E., Serianni G.: "Design and development of an Allison type emittance scanner for the SPIDER ion source", 18th International Conference on Ion Sources (ICIS'19), September 1-6 2019, Lanzhou, China – to be published in Rev. Sci. Instrum. **91**, (2020)

*P.80. Cavenago M., Delogu R. S., Barbisan M., Pimazzoni A., Poggi C., Agostini M., Antoni V., Balltador C., Cervaro V., De Muri M., Giora D., Jain P., Laterza B., Maero G., Maniero M., Martini D., Minarello A., Ravarottto D. , Recchia M., Rizzolo A., Romé M., Sartori E., Sattin M., Serianni G., Taccogna F., Ugoletti M., Variale V., Veltri P.: "Improvements of the NIO1 Installation for Negative Ion Sources", 18th International Conference on Ion Sources (ICIS'19), September 1-6 2019, Lanzhou, China – to be published in Rev. Sci. Instrum. **91**, (2020)*

*P.81. Variale V., Valentino V., Cavenago M., Balltador C., Sartori E. and Serianni G.: "Beam Energy Recovery for Fusion: Collector design for the test on NIO1 source", 18th International Conference on Ion Sources (ICIS'19), September 1-6 2019, Lanzhou, China – to be published in Rev. Sci. Instrum. **91**, (2020)*

*P.82. Wimmer C., Bonomo F., Hurlbatt A., Schiesko L., Fantz U., Heinemann B., Orozco G., Agostini M., Barbisan M., Brombin M., Delogu R. S., Pimazzoni A., Serianni G., Ugoletti M., Veltri P.: "Novel comparative measurement of H− beam divergences at the BATMAN Upgrade test facility: single beamlet and a group of beamlets", 18th International Conference on Ion Sources (ICIS'19), September 1-6 2019, Lanzhou, China – to be published in Rev. Sci. Instrum. **91**, (2020)*

*P.83. Cristofaro S., Fröschle M., Mimo A., Rizzolo A., DeMuri M., Barbisan M. and Fantz U.: "Design and comparison of the Cs ovens for the test facilities ELISE and SPIDER", 18th International Conference on Ion Sources (ICIS'19), September 1-6 2019, Lanzhou, China – to be published in Rev. Sci. Instrum. **91**, (2020)*

MeVArc 2019 – 8th International Workshop on Mechanisms of Vacuum Arcs (MeVArc19) 16-19 September 2019, Padova, Italy

P.84. Spada E., De Lorenzi A., Lotto L., Pilan N., Zuin M.: "The Breakdown Induced by Rupture of Dielectric layer (BIRD) model: insights and future developments", MeVArc 2019 – 8th International Workshop on Mechanisms of Vacuum Arcs (MeVArc19) - 16-19 September 2019, Padova, Italy - oral

P.85. Zamengo A., Agostini M.: "RF Breakdowns in the SPIDER experiment during its first operational phase", MeVArc 2019 – 8th International Workshop on Mechanisms of Vacuum Arcs (MeVArc19) - 16-19 September 2019, Padova, Italy - oral

P.86. Toigo V., Dal Bello S., Boilson D., Rotti C., Bonicelli T., Paolucci F., Chakraborty A., Kashiwagi M.: "Progress of the ITER Neutral Beam Test Facility project", 8th International

Workshop on Mechanisms of Vacuum Arcs (MeVArc19) - 16-19 September 2019, Padova, Italy- oral

P.87. Serianni G., Toigo V.: " First year of operation of SPIDER, prototype source of ITER neu-tral beam injectors", 8th International Workshop on Mechanisms of Vacuum Arcs (MeVArc19) - 16-19 September 2019, Padova, Italy - oral

P.88. Chitarin G., Aprile D., Patton T., Pilan N.: "Design of the first vacuum and low-pressure gas insulation testsfor the MITICA 1 MV electrostatic Accelerator", 8th International Workshop on Mechanisms of Vacuum Arcs (MeVArc19) - 16-19 September 2019, Padova, Italy - oral

P.89. Cordaro L., Cavazzana R.., Zuin M., Berton G., Peruzzo S.: "Surface coatings for arc prevention between plasma facing com-ponents", 8th International Workshop on Mechanisms of Vacuum Arcs (MeVArc19) - 16-19 September 2019, Padova, Italy - oral

P.90. Patton T., Chitarin G., Pilan N., Aprile D.: "Electrical Design and Voltage Holding Analyses of the MITICABeam Source Mock-up and its Intermediate Electrostatic Shield", 8th International Workshop on Mechanisms of Vacuum Arcs (MeVArc19) - 16-19 September 2019, Padova, Italy

P.91. Pilan N., Deambrosis S., De Lorenzi A., Cavenago M., Cervaro V., Fincato M., Fontana C., Lotto L., Martines E., Pasqualotto R., Pino F., Rossetto F., Spada E., Spagnolo S., Veltri P., Zuin M.: "Mutual exchange of charged particles in high voltage dc devicesinsulated by high vacuum", 8th International Workshop on Mechanisms of Vacuum Arcs (MeVArc19) - 16-19 September 2019, Padova, Italy – oral

P.92. Pilan N., De Lorenzi A. , Deambrosis S.M., Fincato M. , Fontana C. , Gobbo R. , Lotto L. , Martines E. , Pasqualotto R. , Patton T., Felix Pino , Spada E. , Spagnolo S. , Zuin M.: "HVDC insulation between shaped electrodes separated by large vacuum gaps", 8th International Workshop on Mechanisms of Vacuum Arcs (MeVArc19) - 16-19 September 2019, Padova, Italy – oral

P.93. Spagnolo S., Pilan N., De Lorenzi A., Fontana C., Renato Gobo, Lotto L., Martines E., Pino F., Rossetto F., Spada E., Zuin M.: "Statistical analysis of current and x-rays signals for a vacuum high voltage holding experiment", 8th International Workshop on Mechanisms of Vacuum Arcs (MeVArc19) - 16-19 September 2019, Padova, Italy - oral

P.94. Cavazzana R., Zuin M., Cordaro L., Peruzzo S.: "Electrode conditioning for prevention of DC arc formation in pres-ence of a cold plasma background", 8th International Workshop on Mechanisms of Vacuum Arcs (MeVArc19) - 16-19 September 2019, Padova, Italy

P.95. Croci G., Muraro A., Gorini G., Perelli Cippo E., Tardocchi M., Grosso G., Rigamonti D., Pilan N., Pasqualotto R., McCormack O.: "X-rays spectrum characterization during high voltage condition-ing in .vacuum insulated system using high rate detectors", 8th International Workshop on Mechanisms of Vacuum Arcs (MeVArc19) - 16-19 September 2019, Padova, Italy

10th IAEA Technical Meeting on Steady State Operation of Magnetic Fusion Devices (IAEA-TMSSO 2019), 9–11 September 2019, Hefei, China

P.96. Piron C., Garcia J., Goodman T., Agostini M., Fontana M., Giruzzi G., Gobbin M., Karpushov A., Kong M., Merle A., Morales J., Nowak S., Pigatto L., Sauter O., Testa D., Vallar M., Yoshida M., the TCV team and the MST1 team: "Extension of the operating space of steady state regimes on TCV", 10th IAEA Technical Meeting on Steady State Operation of Magnetic Fusion Devices (IAEA-TMSSO 2019), 9–11 September 2019, Hefei, China
LAPD19 Symposium - September 22-26, 2019 | Whitefish, MT

P.97. Fassina A., Fiorucci D., Giudicotti L., Vincenzi P.: "Performance analysis and application study of a laser enhancement cavity for photo-neutralization of Negative Ion Beams in large fusion experiments", LAPD19 Symposium - September 22-26, 2019 | Whitefish, MT, to be published in Journal of Instrumentation (JINST)

P.98. Giudicotti L., Pasqualotto R., Fassina A.: "Design of Thomson scattering diagnostics for the Divertor Tokamak Test (DTT) Facility", LAPD19 Symposium - September 22-26, 2019 | Whitefish, MT, to be published in Journal of Instrumentation (JINST)

P.99. Innocente P., Balbinot L., Fiorucci D., Mazzotta C., Tudisco O.: "Dispersion scanning beam medium infra-red interferometry for divertor plasma density measurements in DTT", to be published in Journal of Instrumentation (JINST)

P.100. Fiorucci D., Innocente P., Mazzotta C., Terranova D., Tudisco O.: "Design of an interferometer/polarimeter for DTT", LAPD19 Symposium - September 22-26, 2019 | Whitefish, MT

14th International Symposium on Fusion Nuclear Technology ISFNT14, 22-27 September 2019, Budapest, Hungary

P.101. Gaio E., Ferro A., Maistrello A., Dan M., Lunardon F., Barucca L., Ciattaglia S., Federici G., Benfatto I.: "The DEMO Plant Electrical System: issues and perspective", 14th International Symposium on Fusion Nuclear Technology ISFNT14, 22-27 September 2019, Budapest, Hungary – O3-3.4 oral

P.102. Peruzzo S., Dalla Palma M., Rizzolo A., Rossetto F. and Siragusa M.: "Design and test of the vacuum-tight electrically-insulated crossed joints of the new Vacuum Vessel for the RFX-mod2 experiment", 14th International Symposium on Fusion Nuclear Technology ISFNT14, 22-27 September 2019, Budapest, Hungary – P3-095

P.103. Dalla Palma M., Berton G., Canton A., Cavazzana R., Gambetta G., Innocente P., Peruzzo S., Siragusa M., Spagnolo S., Spolaore M.: "Design of the RFX-mod2 first wall", 14th International Symposium on Fusion Nuclear Technology ISFNT14, 22-27 September 2019, Budapest, Hungary – P1.004

P.104. Maistrello A., Recchia M., Marconato N., Patton T., Pavei M., Sartori E., Serianni G.: "Voltage Hold Off Test of the Insulating Supports for the Plasma Grid Mask of SPIDER", 14th International Symposium on Fusion Nuclear Technology ISFNT14, 22-27 September 2019, Budapest, Hungary – P2-061

P.105. Pavei M., Dal Bello S., Gambetta G., Maistrello A., Marcuzzi D., Sartori E. , Serianni G., Cervaro V., Degli Agostini F., Franchin L., Tollin M.: "SPIDER Plasma Grid masking for reducing gas conductance and pressure in the Vacuum Vessel", 14th International Symposium on Fusion Nuclear Technology ISFNT14, 22-27 September 2019, Budapest, Hungary – P2-071

P.106. Agostinetti P., Franke T., Fantz U., Hopf C., Mantel N., Tran M.Q.: "RAMI Evaluation of the Beam Source for the DEMO Neutral Beam Injectors", 14th International Symposium on Fusion Nuclear Technology ISFNT14, 22-27 September 2019, Budapest, Hungary – P2-026

P.107. Lunardon F., Maistrello A., Spresian I., Gaio E., Piovan P., Ciattaglia S.: "MEST, a new Magnetic Energy Storage and Transfer system: application studies to the European DEMO", 14th International Symposium on Fusion Nuclear Technology ISFNT14, 22-27 September 2019, Budapest, Hungary – P3-091

P.108. Hopf C., Starnella G., Harder N., Agostinetti P., Fantz U.: "Residual Ion Energy Recovery for the DEMO NBI –a Conceptual Design Study", 14th International Symposium on Fusion Nuclear Technology ISFNT14, 22-27 September 2019, Budapest, Hungary- P2-047

P.109. Tobari H., Kashiwagi M., Watanabe K., Maejima T., Yamashita Y., Boldrin M., Zanotto L., Dal Bello S., Toigo V., Simon M., Escudero Gomez G., Paolucci F., Bonicelli T., Decamps H.: "Achievement of DC 1 MV Insulation in High-Voltage Power Supply for ITER Neutral Beam Test Facility", 14th International Symposium on Fusion Nuclear Technology ISFNT14, 22-27 September 2019, Budapest, Hungary – P2-116

P.110. Ciattaglia S., Federici G., Barucca L., De Magistris M., Gaio E., Gliss C., Koerber M., Moscato I., Porfiri M.T., Riedl F., Tarallo A.: "EU DEMO Plant and Building Layout Criteria", 14th Internationl Symposium on Fusion Nuclear Technology ISFNT14, 22-27 September 2019, Budapest, Hungary – P3-106

105° Congresso Nazionale SIF, L'Aquila, 23-27 settembre 2019

P.111. De Masi G., Cordaro L., Fassina A., Pimazzoni A., Gareri C., Cavazzana R., Martines E., Zaniol B., Zuin M., Brun P., Mignogna C., Folino P., Tamme L., De Rosa S., Indolfi C. : "Physical properties of an atmospheric plasma jet and its effect on blood coagulation" 105° Congresso Nazionale SIF, L'Aquila, 23-27 settembre 2019

P.112. Paccagnella R.: "Helicity transport and dynamo sustainment for helical plasma states", 105° Congresso Nazionale SIF, L'Aquila, 23-27 settembre 2019

FisMat 2019, September 30- October 4, 2019, Catania, Italy

P.113. Veranda M., Bonfiglio D., Cappello S., Chacon L., Escande D.F., Di Giannatale G.: "Helical magnetic self-organization of plasmas in toroidal pinches with transport barrier formation", FisMat 2019, September 30- October 4, 2019, Catania, Italy - Invited

18th European Fusion Theory Conference EFTC2019, October 7-10, 2019, Ghent, Belgium

P.114. Bonfiglio D., Cappello S., Chacon L., Escande D.F., Di Giannatale G., Kryzhanovskyy A., Veranda M., Marrelli L., Zanca P.: "Effect of a refined magnetic boundary on MHD modelling of helical self-organization in the RFP" , 18th European Fusion Theory Conference EFTC2019, October 7-10, 2019, Ghent, Belgium

P.115. Cappello S., Bonfiglio D., Di Giannatale G., Kryzhanovskyy A., Veranda M., Chacón L., Escande. D.F., and the RFX Team: "Recent Developments in the Studies of Plasma Self-Organization in the Reversed-Field Pinch and Impact on Transport Properties", 18th European Fusion Theory Conference EFTC2019, October 7-10, 2019, Ghent, Belgium - Invited

P.116. Murari A. and JET Contributors: "Data Driven Theory to Support Model Formulation and the Design of New Experiments", 18th European Fusion Theory Conference EFTC2019, October 7-10, 2019, Ghent, Belgium

P.117. Weisen H.,Maggi C.F., Menmuir S., Horvath L., Bache T.W.,.Casson F.J., Oberparleiter M., Saarelma S., Auriemma F., Chankin A., Delabie E., Giroud C., King D., Lorenzini R., Viezzer E., Siren P., Varje J. and JET contributors: "Isotope dependence of energy, momentum and particle confinement in tokamaks", 18th European Fusion Theory Conference EFTC2019, October 7-10, 2019, Ghent, Belgium

P.118. Macusova E., Ficker O., Markovic T., Gobbin M., Casolari A., Mlynar J., Cerovsky J., Jaulmes Kripner, Decker J., Peysson Y., Papp G., Pokol G., Carnevale D., Farnik M., Havlicek J., Havranek A., Hron M., Naydenkova D., Panek R., Plyusnin V., Tomes M., Urban J., Vondracek P., Weinzett V., COMPASS team and the EUROfusion MST Team: "The impact of resonant magnetic perturbations on runaway electron dynamics", 18th European Fusion Theory Conference EFTC2019, October 7-10, 2019, Ghent, Belgium

P.119. Kryzhanovskyy A., Bonfiglio D., Zuin M., Cappello S., Veranda M.: "Alfvén waves in nonlinear 3D MHD modelling of RFP plasmas", 18th European Fusion Theory Conference EFTC2019, October 7-10, 2019, Ghent, Belgium

61st Annual Meeting of the APS Division of Plasma Physics, October 21-25, 2019 • Fort Lauderdale, Florida

P.120. P. Martin, Albanese R., Ambrosino R., Baruzzo M., Bolzonella T., Carlevaro N., Casiraghi I., Crisanti F., Di Gironimo G., Di Zenobio A., Falessi M., Gobbin M., Granucci G., Innocente P., Mantica P., Martone R., Mazzitelli G., Pigatto L., Pironti A., Pizzuto A., Polli G., Ramogida G., Rubino G., Spizzo G., Subba F., Tuccillo A., Valisa M., Vallar M., Vianello N., Villari R., Vincenzi P., Vlad G., Zonca F.: "Present status of the divertor tokamak test facility", 61st Annual Meeting of the APS Division of Plasma Physics, October 21-25, 2019 • Fort Lauderdale, Florida, Bullettin of the American Physical Society, Volume 64, Number 11, 2019

P.121. Cordaro L., Zuin M., Anderson J. K., Stevanato L., Fontana C., Bonesso I., Kim J.: "New neutron-gamma scintillator diagnostics at the Madison Symmetric Torus", 61st Annual Meeting of the APS Division of Plasma Physics, October 21-25, 2019 • Fort Lauderdale, Florida, Bullettin of the American Physical Society, Volume 64, Number 11, 2019

P.122. Abate D., Marchiori G., Bettini P.: "A feasibility study of RFX-mod2 tokamak equilibria scenarios with DEMO-like shape conditions and negative triangularity", 61st Annual Meeting of the APS Division of Plasma Physics, October 21-25, 2019 • Fort Lauderdale, Florida, Bullettin of the American Physical Society, Volume 64, Number 11, 2019

P.123. Smith S., Meneghini O., Eldon D., Mccle-Naghan J., Lyons B., Knolker M., Thome K., Grierson B., Logan N., Ashourvan A., Hu Q., Haskey S., Holland C., Wilks T., Park J., Kim K., Izzo V., Moynihan C., Pigatto L., Trevisan G., Omfit Team: "Using The Omfit Framework To Streamline Hpc Workflws", 61st Annual Meeting of the APS Division of Plasma Physics, October 21-25, 2019 • Fort Lauderdale, Florida, Bullettin of the American Physical Society, Volume 64, Number 11, 2019

P.124. Zhang N., Liu Y., Piovesan P., D S. Wang.Yu,, Dong G., Hao G., G, Xia: "Toroidal Modelling Of Core Plasma Ow Damping Induced Byrmp Elds In Asdex Upgrade", 61st Annual Meeting of the APS Division of Plasma Physics, October 21-25, 2019 • Fort Lauderdale, Florida, Bullettin of the American Physical Society, Volume 64, Number 11, 2019

Third IAEA Technical Meeting on Divertor Concepts, 4-7 November 2019 IAEA Headquarters, Vienna, Austria

P.125. Vianello N., Ambrosino R., Innocente P. and DTT Contributors: "Power exhaust studies in the Divertor Tokamak Test facility", Third IAEA Technical Meeting on Divertor Concepts, 4-7 November 2019 IAEA Headquarters, Vienna, Austria

P.126. Balbinot L., Rubino G., Innocente P.: "Edge and divertor modelling of JT-60SA ITER-like scenario with carbon wall", Third IAEA Technical Meeting on Divertor Concepts, 4-7 November 2019 IAEA Headquarters, Vienna, Austria

P.127. Martin P.: "The Divertor Tokamak Test facility", Third IAEA Technical Meeting on Divertor Concepts, 4-7 November 2019 IAEA Headquarters, Vienna, Austria

P.128. Galassi D., Reimerdes H., Theiler C., Wensing M., Bufferand H., Ciraolo G., Innocente P., Marandet Y., Tamain P., Baquero M., Brida D., De Oliveira H., Duval B., Février O., Henderson S., Komm M., Maurizio R., Tsui C. K., the TCV team and the EUROfusionMST1 Team: "Multi-code simulations of the gas baffle effects on TCV Lower Single Null edge plasmas", Third IAEA Technical Meeting on Divertor Concepts, 4-7 November 2019 IAEA Headquarters, Vienna, Austria

P.129. Rubino G., Balbinot L., Calabró G., Innocente P., Subba F.: "Study of Single Null divertor in DTT with Nitrogen, Neon and Argon seeding", Third IAEA Technical Meeting on Divertor Concepts, 4-7 November 2019 IAEA Headquarters, Vienna, Austria

AAPPS-DPP 2019 - 3rd Asia-Pacific Conference on Plasma Physics, November 17-22, 2019, Hefei, Anhui, China

P.130. Di Giannatale G., Bonfiglio D., Cappello S., Veranda M., M Falessi.V., Grasso D., Pegoraro F.: "Lagrangian Coherent Structures as skeleton of transport in low collisionality and chaotic magnetic systems", AAPPS-DPP 2019 - 3rd Asia-Pacific Conference on Plasma Physics, November 17-22, 2019, Hefei, Anhui, China

P.131. Spolaore M.: "Current carrying Edge Localized Modes fine structure in the Scrape-Off Layer of tokamak discharges", AAPPS-DPP 2019 - 3rd Asia-Pacific Conference on Plasma Physics, November 17-22, 2019, Hefei, Anhui, China - Invited

P.132. Bonfiglio D., Cappello S., Chacón L., Escande D.F., Di Giannatale G., Kryzhanovskyy A., Veranda M., Marrelli L., Zanca P.: "Nonlinear MHD modelling of helical self-organization in the RFP: effect of a realistic boundary and predictions for RFX-mod2", AAPPS-DPP 2019 - 3rd Asia-Pacific Conference on Plasma Physics, November 17-22, 2019, Hefei, Anhui, China - Invited

P.133. Sattin F., Escande D.F., Gondret V.: "Relevant heating of the solar corona by quenching Alfvén waves : a result of adiabaticity breakdown" , AAPPS-DPP 2019 - 3rd Asia-Pacific Conference on Plasma Physics, November 17-22, 2019, Hefei, Anhui, China – Invited

APPC 2019 - 14th Asia-Pacific Physics Conference, November 17 – 22 2019, Kuching, Sarawak, Malaysia

P.134. Auriemma: "TRANSP Predictive Modelling for Exb Studies in Pure D and T H-Mode JET Plasmas" F., APPC 2019 - 14th Asia-Pacific Physics Conference, November 17 – 22 2019, Kuching, Sarawak, Malaysia – Invited